



University
of Glasgow

<https://theses.gla.ac.uk/>

Theses Digitisation:

<https://www.gla.ac.uk/myglasgow/research/enlighten/theses/digitisation/>

This is a digitised version of the original print thesis.

Copyright and moral rights for this work are retained by the author

A copy can be downloaded for personal non-commercial research or study, without prior permission or charge

This work cannot be reproduced or quoted extensively from without first obtaining permission in writing from the author

The content must not be changed in any way or sold commercially in any format or medium without the formal permission of the author

When referring to this work, full bibliographic details including the author, title, awarding institution and date of the thesis must be given

Enlighten: Theses

<https://theses.gla.ac.uk/>
research-enlighten@glasgow.ac.uk

TECTONICS AND PETROFABRIC STRUCTURES IN BALLACHULISH AND

GLEN COE, ARGYLLSHIRE

Mary Cameron Vogt
University of Glasgow
Glasgow, Scotland
September, 1954

ProQuest Number: 10656245

All rights reserved

INFORMATION TO ALL USERS

The quality of this reproduction is dependent upon the quality of the copy submitted.

In the unlikely event that the author did not send a complete manuscript and there are missing pages, these will be noted. Also, if material had to be removed, a note will indicate the deletion.



ProQuest 10656245

Published by ProQuest LLC (2017). Copyright of the Dissertation is held by the Author.

All rights reserved.

This work is protected against unauthorized copying under Title 17, United States Code
Microform Edition © ProQuest LLC.

ProQuest LLC.
789 East Eisenhower Parkway
P.O. Box 1346
Ann Arbor, MI 48106 – 1346

ABSTRACT

A detailed macroscopic examination has been made of bedding, flow cleavage, false cleavage, lineation, fold axes, and axial directions in the Dalradian rocks of Ballachulish and Glen Coe, Argyllshire. This has been supplemented by the microscopic study of 594 thin-sections and by 62 petrofabric analyses. From these data two structural directions have emerged, the stronger one trending northeast-southwest, with a southwesterly plunge, and the weaker one trending northwest-southeast, with a northwesterly plunge. It has not been possible to elucidate the tectonic history from the structural data of one limited, complex area.

ABSTRACT

PREFACE

CHAPTER I: INTRODUCTION

- A. Location of area and brief physiographic description
- B. Field work
 - 1. General comments
 - 2. Collection of specimens
 - 3. Preparation of thin-sections
- C. General lithology
 - 1. Rock types
 - 2. Age of the Dalradian series
 - 3. Stratigraphic succession
- D. General tectonic picture

CHAPTER II: LITHOLOGY

- A. Preparation of the geology map (Map I)
- B. Characteristics of the stratigraphic succession
 - 1. Binnein quartzite
 - 2. Binnein schist
 - 3. Glencoe quartzite
 - 4. Banded Passage Beds (part of the Leven schist)
 - 5. Leven schist
 - 6. Ballachulish limestone
 - 7. Ballachulish slate
 - 8. Striped Transition Series (part of Appin quartzite)
 - 9. Appin quartzite
 - 10. Appin limestone
 - 11. Appin phyllite

CHAPTER III: TECTONICS -- PLANAR STRUCTURES

- A. Collection of field data
- B. Description of planar structures
 - 1. Primary
 - a. Bedding
 - b. Map II: Strike and dip of bedding
 - 2. Secondary
 - a. Foliation
 - (1) Terminology
 - (2) Types
 - b. Cleavage
 - (1) Flow cleavage
 - (a) Characteristics
 - (b) Relation of flow cleavage to bedding and folding
 - (c) Map III: Strike and dip of flow cleavage
 - (d) Origin of flow cleavage

(2) False cleavage, including fracture cleavage	
(a) Characteristics	4
(b) Relation of false cleavage to bedding, flow cleavage, and folding	4
(c) Map III: Strike and dip of false cleavage	5
(d) Origin of false cleavage	5
(3) Use of cleavage to determine superposition	5
c. Slickensides	5
d. Shear zones	5
e. Joints	5
(1) Types	5
(2) Stereogram	56
(3) Origin	57
f. Faults	57
(1) Regional	57
(2) Medium-scale	58
(3) Small-scale	59
 CHAPTER IV: TECTONICS -- FOLDED STRUCTURES	60-
A. Folding	60-
1. Competence	60
2. Stress	61
a. Compressive	61
b. Tensile	62
c. Shearing	62
3. Relation of competence and stress	62
B. Types of folds	63-
1. Compression	63
a. Flexure folds	63
b. Flexural-slip folds	64
c. Flow folds	65
2. Shear	65
3. Combinations of folds	65
 CHAPTER V: TECTONICS -- LINEAR STRUCTURES	66-9
A. Lineations	66-7
1. Types	66
2. Map IV: Directions and plunge of lineations	68
3. Stereograms	70
B. Fold axes	72-
1. Definition	72
2. Measurement	72
a. Direct measurement	72
b. Geometrical construction	73
c. "b"-lineations	75
3. Map V: Direction and plunge of fold axes	77
4. Stereograms	78

a. Based on scale of folds	78
b. Based on lithology	80
c. Based on geographic distribution	82
5. Axial directions	86
a. Geometric construction	86
b. Stereograms and Map VI	87
(1) Axial direction of total area	87
(2) Axial directions of major divisions	88
(3) Axial directions of subdivisions	90
CHAPTER VI: PETROFABRIC STRUCTURES	92-100
A. General principles of petrofabric analysis	92-9
B. Preparation and orientation of petrofabric diagrams	94-5
C. Analysis of the Ballachulish-Glencoe petrofabric diagrams	95-1
1. Relation of quartz orientation to maxima	95
2. Relation of quartz orientation to girdles	98
3. Relation of girdle patterns to linear structures	101
4. Symmetry of fabric	102
5. Homogeneity of fabric	103
6. Map VII: Geographic orientation of quartz optic axes	104
SUMMARY AND CONCLUSIONS	106-1
BIBLIOGRAPHY	
LIST OF TEXT-FIGURES	
LIST OF PLATES	
LIST OF MAPS	
APPENDIX	

TECTONICS AND PETROFABRIC STRUCTURES IN BALLACHULISH AND GLEN COE, ARGYLLSHIRE

PREFACE

Stimulated by the Eighteenth International Geological Congress excursion to Ballachulish and Glen Coe, Argyllshire, in 1948, the author has undertaken a detailed structural examination of the metamorphic rocks between the Ballachulish igneous complex on the west, Loch Leven on the north, the Glen Coe cauldron on the east, and an arbitrary boundary on the south, as shown on Map I and roughly outlined on the map of Scotland, Text - fig.1. Thirty weeks were spent in the field between October 1950 and August 1952, and most of the accessible rock outcrops studied. With a Brunton compass the strike and dip of bedding, cleavage, joint, and fault planes and the direction and plunge of fold axes and lineations were measured. The lithology was drawn on six inches to one mile (1:10,560) Ordnance Survey maps (second edition, 1900). The map data were supplemented by a series of 84 vertical aerial photographs, taken in 1946 and 1947 by the Air Ministry on the scale 1:10,000 and by the third edition of the geological map, Sheet 53, published in 1948 by the Geological Survey, on the scale of one inch to one mile (1:63,360). 709 rock specimens were collected, 614 of which were orientated. 594 thin-sections have been prepared; 436 are orientated. The specimens and thin-sections are numbered consecutively and are prefixed by the letters VB. This thesis describes all of the data obtained from the author's field and laboratory work, her methods of analysis, and her conclusions. The specimens, thin-sections, maps, and notebooks are in the Department of Geology, University of Glasgow.

The author is indebted to the United States Department of State for a Fulbright grant for 1950-52 to pursue research at the University of Glasgow.

Her deepest thanks go to her sponsors; Dr. J. C. Haff, Department of Geology, Mount Holyoke College; Dr. H. A. Meyerhoff, head of the Scientific Manpower Commission, Washington, D.C.; and Dr. H. Stobbe, Department of Geology, Smith College.

The laboratory work has been carried out in the departments of geology of the University of Glasgow and of Bedford College, University of London. The writer greatly appreciates the cooperation, suggestions, and criticisms of Prof. T. N. George and Dr. B. C. King at the University of Glasgow and of Prof. L. Hawkes at Bedford College. Mr. B. G. Woodland assisted materially in the checking and preparation of maps and diagrams and for brief periods in the field.

CHAPTER I: INTRODUCTION

A. Location and description of area

The Ballachulish-Glen Coe district, Argyllshire, lies in the western part of the Grampian Highlands of central Scotland south-southeast of the boundary marked by the Great Glen fault (Text - fig.1). The Grampian physiographic province is characterized by northeast-southwest-trending crush belts, a well-dissected landscape, and a fjord coastline. These features are exemplified in Ballachulish and Glen Coe by the numerous northeast-southwest-trending dikes, the sharp ridges and peaks rising to heights exceeding 3000 ft., (Pl.VII, Fig. XXIX, Fig.1) and the trough shapes of Loch Leven, a salt-water lake, and Glen Coe (Pl.VII, Fig.2).

The section examined by the author is trapezohedral in outline, and lies between Lon. $5^{\circ} 2' 55''$ W and $5^{\circ} 14' 15''$ W and between Lat. $56^{\circ} 38' 45''$ N and $56^{\circ} 42' 30''$ N. The land area mapped is approximately 16 sq. mi. The highest



Text-figure 1. The physiographic provinces of Scotland showing the location of the Ballachulish-Glen Coe area.

peaks are Sgorr Dhearg (National Grid Reference on Map I, 056558), 3362 ft., Sgòr nam Fiannaidh (142581), 3168 ft., and Beinn Fhiodha (062562), 3104 ft. Sgòr na Ciche or the Pap of Glen Coe (126594), 2430 ft., Meall Mor (108560), 2215 ft., and Sgorr a' Choise (085550), 2169 ft., comprise a 2000 ft. group. The lowest peaks rising southward from the shores of Loch Leven are Beinn Bhan (068573), 1645 ft., Meall a' Chaolais (057576), 1550 ft., and Am Meall (095575), 1350 ft. (see Map I; Pl. VII, Fig. 1; XVI, Fig. 1; XXIX, Fig. 1).

Glacial modifications of the topography besides the trough valleys include cirques, such as Coire Riabhaich (065566) (Pl. XXIX, Fig. 2) and Coire an Lochain (135588), arêtes and cols, such as make up the horseshoe-shaped ridge extending from Meall a' Chaolais southward to Sgorr Dhearg, east-northeastward to Beinn Fhiodha, and northward to Beinn Bhan (Map I; Pl. XXIX, Fig. 1), and morainic deposits on valley slopes (Pl. XXIX, Fig. 2).

B. Field work

1. General comments. The best rock exposures are found in the shore section and road cuttings along Loch Leven, in the courses of the main streams (the Giúbhachain, Laroach, Riabhach, Socalach, Leac-na-muidhe, and the upper portion of the Coe), and in the rock prominences which generally occur above 1200 ft. The lower slopes in the area have a thick cover of glacial debris, as mentioned above, overlain by spongy sod or peat which obscures the underlying rock to a marked degree. The steep upper slopes frequently have a cover of scree or spongy sod which mask structures. The absence of paths southward from Ballachulish is a deterrent to field work because several hours are required to get to the southern slopes of Sgorr Dhearg, Sgorr a' Choise, and Meall Mor before the day's program can be started.

In spring and fall the winds blow at such velocities it is impossible to stand up even on the lower peaks, and it is most difficult to use maps, aerial photographs, and stereographic nets except in the occasional sheltered spot. Frequent rains delay detailed field work appreciably because orientational arrows do not stick to wet specimens, plotting measurements on a stereographic net can not be done at the locality, and aerial photographs can not be used effectively. In mid-October the snows begin to fall on the slopes above 2000 ft., and until the latter part of May the three highest peaks, Sgòrr Dhearg, Beinn Fhiodha, and Sgòr nam Fiannaidh, remain snow-covered. In summer there is sufficient daylight to be out-of-doors until 10 p.m., in the late spring and fall until 7 p.m., and in early spring and late fall until 5 p.m.

2. Collection of specimens

Most of the hand-specimens collected (614 of 709) are geographically orientated, and consequently can be studied in a variety of ways. Bedding planes were selected for measurement in the field wherever possible, but sometimes cleavage planes or joint planes had to be measured because of poor exposures of bedding on the outcrop or because of insufficient space in which to maneuver the Brunton compass. The strike and dip of the measured surface were marked in colored pencil on the rock surface by using the compass rim as a straight edge, and the values recorded in field notebooks. An arrow pointing approximately to north was also sketched on the specimen with colored pencil together with the specimen number. Somewhat of a problem in the rainy high-lands was the necessity of having the rock surface perfectly dry so that the

colored pencil would adhere. Each specimen had to be wrapped carefully to prevent erasure of the orientation marks. Later the rocks were cleaned and re-marked in waterproof India ink. An index card of macroscopic details has been completed for each specimen. 27 rock specimens have been photographed to illustrate the text.

A rather crude type of universal joint was set up in the laboratory whereby specimens can be clamped and then orientated by means of the Brunton compass into their original geographic position in the field. This enabled the strike and dip of planes other than the one determined in the field to be measured reasonably accurately. These laboratory measurements have added greatly to the completeness of the bedding, cleavage, lineation, and fold maps.

3. Preparation of thin-sections

A total of 449 rocks were selected for thin-sectioning; the majority exhibit at least one foliation plane. If this foliation contained a linear structure, the specimen has been cut perpendicular to the lineation, and sometimes parallel to the foliation plane. If there were more than one lineation the specimen may have been cut perpendicular to each one. Where no linear structure was apparent, the rock has been arbitrarily cut normal to the foliation and usually normal, too, to its strike. If there was no visible foliation, the specimen has been cut normal to a joint plane and usually normal to its strike.

Some technical difficulties arose when slicing specimens to cut exactly along the line marked on them and particularly to protect the India ink system from being removed by the oil or by subsequent scrubbing to remove the oil. Sometimes a rock had to be re-cut. Every time several layers of adhesive

and sellotape were put over the inked symbols and left on until after the rock was washed to prevent erasure.

After a slice had been cut from a specimen, the side of the slice away from the top of the specimen -- the "down" side -- was ground smooth and marked with an arrow in India ink. Only half of the arrowhead and a half bar were drawn in order to indicate more readily which portion of the slice was used. The arrowhead always points to the top of the specimen. If the slice was normal to the lineation, a small "b" was drawn alongside. (Conventionally the trend of a prominent linear structure on a foliation plane is taken as megascopic reference axis "b". Reference axis "a" lies at right angles to "b" and in the same plane. Reference axis "c" is perpendicular to the "ab" plane. If there is more than one lineation, the notations "b₁", "b₂", etc. are used so that each deformation may be referred to a distinct set of coordinates.) The corresponding mate to each arrow was drawn in India ink on the cut surface of the rock. e.g. Pl. XII, Fig.3. If the rock slice was friable, it was impregnated with Gum Damar before being ground smooth.

The marked side of the slice was affixed with Canada balsam, or in difficult cases with Santolite M. H. P. or Lakeside #70 plastic, to a 2"x1" glass slide so that the arrow shaft was parallel to the edge of the slide. (Glass slides of larger dimensions are not maneuverable with the Schmidt slide on the Universal Stage). In most cases the slices were then ground very thin so that the quartz grains were gray to pale yellow under crossed nicols, never of a higher order color than first-order yellow or else the true extinction position of the grains was obscured and errors of measurement would be introduced into the petrofabric analyses. A cover glass was affixed to the section, and the specimen number and arrow were scratched on one end of the slide for permanent identification.

Each thin-section has been examined under the polarizing microscope for structure, texture, mineral content, and grain size and shape, and the data recorded on an index card. Photomicrographs have been taken of nine thin-sections. In Appendix I are listed the numbers of thin-sections which are of special interest.

C. General lithology

1. Rock types

The lithology of the Ballachulish-Glen Coe district is one of metamorphic rocks of sedimentary origin which belong to the Dalradian series of Highland Schists. They are regionally metamorphosed slate, phyllite, schists, quartzites, limestones, and marble; some have been thermally altered by the subsequent intrusion of the Ballachulish granite on the west and Glencoe granite on the east. Dikes cut across the metamorphic and igneous rocks. Although the highest peaks are quartzite and the main valley, Glen Coe, is limestone (see Map I), no definite relationship between the topography and lithology may be inferred for the lower elevations. For example, the north slope and summit of Sgorr a' Choise are slate, while the backbone of the ridge is quartzite (Pl. XVI, Fig. 1), and on Am Meall the contact between Ballachulish slate and Ballachulish limestone cuts across the summit.

2. Age of the Dalradian series

The age of the Dalradian series is in dispute. Some geologists consider it Pre-Cambrian. The Geological Survey states that the series is of uncertain age, possibly Pre-Cambrian (Read and MacGregor, 1948, p. 7). Others believe that some or all of the Dalradian is Cambrian (p. 34). Fossils, by which to date the strata, are lacking. The author found no trace of any in the field.

nor any graphite, which might indicate former organic life. The inference is that there never were any fossils in the Dalradian. The strata are either Pre-Cambrian or non-fossiliferous lower Paleozoic (pre-Caledonian).

3. Stratigraphic succession

The general stratigraphic succession of the Dalradian series has been worked out broadly for the central Grampian Highlands, but the complexity of the local successions to the northwest, southwest, and northeast has prevented their correlation with each other and with the standard Perthshire succession. One of these local "orphan" groups is the Ballachulish-Appin-Loch Eilde tectonic unit, which has been studied intensively by E.B. Bailey (1922, 1930, 1934, 1938). On the basis of Bailey's field work, with modifications by R.G. Carruthers and T. Vogt, the generally accepted succession in the Ballachulish-Glen Coe area studied by the author is as follows, in stratigraphical order with the youngest beds at the top (Read and MacGregor, 1943, p. 26):

- Appin phyllite (or mica schist), often with much flaggy quartzite
- Appin limestone, dolomitic, sometimes with central band of quartzite and phyllite
- Appin quartzite, pebbly
- Appin Striped Transition Series
- Ballachulish slate, black graphitic and pyritous
- Ballachulish limestone
 - Dark gray or black limestone
 - Calcareous and quartzose mica schist
 - Cream-colored limestone
- Leven schist
 - Pelitic series
 - Banded series (Banded Passage Beds)
- Glencoe quartzite
- Binnein schist
- Binnein quartzite
- Eilde schist

This is the sequence shown on the third edition of the geological map, Sheet and used by the writer for her geological map, Map I, on the scale of two-and-one-half inches to one mile (1:25, 000).

J. F. N. Green (1931, correlation table preceding p. 547) has arranged a very different lithologic succession by grouping together the Appin Limestone with the cream-colored Ballachulish limestone and the Leven schist with Appin phyllite, and by inferring a special type of unconformity between the dark-colored Ballachulish limestone and Appin quartzite.

The only recent workers south of Loch Leven have been W.G. Hardie (1952) who has confined his attention to the district east of Caolasnacon, adjoining the eastern margin of the area under discussion, and I.D. Muir (1953), who has studied the Ballachulish granodiorite southwest of the limits of this paper.

D. General tectonics

The tectonic picture of Dalradian distribution is even more complex than the stratigraphic picture. The principal tectonic worker in Ballachulish has also been E.B. Bailey (1910, 1914, 1922, 1934, 1938). From his field observations both here and in the Alps he has evolved an approach to highland geology which is radically different from that of his British contemporaries the concept that recumbent folding and fold-faulting (sliding) form the basis of Dalradian tectonics. Bailey "envisages recumbently folded rocks with associated slides as having been bent into secondary recumbent folds, all with gently pitching axes ... Locally, as at Loch Leven..., he infers that subsequent 'sideways' or 'twisting' movements were superimposed on this complex fold and slide system and produced in it major or minor strike-bends or strike corrugations with steeply pitching axes". (Read and MacGregor, 1998 pp. 32-3)

According to Green (1931 p.546) the structural picture is one of gentle synclines and anticlines, rather than "abnormal" large-scale structures but this interpretation is not borne out by field evidence.

Subsequent mapping in other Dalradian localities by other geologists have partly substantiated and partly modified Bailey's hypothesis. No further detailed work, however, has been published on the classic tectonic area of Ballachulish and Glen Coe. The author has undertaken to apply to this section the Wegmann (1929) technique of fold analysis, which is based on work by Argand and Lugeon in Switzerland and which is an extension of Bailey's methods. In addition, the technique of petrofabric analysis has been used to obtain microscopic structural data to compare with the macroscopic structural data.

CHAPTER II: LITHOLOGY

A. Preparation of the geology map

The lithology was mapped on six inches to one mile Ordnance Survey maps second edition (Argyllshire sheets XXX S. E., XXX S. W., XXXI S. W., XXXI N. E., XLIV N. E., and XLV N. W.), not for the purpose of re-mapping the area, but in order to understand better the rock specimens collected and their structural relationships and to check roughly the published geological map. Aerial photographs proved invaluable for verification of locality positions on lower slopes and on ridges, particularly as the six-inch maps are not contoured. Use was made of the one-inch geological map, Sheet 53, third edition, as a general guide to the section and for the lithology of precarious steep slopes around Sgorr Dhearg, Beinn Fhiodha, Sgòr na Ciche, and Sgòr nam Fiannaidh which the author did not attempt to examine.

The field data on the resultant lithologic map have been transferred to a two and one-half inches to one mile contoured map of this area (Map I). It should be noted that the lithologic pattern is in general the same as that of the one-inch geological map, with minor differences on Sgorr a' Choise, on the south slope of Sgòr nam Fiannaidh, on the east slope of Am Meall, and to the north of Glen Coe House. These modifications are due partly to the different scales of the two maps and partly to somewhat different field interpretations.

B. Characteristics of the stratigraphic succession

From a macroscopic and microscopic examination of the metamorphic hand specimens collected the characteristics of each rock formation are given below, starting with the oldest. Future mention of rock types in the text will refer

to these descriptions. The descriptive terms "massive", "blocky", "slabby", and "flaggy" are used as advocated by McKee and Weir (1953). The quantitative terms used to express grain size are: fine, less than 0.1 mm. in diameter; small, between 0.1-0.3 mm.; medium, between 0.4-0.8 mm.; large, greater than 0.9 mm. The quantitative terms describing lineation are: very fine, less than 0.1 mm. in width across a pucker; fine, between 0.1-0.2 mm.; medium, between 0.2-0.3 mm.; medium-coarse, 0.4-0.5 mm.; and coarse, greater than 0.5 mm.

Cataclastic structure is a common feature in all of the formations. It is shown by secondary twinning and gliding in the calcite of the limestones, by secondary twinning and gliding in the plagioclase porphyroblasts of the Banded Passage Beds, by bending of the mica and chlorite in Leven schist, and strain shadows in the quartz of Binnein quartzite, Binnein schist, Glencoe quartzite, Banded Passage Beds, Leven schist, and Appin quartzite.

All of the formations show recrystallization to some degree; it has occurred either broadly penecontemporaneous with deformation or continuing after deformation.

"From a physico-chemical standpoint the growth of crystals in a heterogeneous anisotropic solid medium is highly complex, and its effect correspondingly difficult to predict. Stable minerals form at the expense of minerals less stable under prevailing physical conditions in the particular chemical environment provided by the pore fluids. Moreover, individual grains of a single mineral vary in stability, so that some grains persist and develop while others are eliminated. Factors which tend to decrease stability are small grain size, irregular outline, local application of stress on the crystal surfaces, strained condition of the crystal lattice and presence of impurities within the grain concerned. In the anisotropic growth medium afforded by a rock cut by regularly oriented slip surfaces and micro-fractures, the crystallographic orientation of a grain in relation to the rock fabric is probably an important factor in determining whether the grain will survive or will be suppressed" [Turner, 1948, (2), p. 560]

Details of chemical analyses of Binnein quartzite, Appin quartzite, Ballachulish limestone, and Appin limestone which have been carried out mainly by the Geological Survey of Great Britain are given in Appendix II.

1. BINNEIN QUARTZITE

Macroscopic features (Pl. I)

Granulose; medium-grained, granoblastic; white, due to white opaque feldspar grains in glassy quartz matrix (VB230); current-bedding conspicuous (VB237); jointed; rodding and fine lineation common on bedding foliation (VB231); chemical analyses of five samples (Appendix II) show typical great purity.

Microscopic features

Thick bands of medium to small, subangular to subrounded, recrystallized quartz grains alternate with similar bands of small to tiny quartz grains and with narrow, discontinuous bands of small lath traces of muscovite, inclined to bedding foliation anywhere from 15° to 63° (VB98, 101, 107); sometimes there are a few large grains scattered throughout, with strain shadows inclined to the foliation (VB101, 231-2); or the medium-sized grains may show strain shadows and embayment of boundaries, indicating only partial recrystallization (VB107); Böhm lamellae may be conspicuous (VB232); where microfaults occur, very small attenuated quartz grains may lie along the fault planes (VB232).

2. BINNEIN SCHIST

Macroscopic features (Pl. II, Fig. 1; Pl. III)

Gneissose to schistose $\frac{1}{4}$ " - 1" bands of white quartzite, often tightly folded, are transitional to the underlying Binnein quartzite and to the overlying Glencoe quartzite (VB328); medium - to fine-grained; silvery to dark gray; biotite porphyroblasts may cross-cut the finer-grained schistose bands (VB231); lineation tends to be coarse on quartzite and fine on micaceous laminae.

Microscopic features

Bands of medium to tiny, angular, recrystallized quartz grains alternate with continuous or discontinuous bands of lath traces of muscovite (VB108, 217); in the more schistose portions the mica laths take on a herringbone pattern due to flow cleavage intersecting the original, but now folded, bedding, and the quartz is interspersed throughout this matrix (VB215, 233); large, distorted albite porphyroblasts may also occur, speckled with small secondary quartz grains having a tendency towards attenuation in a rough swirl, implying rotation (VB215), or speckled with poikiloblasts of plagioclase, quartz, and mica (VB215); the larger quartz grains frequently show strain shadows inclined to the foliation (VB217, 236-1); occasionally there are garnets enclosing small quartz grains attenuated at an angle to the foliation (VB220); the quartz bands may be composed of fine-grained layers alternating with coarser-grained layers (VB220, 363), and may be undulatory (VB220), or the bands may contain small clusters of tiny grains (VB364-2); sometimes there are small laths of chlorite scattered throughout (VB363) or large porphyroblasts of secondary biotite (VB220).

3. GLENCOE QUARTZITE

Macroscopic features (Pl. II, Fig. 2)

Granulose, locally cataclastic (VB110-2) and schistose (VB109); medium-grained, granoblastic; white to buff or gray, locally reddish where hornfelsed (VB258); gritty quartzose bands in the lower portion of the formation contain large grains of white and pink feldspar (VB238); current-bedding conspicuous (VB147, 256); jointed; lineation tends to be coarse on quartzite and fine on micaceous laminae.

Microscopic features

Thick bands of large to medium or of medium to small, subrounded to subangular, partially recrystallized quartz grains, with some strain shadows the larger grains (VB126, 219, 445) and Böhm lamellae (VB68-1, 175, 521), and with minor lath traces of muscovite and biotite inclined to the bedding foliation (VB253, 369, 525), sometimes forming discontinuous bands showing foliation cleavage (VB122, 146, 432); there may be chlorite laths, too (VB110, 292, 370-2); minor small grains of feldspar, frequently weathered, may be scattered throughout (VB110-2, 314, 523) or in discontinuous bands (VB537); occasionally there are very large albite porphyroblasts with polysynthetic twinning (VB231) which may have become sheared (VB182); sometimes albite may be turbid (VB258); sericitization may attack quartz (VB445) as well as feldspar (VB316); very large quartz grains may contain poikiloblasts of tiny quartz and mica (VB68-1, 175), and tend to fracture along rhombohedral cleavages (VB174, 254); they are frequently embayed (not recrystallized); the presence of tiny grains around them points to incipient granulitization (VB187, 221-2, 257); sometimes the thick quartz bands alternate with very narrow bands of tiny quartz (VB182, 238, 314); the bands may be undulatory with blotchy aggregates of mica aggregates (VB313); where the rock is cut by microfaults, tiny quartz grains are attenuated along the fault planes (VB125); in schistose portions two sets of micas produce an "open lace-work" pattern of lath traces (VB109, 240), in some cases bending around garnets (VB240); rarely are there small zircons (VB319, 445), large-to medium-sized calcite porphyroblasts (VB110, 298), small pyrite cubes (VB110, 123) and large porphyroblasts of biotite (VB123) and

chlorite (VB398); in the Glen Coe granite aureole the matrix of quartz and m is finer-grained, the medium to small quartz grains have been completely recrystallized (VB255); they are sometimes in discontinuous bands and lenticles (VB177), alternating with broad, mesh-like bands of tiny sericite laths, with chlorite forming from feldspar (VB177); garnet and epidote are sometimes accessory (VB187, 512-2).

4. BANDED PASSAGE BEDS (PART OF LEVEN SCHIST)

Macroscopic features (Pl. IV; V; XXX, Fig. 1)

Bands of granulose, medium-grained, granoblastic, white quartz alternate with schistose, fine-grained, blackish bands (VB513); narrow, light-colored quartzose bands become increasingly frequent in the schist as the contact with the underlying Glencoe quartzite is approached (compare VB224 and VB400); locally maculose (VB148A); flow cleavage common in schistose portions (VB224 recumbent (VB647) and isoclinal (VB448) folding conspicuous; lineation tends to be coarse on quartzite and fine on micaceous layers.

Microscopic features (Pl. VI)

Thick to thin, continuous and discontinuous bands of angular to subrounded at least partially recrystallized quartz grains alternate with thick to thin, continuous and discontinuous bands of medium to small lath traces of muscovite and biotite, often inclined a few degrees to the foliation (VB69, 565, 647); sometimes the quartz bands are segregated into narrow layers of large, medium and small grains (VB196, 563) and may be lenticular in shape (VB513, 682); the larger grains may show pressure shadows (VB149, 201) and Böhm lamellae (VB632).

sometimes the mica bands are segregated into biotite (VB195) or muscovite (VB4, 229) and often reflect false cleavage crosscutting the bedding foliation (VB229, 401, 541); occasionally biotite laths may enclose a black nucleus of magnetite (VB4); some portions contain quite a high percentage of untwinned medium to small plagioclase grains (VB682), often sericitized (VB542); very schistose portions contain enormous porphyroblasts of untwinned albite, with poikiloblasts of small, recrystallized quartz grains (VB148A), or large turbid porphyroblasts of orthoclase altering to sericite (VB403); large biotite porphyroblasts commonly crosscut the bedding foliation (VB148A, 226, 565); chlorite may be pseudomorphous after biotite (VB402, 436) and garnet (VB229); large crystals of chloritoid parallel muscovite cleavage (VB541); pyrite grains may form rough bands parallel to the bedding (VB647) or may be scattered throughout (VB150, 624); medium-sized calcite grains frequently heal microfractures (VB47, 196); rarely tiny grains of epidote (VB4) and zircon (VB436) may be scattered throughout the matrix, and occasionally a garnet (VB224); in the Ballachulish granite and Glen Coe granite aureoles the biotite is commonly altering and coloring the matrix a bright yellow (VB478).

5. LEVEN SCHIST

Macroscopic features (Pl. VIII, IX, Fig. 1)

Schistose, maculose near contact with Ballachulish limestone; fine-grained banded; silvery to green, locally black near contact with Ballachulish limestone grades from green, cleaved phyllite (VB616) to green mica schist with red garnet porphyroblasts (VB419) to silvery mica schist with biotite porphyroblasts crosscutting the foliation (VB360, 389); coarse to fine lineations on all foliation surfaces.

Microscopic features (Pl. IX, Fig. 2; X, Fig. 1)

Continuous and discontinuous bands of small mica laths (biotite, muscov and chlorite in varying proportions), sometimes marking the bedding foliation (VB455, 534), sometimes in a herringbone or open mesh pattern due to flow cleavage intersecting bedding (VB458), which has usually been folded either isoclinally (VB531) or similarly (VB407, 462), or marking false cleavage intersecting flow cleavage (VB580) or bedding (VB57-1, 287, 613); flow cleavage replaces limbs of small folds in VB419-1A; subordinate amounts of medium to small, sharply angular to subangular, recrystallized quartz occur either in intercalated bands (VB407, 456, 528,) streaks (VB207, 393), lenticles and pockets (VB209, 388-3, 676), or scattered throughout the matrix (VB359, 419) occasional large grains show strain shadows (VB393); large, recrystallized quartz occur in crosscutting quartz veinlets (VB613); large-to medium-sized calcite porphyroblasts are common near contacts with Ballachulish limestone (VB458, 702); sometimes they contain poikiloblasts of mica, quartz, and epidote (VB532) large porphyroblasts of biotite (VB62, 291, 457) and of chlorite (VB287, 461) may crosscut the foliation; accessory minerals are garnets, often undergoing incipient alteration and partly filled with poikiloblasts of small, recrystallized quartz grains attenuated parallel with the original bedding (VB62, 390, 407), epidote (VB62, 405), sometimes lying in the plane of foliation with biotite bending around the crystals and also crosscutting the foliation ca. 45° (VB458) or sometimes in irregular masses bounded by chlorite (VB389-4) magnetite (VB270A, 395), rarely ilmenite surrounded by leucoxene (VB462-2),

pyrite (VB287, 420), apatite (VB270A), fibrous needles of zoisite (VB419-2), tourmaline (VB57-1, 419-2); in some hand-specimens micas have grown secondary across parallel micas (VB702) and chlorite is replacing mica (VB270A, 702), garnet (VB532), and calcite (VB408); micaceous pseudomorphs after ottrelite be the cause of the porous appearance of large laths filled with poikiloblast quartz, mica, and zoisite (VB461A-2, 462-2); in the Glen Coe granite aureole narrow bands of feather micaceous aggregates, mainly muscovite and sericite, alternate with discontinuous narrow bands of medium to small quartz grains, sometimes crenulate (minor recrystallization), sometimes subangular (partial recrystallization) (VB530, 672, 676); secondary chlorite is common (VB207, 6 rarely with β -zoisite (VB530).

6. BALLACHULISH LIMESTONE

Macroscopic features (Pl. X, Fig. 2; XI; XII; XIII; XIV, Fig. 1)

In part, granulose, locally maculose, with garnet porphyroblasts near contact with Leven schist (VB644), to gneissose; medium-grained, granoblastic cream-colored (VB666) to blue-gray (VB454), weathered surface of both usually characteristic orange-brown color (VB416); in part, schistose to gneissose; coarse- to medium-grained, with alternating bands of calcite and of quartz; silvery to buff, greenish, or gray-blue; differential weathering produces small pits in purer portions (VB46), sometimes with ribs of mica schist (VB416); similar (VB643) and contorted (VB664) folding common; in the Glencoe granite aureole the limestone has been thermally altered to coarse-grained tremolite schists (VB271, 410), sometimes with actinolite (VB377); near the granite contact calcsilicate-hornfels has developed (VB674); coarse to fine lineatic

on all foliation surfaces; chemical analysis of one sample (Appendix II) shows up a fairly large (12%) siliceous impurity, which is to be expected from the alternation of calcareous and quartzitic bands.

Microscopic features (Pl. XIV Fig. 2)

In the purer portions, thick bands of medium to small, subangular to subrounded, partially recrystallized calcite grains, often twinned, and with subordinate amounts of medium to tiny, angular to subangular, recrystallized quartz grains and small muscovite laths both parallel and inclined to the foliation (VB130, 284, 454); the calcite bands may contain alternating layers of small grains and fine grains (VB331), and may be cross-cut by veinlets of larger grains (VB44, 504); sometimes calcite occurs in individual large grains (VB544), pockets (VB612), lenticles (VB44), and rarely in bands (VB131, 644); quartz seldom occurs in large grains with pressure shadows (VB415) and Böhm lamellae (VB130); the large grains are generally recrystallized, either healed microjoints (VB331) and veins (VB286) or filling lenticles (VB70, 454), in which case they are often poikiloblastic; lenticles or pockets of medium to small recrystallized quartz may be intercalated in a calcite matrix (VB324, 331); thick to thin bands of small muscovite laths may also be intercalated (VB576) sometimes with laths in radiating clusters (VB557), and often show false cleavage (VB331, 544, 566); biotite is much less common, it may occur as small laths (VB415), large laths in discontinuous bands (VB388), large porphyroblasts inclined to the foliation (VB576), or, rarely, in quartz veinlets (VB415); chlorite may be intergrown with mica (VB212, 644) and may even show some she

(VB212, 415), it may be pseudomorphous after garnet and mica, with poikiloblasts of quartz attenuated perpendicular to the bedding (VB644); rarely there are slivers of rutile along cleavage planes (VB644); occasionally pyrite (VB351), garnet (VB644), and large feldspar grains, with poikiloblasts of calcite and quartz (VB642), are accessory; within the Glen Coe granite aureole thick bands of small, rounded calcite grains are accompanied by long blades of actinolite, diopside, and large muscovite porphyroblasts, with very minor quartz and small muscovite laths (VB378); the calcite may also appear in attenuated aggregates of large grains, in blobs of medium-sized grains scattered throughout the matrix and in large poikiloblastic porphyroblasts together with long chlorite laths in discontinuous bands, large to small recrystallized quartz grains, and the accessories sphene (VB271) and iron-free zoisite (VB376); nearer the granite contact the calcite practically disappears (VB178), being replaced by tremolite (VB206, 410, 449), sometimes diopside (VB194, 650, 671), and epidote (VB204, 449, 675); the quartz is largely recrystallized (VB204), it often occurs in lentils and pockets of medium to small grains (VB204), perhaps attenuated parallel with the foliation (VB650), occasionally, however, the grains may have crenulate, interlocking boundaries and strain shadows (VB651); biotite may occur in tiny laths (VB204) or in fairly continuous bands of large- to medium-sized laths (VB206, 411); muscovite may be in laths (VB449) or in large porphyroblasts (VB410); chlorite is also minor (VB204, 206), replacing biotite (VB671) or in large porphyroblasts (VB674); accessory are large porphyroblasts of albicase, with poikilitic inclusions of mica (VB206), sphene (VB178), and β -zoisite (VB271, 410).

7. BALLACHULISH SLATE

Macroscopic features (Pl. XV; XVI, Fig. 1; XVII; XVIII, Fig. 1)

Schistose; fine-grained; dark gray; flow cleavage and false cleavage commonly cross-cut bedding foliation (VB55, 353); foliation surfaces often dotted with pyrite cubes (VB467); high polish on some fault planes (VB160); veins of white quartz abundant, as well as veinlets filling tension cracks along folds (VB161); locally thin bands or lenticles of quartzite (VB157) and limestone (VB158) may be intercalated; coarse to fine lineations on all foliation surfaces.

Microscopic features (Pl. XVI, Fig. 2)

Continuous and discontinuous bands of small to tiny mica folia (muscovite and biotite), frequently showing false cleavage (VB510, 519-1) and flow cleavage (VB662, 663), with folded bedding (VB203, 662); sometimes streaks and lenticles of small to tiny, subrounded to subangular, partially recrystallized, attenuated quartz grains are intercalated in mica bands (VB55, 343-1, 592-1), or narrow bands of medium to small recrystallized quartz grains alternate with mica bands (VB510); occasionally large biotite porphyroblasts are inclined to the foliation (VB510, 543, 663); crosscutting veinlets usually contain medium to small quartz grains (VB161), rarely chlorite (VB606); large calcite porphyroblasts (VB343, 447, 543), large albite porphyroblasts (VB519-1), small garnet crystals, in which tiny quartz grains are attenuated parallel with the original bedding (VB447), very rarely β -zoisite (VB543) and zircon (VB161) are accessory.

8. STRIPED TRANSITION SERIES (PART OF APPIN QUARTZITE)

Macroscopic features (Pl. XIX, Fig. 1; XXI, Fig. 2; XXII; XXIII)

Bands of granulose, medium-grained, granoblastic, white quartzite alternate with bands of schistose, fine-grained, black slate; narrow slaty bands become increasingly frequent in the quartzite as the contact with the underlying Ballachulish slate is approached (compare VB75 and 607); foliation may be defined with pyrite cubes (VB348, 591); flow cleavage common in slaty portion; original bedding may appear as color bands on cleavage (VB469); tension fractures may be healed with white quartz (VB587); recumbent folding on the scale of a few inches to 20 feet in width often occurs; graded bedding may be conspicuous (VB277); lineation tends to be coarser on the quartzite and finer on the slate.

Microscopic features (Pl. XIX, Fig. 2; XX; XXI, Fig. 1)

Thick to thin, continuous and discontinuous bands of medium to small, subangular to subrounded, partially recrystallized quartz grains alternate with thick to thin, continuous and discontinuous bands of small to tiny mica laths and medium to tiny, partially recrystallized quartz grains (VB121, 268, 472); the mica laths are frequently in clusters, sometimes outlining individual quartz grains (VB36, 303, 472), the laths reflect false cleavage (VB40, 354, 503) and flow cleavage (VB609, 688) crosscutting the bedding foliation; the larger quartz grains are often embayed (not recrystallized) and show strain shadows (VB277, 337, 347) and Bøhm lamellae (VB75, 95, 115); large recrystallized grains form microjoints (VB115, 309) or form lenticles or pockets in a finer-grained matrix (VB75, 275, 573) due to cataclasis of original very large grains; discontinuous bands of weathered biotite (VB573-2, 593) and chlorite (VB688) appear in rock which flow cleavage crosscuts the bedding, occasionally there are large biotite

porphyroblasts inclined to the foliation (VB569); other micas may bend around them (VB503); abundant small recrystallized grains of microcline and plagioclase are scattered throughout, with a few large grains partly sericitized (VB75, 347); pyrite occurs as elongate grains roughly parallel with the foliation (VB428, 472), as "ghost" cubes filled with quartz (VB486), or as irregular grains (VB33) or tiny cubes (VB113, 142) scattered throughout the matrix; calcite and dolomite occur in subordinate amounts in the matrix in large to small grains, ^{angular} subrounded, attenuated, sometimes twinned (VB24, 22, 335), or healing microjoints (VB42); more rarely small grains of zircon (VB23A, 367-2, 468) and tourmaline (VB24, 569) are accessory.

9. APPIN QUARTZITE

Macroscopic features (Pl. XXIV; XXV; XXX, Figs. 2, 3)

Granulose, locally cataclastic (VB266); coarse- to medium-grained, granoblastic; white to buff; pebbly nature due to high proportion of large grains of pink feldspar in a finer-grained glassy matrix of white quartz (VB266); current-bedding (VB31) and graded-bedding (VB303) are present locally; joint lineation tends to be coarse on quartzite and fine on micaceous laminae; chemical analyses of two samples (Appendix II) show the great purity of this formation when feldspar is a minor constituent.

Microscopic features

Large to medium or small, subangular to subrounded, largely recrystallized quartz grains (VB136) occur in thick bands, sometimes with narrow intercalated mica bands, which may contain small quartz grains (VB117, 141-1) or alternate with narrow bands of tiny quartz grains (VB52, 83); frequently there are str

shadows (VB27, 60, 80) and Böhm lamellae (VB16, 82, 488) in the larger quartz grains, also embayed outlines (no recrystallization) (VB488) and poikiloblasts of tiny quartz (VB27) and mica (VB31, 263-1), rhombohedral cleavage may be conspicuous (VB266); plagioclase often occurs in subordinate amounts as large to small, twinned, subrounded grains (VB133, 514-1), or in large microperthite grains (VB60); where cataclasis is partially developed, there are pockets of large-to medium-sized quartz grains in a matrix of small to tiny quartz grains (VB133, 306, 355), or medium to tiny grains may bound the larger grains (VB263-2, 303); the micas may be in discontinuous bands (VB604-1) or as individual laths scattered throughout the matrix (VB27, 53, 514-1); occasional large blobs of calcite filling microjoints (VB52), medium-sized calcite porphyroblasts (VB118, 133, 345), and pyrite cubes (VB16, 60, 117) occur; in the Ballachulish granite aureole bands of small quartz grains alternate with bands of medium-sized grains and occasionally with bands of large grains (VB263-1); there has been partial recrystallization; Böhm lamellae and pre-shadows are prominent in the larger grains (VB263-1); pyrite is abundant throughout (VB636).

10. APPIN LIMESTONE

Macroscopic features (Pl. XXVI)

Granulose; coarse- to medium-grained, locally fine-grained marble (VB1), granoblastic to banded; cream-colored (VB87) to pink (VB621), locally green purple (VB500); may contain folded micaceous bands (VB357, 617) or show flow folding well (VB693); narrow veinlets of quartz (VB87) or calcite (VB346-1) may heal joints; lineation tends to be coarse on limestone and fine on mica.

laminae; the contrast in silica content (1.70%-25.88%) in the chemical analysis of four samples (Appendix II) indicates very well the variation in purity.

Microscopic features

Closely-knit fabric of tiny, subangular to subrounded, recrystallized calcite grains, with subordinate, small, subangular, recrystallized quartz grains scattered throughout (VB356, 362-1, 600); crosscutting veinlets contain large recrystallized grains of quartz and calcite (VB87); sometimes tiny laths of muscovite are scattered throughout, they may be parallel with or inclined to foliation; the calcite is frequently twinned, especially the larger grains, occasionally narrow bands of calcite alternate with narrow bands of quartz; grain size tends to increase markedly over that of the matrix (VB357), rarely there are lenticles of coarse-grained calcite rather than bands (VB346); where quartz is absent, the calcite tends to be very large (VB281, 282) and twinned with irregular embayed boundaries (probably not recrystallized) (VB440, 489); the Ballachulish granite aureole diopside has developed in clusters of tiny grains at the expense of the calcite (VB494, 499, 500); sometimes there are still small calcite grains in a ratio of 1:1 with small quartz, and with large porphyroblasts of calcite scattered throughout (VB496), or, in the absence of quartz, medium small calcite grains may be scattered among the diopside (VB502), occasionally rough bands of quartz and calcite alternate with bands of calcite and diopside (VB697); pyrite and sphene (VB493) are minor accessories.

11. APPIN PHYLLITE

Macroscopic features (Pl. XXVII; XXVIII, Fig. 2; XXX, Fig. 4)

In part, schistose, maculose locally (VB628); fine-grained; silvery to purple; flow cleavage common, with original bedding appearing as color bands and cleavage (VB89, 695); in part, gneissose, with $\frac{1}{2}$ "-2" thick quartzite bands

intercalated in phyllite; fine- to medium-grained (VB259); silvery (VB598) greenish (VB685) or purple (VB696), locally dark gray where hornfelsed (VB7) thrusting may cut out limbs of folds (VB687); coarse to fine lineations on foliation surfaces.

Microscopic features (Pl. XXVIII, Fig. 1)

Narrow, continuous and discontinuous bands of small to tiny mica laths alternate with bands of medium, small, and tiny quartz grains (VB5, 88, 312) sometimes attenuated parallel with the foliation (VB601, 684, 692); micaceous bands may show false cleavage (VB5, 18, 422) and may be composed of muscovite, sericite, biotite, and chlorite in varying amounts (VB361, 686, 690); quartz generally subangular to subrounded and partially recrystallized (VB311, 699) in the upper reaches of the River Laroch crenulate boundaries (VB91, 338) and strain shadows (VB338, 685) indicate incipient recrystallization, occasional there are pockets of larger grains in a finer-grained matrix (VB18, 628) or pockets of tiny grains in a coarse-grained matrix (VB709) due to cataclasis; large grains of secondary, recrystallized quartz fill cavities and heal microfractures (VB5, 88, 339); porphyroblasts of biotite (VB556, 700) and rarely garnet (VB5), scapolite (VB629), kyanite (?) (VB311, 709), diopside (VB629, 683, 685), tremolite (?) (VB699), rutile (?) (VB630), and cordierite (VB628) may also occur; chlorite may be pseudomorphous after mica sometimes parallel with and sometimes cross-cutting the foliation (VB690); small plagioclase grains may occur in minor amounts (VB93, 685) or may make up a third of the matrix (VB490); large to medium-sized calcite grains may be present in blotches (VB341, 686), in an occasional band with diopside (VB683) or with quartz (VB422, 602, 630), or heal microjoints (VB18, 91); small grains of pyrite (VB361, 427, 601) and zircon (VB88, 630) may be scattered throughout

the matrix; near the Ballachulish granite contact quartz may be completely absent, in its place are large, twinned porphyroblasts of cordierite in a fine grained matrix of cordierite (VB556), the large cordierites contain poikiloblasts of spinel (VB560) or tourmaline and mica (VB556); there may be narrow bands of sericitized albite (VB560); other accessories may be andalusite (VB556, 560), magnetite (VB556, 560), sillimanite (VB 560), and corundum (VB560); where quartz is present, it is associated with poikilitic plates of orthoclase, large medium-sized grains of poikiloblastic albite, and large to tiny biotite lath (VB7-1).

CHAPTER III: TECTONICS -- PLANAR STRUCTURES

A. Collection of field data

At each outcrop the general lithology and structure were first ascertained. Where the crop was partially obscured, excavation through a cover of peaty sod, or occasionally scree, was necessary. Planar measurements were made with a Brunton compass. Sometimes adjacent rock had to be chipped away to make room for the compass. If a hand-specimen was desired, the portion of strata already bearing the pencil lines was chiseled out, and the approximate north arrow and specimen number added to it, as described in the Introduction, Chapter I.

If the bedding was not folded, one or two readings of bedding strike and dip sufficed. Usually, however, the rocks were bent into broad, open folds or into tighter, isoclinal folds. Then the fold axis direction and plunge had to be determined. Sometimes the axis was exposed and could be measured directly with the Brunton. Otherwise successive measurements of the bedding were taken across both limbs of a fold, poles to these surfaces were plotted on a Wulff stereonet, and the fold axis constructed normal to the zone in which these poles lay (Wegmann, 1929). This procedure is described in detail under linear structures.

Bedding was frequently difficult to trace in very massive quartzites like the Appin and Glencoe; prominent flat surfaces were usually joint planes. Sometimes only the joints could be measured in the field; the bedding had to be determined later in the laboratory by re-orienting the specimen in the universal clamp and measuring with the Brunton. In a few cases the bedding was not determinable even in the laboratory.

In slate, phyllite, and schists the prominent surfaces were often flow cleavage planes or, less often, false cleavages. Laboratory re-orientation of such specimens has usually enabled measurements of bedding, additional cleavages, and joints to be made.

The presence of lineations, slickensides, joints, and faults was noted at each outcrop. If any of these features was conspicuous on a small-scale, a specimen was collected for further detailed examination in the laboratory.

B. Description of planar structures

The tectonic detail for Ballachulish and Glen Coe may be divided into three categories: one-dimensional (linear) structures, two-dimensional (planar) structures, and three-dimensional (folded) structures. For convenience the linear structures will be discussed last.

1. Primary Planar Structures

a. Bedding

Bedding is well-preserved in the quartzose strata transitional to slate and schist (Pl.V, Fig. 1; XXI, Fig.2) and generally in the rather thick-bedded Appin, Glencoe, and Binnein quartzites (Pl.I; II, Fig.2; XXIV, Fig.1). However, in some places on Sgorr Dhearg, Sgorr a' Chose, and in Allt an t-Sil the massiveness of the quartzite masks the bedding and makes its determination quite difficult.

Graded bedding occurs in the Appin quartzite and Striped Transition Series of Beinn Bhàn and Allt a' Coire Riabhach and in the Glencoe quartzite on Sgor nam Fiannaidh. On Beinn Bhàn thick layers of mottled quartzite alternate with thinner layers of streaked quartzite. The mottling is due to the high content of feldspar. A typical specimen is shown in Pl.XXIV, Fig. 2. The

upper portion consists of a fine-grained band 1 cm. thick of colorless, translucent quartz and pink opaque microcline grains 0.5-1 mm. in diameter. Below this is a coarser-grained band, 5.5 cm. thick, with both the quartz and feldspar grains increasing in diameter from 1 mm. at the top to 3-4 mm. at bottom of the band. Below this is an extremely fine-grained band, 1.5 cm. thick in which the streakiness is due to the bedding alignment of tiny feldspar grains in a very fine quartz matrix. This band is followed by another coarse-grained band 0.7 cm. thick.

The localities of graded bedding particularly noted in the field are tabulated in Appendix III.

Current bedding is conspicuous in the Binnein (Pl. I, Fig. 1) and Glen quartzites, but less prevalent in the Appin quartzite. The strata are the right way up in all cases but one, the latter possibly being an infold. The instances examined by the author are tabulated in Appendix III.

Bedding in the schistose rocks can be determined only very near their contacts with quartzite or from a series of intercalated bands of different compositions (Pl. II, Fig. 1; XI, Fig. 3; XII, Figs. 2, 3; XXVII, Fig. 2), slate, phyllite, and schist cleave so readily. In Appin phyllite (Pl. XXVI, Fig. 1) and in Ballachulish slate (VB353) bedding often appears as color bands on flow cleavage or false cleavage. In the fine-grained rocks bedding may only appear conclusively in thin-section.

b. Map II: Strike and dip of bedding

The majority of bedding strike and dip measurements (1212 out of 1600) are plotted on Map II. As a whole, the strike pattern reflects the pattern of the lithologic contacts. The general trend from Meall a' Chaolais and Sgorr Dhearg eastwards to the River Coe is north-northeast-south-southwest

with local modifications due to medium-scale plunging folds, such as on the north slope of Meall Mor (099567), and to large-scale plunging folded structures, such as the Beinn Bhan syncline (067573) (see aerial photograph, Pl. XXXIII). The general strike trend on the Sgòr na Ciche-Sgòr nam Fiannaidh range is northwest-southeast, with local modifications due to medium-scale, fairly steeply plunging folds, such as in the shore outcrop at Camas Calltui (102599) (Pl. XXI, Fig. 2), or due to more gently plunging recumbent folds, such as those on the north spur of Sgòr nam Fiannaidh (Pl. I, Fig. 2).

The directions of dip make a much more complicated pattern than the strikes and are not entirely reliable for inferring synforms and antiforms from the map. For example, within the Leven Banded Passage Beds outcrop on the northern slope of Meall a' Chaolais (055588) the most numerous dips are 80° or more. The directions of approximately a third are northwest and of about two-thirds southeast. But these opposing directions are not neatly confined to certain parts of the Leven outcrop; rather, they are scattered over it, with the result that an 88° N.W. dip may be adjacent to an 83° S.E. dip. In the field (e.g. at Loc. 371, 062589) it is apparent that the bedding planes are nearly vertical, but warped into swells and swales. It depends on where the measurements are taken on these undulating surfaces whether the dip will be northwest or southeast. In other words, the limbs of the regional folds are themselves broadly plicated.

A further difficulty in inferring structural features from the direction of dip on the map is due to the frequent recumbent nature of the folds in the area. Two symbols with the same direction of dip and with roughly the same amount of dip may be either part of the same limb of a regional fold or on opposite limbs of a fold, in which case the beds in one limb are right way up

and in the other are upside down. Actually Map II must be used in conjunction with Map III (cleavage) to determine the directions of "younging" (Bailey's term, 1934, p.469) of the beds (see Wilson, 1946, pp. 269-271, and Text-fig.

The amounts of dip on Map II are not significant by themselves. With gradations between recumbent folds and steeply plunging folds the amounts vary from 9° to 90° .

Major tectonic features can be discerned, however, from the strikes and dips -- such as the aforementioned Beinn Bhan syncline (067573), with its outer rim of Appin Striped Transition Series and quartzite and its core of Appin limestone and Appin phyllite. The strike changes from northeast on Meall a' Chaolais to almost east in Allt Giubhsachain to northwest on the northern slopes of Beinn Bhan to northeast again on the southeastern slopes of Beinn Bhan; the dips in general point into the center of the structure. The amount of dip varies from 52° to 80° on the rim, and from 17° to 39° nearer the center.

In like manner an antiform in the backbone of Sgorr a' Choise with a synform nearer the summit can be inferred, but the "obvious" anticline on the southeastern shoulder of Sgorr Dhearg referred to by Bailey (1916, p.47) is not apparent. Tectonically Meall Mor should be the crest of an anticline. If so, the structure is gently plunging and recumbent, for the bedding strikes are almost without exception northeast-southwest, and the dips northwest. A feature which does show up quite well is the synclinal nature of the slate outcrop west of Am Meall (090575).

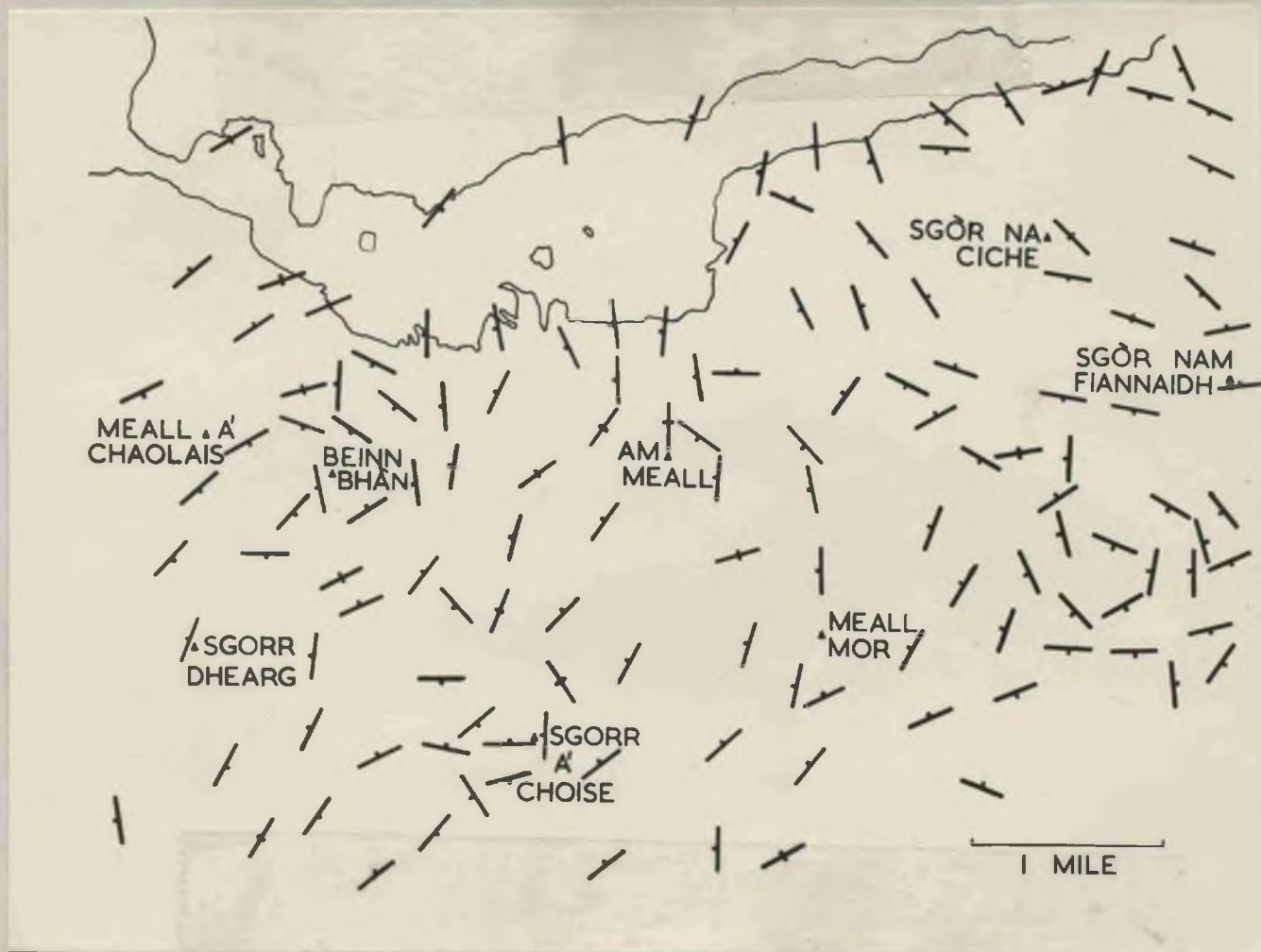
No particular structure can be inferred on Sgorr na Ciche and Sgorr nam Fiannaidh. On the whole the Glencoe quartzite dips steeply (from

43° S.W. to 90° to 72° N.E.; see Pl. II, Fig. 2) -- another instance of warping of near-vertical bedding on a regional scale. This shows very well in the exposed eastern side of the peak of Sgor na Ciche. The regularity of the northwest-southeast trend of the surface outcrops (as opposed to Beinn Bhan, for example) is excellently indicated on the aerial photograph, Pl. XXXI. The structural relations west of Caolasnacon perplex Bailey, too (1934, pp. 484-485):

"The Pap of Glencoe outcrop of quartzite is about $1\frac{1}{2}$ miles broad. This entails a prodigious thickness for the group unless there is some reduplication by folding, such indeed as is indicated by bifurcation of the outcrop not far north of the loch. On the other hand, current-bedding is abundantly displayed in the road-cuttings across the outcrop south of the loch, and gives no indication of folding other than that due to slip at the time of sedimentation. Presumably, sliding has suppressed one or more return limbs".

As the multitude of symbols and dip values on Map II tends to obscure the main bedding trends, the most dominant strikes and dips have been picked out to give a schematic representation of the structural relations in Ballachulish and Glen Coe (Text-fig. 2). From left to right the following major features may be seen: (1) the southwest-plunging Beinn Bhan syncline flanked by near-vertical beds, (2) the southwest-plunging Sgorr a' Choise synform similarly flanked and separated from the former by (3) a less well-defined antiform east and southeast of Sgorr Dhearg, (4) the ill-defined southwest-plunging Am Meall and Meall Mor antiforms separated by a synform, (5) the disrupted pattern south of Sgor nam Fiannaidh due to the intrusion of the Glencoe granite, and (6) the northwest-southeast-trending regional limb of Sgor na Ciche and Sgor nam Fiannaidh.

The igneous rocks are outside the scope of this thesis, and so flow banding, another primary planar structure, has not been studied.



Text-figure 2. Schematic representation of bedding strikes adapted from Mac...
 Long bar of symbol is the predominant strike, short bar is the direction of
 dip, cross-bar means beds are essentially vertical.

2. Secondary planar structures

a. Foliation

(1) Terminology

The words "foliation", "schistosity", and "cleavage" have been used in many different ways to describe metamorphic rocks. They are employed by the author as defined below.

Foliation is a descriptive term for ".... a more or less pronounced aggregation of particular constituent minerals of the metamorphosed rock in lenticles or streaks or inconstant bands, often very rich in some one mineral and contrasting with continuous lenticles or streaks rich in other minerals" (Harker, 1939, p.203).

Schistosity is a generic term for the tendency to a common parallel orientation of the crystal elements perpendicular to the direction of orogenic pressure (Harker, 1939, p. 194):

"....Cleavage is the ability of a rock to part along certain parallel planes, regardless of the nature and origin of these planes (Kvale, 1948, p. 15).

Thus, these three terms are not strictly synonymous, but describe interrelated phenomena which usually grade into one another: (a) a parallelism of minerals, (b) a general tendency for an infinite number of parallel planes to develop throughout a rock due to the parallelism of minerals, and (c) parting along these parallel planes.

(2) Types of foliation

The most common type of foliation in Ballachulish and Glen Coe is bedding foliation, due to "recrystallization in situ of grains, particularly mica, which had an initial arrangement parallel to the bedding at the time of

deposition" (Fairbairn, 1935, p. 592). This is characteristic of the Appin, Glencoe, and Binnein quartzites and of the transitional strata. It can be determined less readily in the pelitic schists, limestones, slate, and phyllite. (The bedding strikes and dips which appear on Map II were generally measured on bedding foliation in the field).

The second type of foliation is due to recrystallization of grains as the result of shortening and elongation of the rock mass during rock flowage. This has been followed by the development of flow cleavage, which is discussed below.

A third type of foliation is due also to recrystallization of grains, but it differs from the second by resulting from shearing between beds after their consolidation (Fairbairn, 1935, p. 592). False cleavage has thus developed; it is discussed after flow cleavage.

Consequently a foliation surface in a hand specimen may be a bedding plane, a flow cleavage plane, or a false cleavage plane. Great care has been taken to differentiate between them in preparing the bedding, cleavage, and lineation maps (Maps II, III, IV).

b. Cleavage

(1) Flow cleavage

(a) Characteristics

All of the lithologic formations except the Binnein, Glencoe, and Appin quartzites contain good examples of flow cleavage, that is, the mineral constituents are arranged in a parallel pattern which is both dimensional and crystallographic, and the rocks have a capacity to part along an infinite number of planes parallel with this pattern. In Appin phyllite (Pl. XXVII, Fig. 1), Ballachulish slate, Leven schist, and Binnein schist the mica

grains are arranged with their bases (i.e. the plane of their greatest and mean dimensions) parallel or nearly parallel with the plane of cleavage -- plane-parallel flow cleavage (Leith, 1905, p. 25). In thin-sections cut parallel with the flow cleavage (VB628) mica is generally in small, angular cleavage sections or radiating, irregular masses of tiny cleavage laths. Sometimes there is a tendency towards parallelism of the crystals within the cleavage plane.

In thin-sections cut perpendicular to flow cleavage and to linear structures in the cleavage plane mica occurs in roughly parallel, continuous or discontinuous bands of small lath traces (Pl. IX, Fig. 2). Sometimes the mica laminae bend around more rigid minerals, such as epidote (VB458) and garnet, or develop along the margins of other minerals, such as quartz (VB573-2), or are broken due to subsequent microfolding and microfaulting. Frequently a series of laths feathers out diagonally one against another as the result of rotation due to changing stresses (VB458). "...The longer diameters or direction of growth of particles developing by recrystallization at any instant normal to the greatest pressure do not quite correspond with the longer diameters or direction of growth of particles developed by crystallization in preceding instants, for these latter have been rotated from the most favourable positions...". (Leith, 1905, p. 114). Biotite often occurs as large porphyroblasts lying at almost any angle with the flow cleavage (VB62). This indicates that it developed later than the deformation producing the flow cleavage.

In the thermally metamorphosed Ballachulish limestone actinolite and tremolite are generally arranged with their longest dimension in the plane

the flow cleavage but the crystals are rarely parallel with each other in this plane (VB379, 383). In the cases of radiating aggregates the crystals lying in the cleavage plane are better developed than those cross-cutting the plane.

Quartz usually occurs in small, angular to subangular (i.e. recrystallized) grains attenuated in the plane of flow cleavage -- a dimensional parallelism. Crystallographic parallelism is not readily apparent from thin-sections, but petrofabric analyses of the orientation of quartz optic axes in 59 rocks reveal an aggregation of the "c"-axes in girdles (see contoured diagrams 1-6, Pl. XXXIV).

Lines of inclusions, generally small, attenuated quartz grains, in garnet (VB407, Pl. IX, Fig. 2) and in calcite (VB458) are sometimes inclined as much as 90° to the plane of flow cleavage. This is an indication that these porphyroblasts were growing while the rock was being deformed, i.e. while the principal minerals were recrystallizing into parallel alignment in flow cleavage planes.

The positions of quartz, feldspar, calcite, garnet, ottrelite, chlorite and andalusite have had much less influence upon the development of good flow cleavage than mica and amphibole.

The flow cleavage planes are numerous and closely-spaced, "... being separated only by the mineral particles or even by the cleavage plates of the mineral particles. The parting is usually parallel to one plane... The structure is developed in planes or lines parallel to the greatest elongation

of the rock mass, usually with the same relations to pressure that the elongation of the rock bears" (Leith, 1905, p.125).

(b) Relation of flow cleavage to bedding and folding

Flow cleavage may be parallel to the bedding, in which case it is impossible to differentiate between the two in hand-specimen, or, as is more usually the case, it may cross-cut the bedding at any angle from a degree or two to 90° (Pl. IX, Fig. 1; X, Fig. 2). One locality brings out the cross-cutting relationship very well. In the bed of a small stream on the north-east slope of Sgorr a' Choise (083561) the phyllitic Ballachulish limestone is being eroded along the bedding planes (strike 17° , dip 53° S.E.). In a pot in the stream bed the limestone is being eroded along the flow cleavage plane (strike 43° , dip 73° N.W.). This has given rise to an apparently unconformable "contact" within the formation.

Flow cleavage frequently parallels the axial plane of a fold, and usually occurs in relatively fine-grained rocks which show a low grade of metamorphism (Fairbairn, 1935, p. 607). There are several examples in Ballachulish and Glen Coe. The flow cleavage in Pl. XXVI, Fig. 2, is parallel with the axial plane of the small fold in Appin marble, and shows up as a series of lines across the fold parallelling the fold axis. In Pl. XV, Fig. 1, coarse lineation in Ballachulish slate marks the trace of a succession of planes parallelling the axial planes of the innumerable plications into which the bedding has been folded.

On a larger scale, the folds in Appin phyllite exposed on the north spur of Sgorr Dhearg (Text - fig. 4) are cut across their apices by cleavage planes parallel with the axial planes of the folds.

Relict bedding in Leven schist which has been folded isoclinally on a small scale occurs on the south slope of Meall Mor (VB417) and in the River (VB407, Pl. IX, Figs. 1 and 2). The bedding is roughly perpendicular to the flow cleavage, which is also an axial plane cleavage.

(c) Map III: Strike and dip of flow cleavage

All measurements (127) of flow cleavage strike and dip are plotted in red on Map III. In the southern part of the area the general trend is north-east-southwest, swinging to north-northeast-south-southwest and to north-south, and even to north-northwest-south-southeast along Loch Leven. These trends are roughly parallel with the regional fold axes (see Chapter V, B and Map V). The cleavage frequently cross-cuts the lithologic contacts at large angles, e.g. along the nose of the Beinn Ehan syncline (070580) and on the northern slope of Meall Mor (100565); in these cases it necessarily cross-cuts the bedding strikes, too (see Map II). Sometimes the cleavage parallels the lithologic contacts and bedding strikes, e.g. along Gleann an Fhiod (075560) and Gleann Leac-na-muidhe (110550).

About 90% of the directions of dip are northwest or southeast (in contrast to the variable bedding dip directions). The amount of dip varies from 15° to 90° , but the mean is around 60° . The distribution of dips indicates that the axial planes of the regional folds dip westerly and that the folds are recumbent towards the east.

(d) Origin of flow cleavage

Mead (1940, p. 1016) gives a lucid description of the development of flow cleavage:

"Flow cleavage is not initiated until the limits of intergranular plasticity are approached, which means that it may not make its appearance until the later stages of folding and thus escapes the distortion and change in orientation that would have been necessary had it developed in the early stages of folding.

"...As folding proceeds by interatomic plasticity and the development of flow cleavage, interatomic plasticity is progressively diminished. Dynamic metamorphism of shales involves changes in composition, both chemical and mineralogical, and develops a slate or a schist less interatomically plastic than the parent-rock. Just as a limit of intergranular plasticity is reached by consolidation, a limit of interatomic plasticity is approached by metamorphism".

There are seven hypotheses on the origin of flow cleavage, (Swanson, 1941, pp. 1248-1249):

"(1) Flattening of grains or portions of the rock mass by differential pressure; (2) solution at points where the differential stress is greatest and deposition where it is least; (3) growth of new minerals along planes of weakness, such as joints or bedding planes, the new minerals being oriented with respect to these planes; (4) growth of new minerals along planes where the supply of material is abundant such as bedding planes or joints serving as channelways for solutions either aqueous or aqueo-igneous, the new minerals again being oriented with respect to these planes; (5) rotation of elongated or platy minerals into a common plane by movement during deformation...; (6) gliding of mineral grains along preferred crystallographic directions in the mineral and along one or more shear planes in the rock, a process similar to that which develops oriented fabrics in the plastic deformation of some metals; and (7) growth of new minerals in such a way that their longest dimensions and cleavages lie in planes normal to the direction of greatest stress".

The first two hypotheses would produce dimensional parallelism but no crystallographic parallelism. The second two hypotheses may explain false cleavage (discussed in detail below), more particularly fracture cleavage, and gneissic structures, but banding is not characteristic of flow cleavage. (5) and (6) are components of the movement hypothesis, and (7) is the recrystallization hypothesis. Two schools of thought have developed from these two major ideas.

The recrystallization school regards metamorphic recrystallization

"....as a contrivance for minimizing the internal stresses which are in existence during recrystallization... The presence of a large differential stress causes tabular or elongated grains of certain minerals (such as mica and chlorite) to form in planes normal to the greatest stress. This relation, aided by the fact that the minerals have cleavages parallel to their larger faces, causes flow cleavage. The presence of shearing stress also affects, adversely or favourably, the stability of different minerals and we may recognize a group of minerals, called stress minerals, whose crystallization seems to be favored by shearing stress.

"Mechanical processes, such as slicing, granulation, and gliding, contribute toward the development of schistosity but do not constitute the main orienting agent nor do they explain the development of new and characteristic minerals. Their effects become progressively less important as the reconstruction of the rock by crystallization proceeds" (Swanson, 1941, p.1250).

The Sander or movement school regards all ordered arrangements of rock fabric as a response to the vectors of movement (Knopf and Ingerson, 1938, p.

"Some tectonite fabrics (i.e. those caused by rock flowage)... can be interpreted as the result of grain gliding, or a combination of grain gliding and movement of rigid grains in a flowing medium. Others can be explained by a combination of rupture and of recrystallization from seeds whose position was determined by the orienting influences. Still other tectonite fabrics, mimetically crystallized, owe their preferred orientation to a post-tectonic crystallization, which records the plan of the deformational movement, even intensifying it in some rocks" (Knopf and Ingerson, 1938, p. 179).

The author considers that the development of new minerals such as mica, actinolite, and tremolite in the pelitic and calcareous rocks of Ballachulish Glen Coe supports the recrystallization hypothesis more than the movement hypothesis in accounting for the northeast-trending flow cleavage of the area.

Swanson (1941, p.1258) makes out a good case against the movement hypothesis on the origin of flow cleavage in discussing the deformation shown by a cross section of a simple fold:

"...Regardless of how the movement planes are oriented with respect to the fold, the amount of movement must be greater on the limbs than the crest of a fold, it must be greater in any one place on a fold if fold is closed than if it is open, and it must vary with the relative thicknesses of the competent and the incompetent beds that are involved.

Certainly the flow cleavage pattern (Map III) in Ballachulish and Glen Coe does not show systematic differences that might reasonably be expected if the movement hypothesis were the dominant cause of flow cleavage.

Moreover, at the crest of a simple fold slipping between beds is at a minimum. "The direction of greatest elongation is perpendicular to the bedding and its amount is shown by the thickening of the incompetent bed" (Swanson, p.1258). The author agrees with Swanson that the amount of strain involved could not cause rotation, twinning, and gliding sufficient to develop the high degree of mineral orientation that is characteristic of flow cleavage in slaty beds. This is borne out by a study of several series of thin-sections cut normal to fold axes in Ballachulish and Glen Coe, e.g. VB115a, b, c from the Striped Transition Series and VB131a, b, c, d from the Ballachulish limestone. The dimensional orientation of the quartz in these slides is parallel with the bedding foliation; if flow cleavage had developed parallel with the axial planes of the folds, the quartz would be attenuated parallel with the cleavage.

As for the recrystallization hypothesis itself,

"there is no reason for believing that the oriented growth of minerals under the influence of differential stress requires a great amount of distortion or even a great amount of differential stress. Many examples are known where an oriented crystal growth has taken place under the influence of what were apparently only minor stress differences. Also across the crest of a simple fold the stress condition is essentially uniform, consisting largely of compression normal to the axial plane, together with more or less hydrostatic pressure. Such a stress condition would account for the uniform character and attitude of flow cleavage in the vicinity of the crests of folds" (Swanson, 1941, p.1259).

(2) False cleavage, including fracture cleavage

(a) Characteristics

The term "false cleavage" is used in this paper to include the varieties of cleavage due to "... low coherence of the rock across individually distinct planes of structural weakness, especially shearing planes". (Hills, 1943, p. 97). In contrast with flow cleavage the number of planes along which a rock will split is decidedly^d limited, and the fissility of the rock is correspondingly less perfect. False cleavage may be caused by closely-spaced shear planes, closely-spaced joint planes, axial planes of weakness in microfolds and small macrofolds, and attenuated limbs of very small-scale folds which, under continued stress, may finally become small-scale reverse faults.

Where fracture has actually occurred, the term "fracture cleavage", as used by Leith (1905, p. 119), is a more precise description. Leith defines fracture cleavage as

"...a cleavage dependent for its existence on the development of incipient parallel fractures or actual fractures which by subsequent welding or cementation remain planes of weakness...Rocks may be fractured along parallel planes quite independently of any arrangement which the mineral constituents may have, and the fractures may be cemented by infiltration of foreign material, by crystallization of new minerals, and by recrystallization of adjacent minerals, or may be welded by bringing adjacent minerals by compression under bonds of molecular attraction".

The most common instances of false cleavage in Ballachulish and Glen Coe are those in which actual fracturing has not occurred, for example the minute crenulations on bedding in Appin Striped Transition Series (VB40, Pl. XXI, Fig. 1), Leven schist (VB57), and Ballachulish limestone (VB416, Pl. XII, Fig. 2) or on flow cleavage in Leven schist (VB462, Pl. X, Fig. 1). The crenulations are regular but unsymmetrical microfolds,

which tend to yield differentially along one limb. This produces a series of nearly parallel shear planes. "Between each pair of shear planes sigmoidal folds are developed on a microscopic scale, and the outlimbs of each minute fold merge tangentially into the shear planes". (Holmes, 1930, pp.378-379). The mica near these shear planes has become oriented nearly parallel with them. Characteristically the false cleavage does not extend into the more quartzose bands in the schists, phyllite, slate, and transitional beds. In the massive formations false cleavage occurs in the thin micaceous films between quartzite layers.

The polished surface of VB692, Appin phyllite (Pl. XXVII, Fig. 2), shows well the false cleavage developing from small-scale asymmetrical folding in alternating layers of quartz and mica. In VB687, Appin phyllite (Pl. XXVIII, Fig. 2), thrusting along one limb of a fold has produced a false cleavage.

Closely-spaced joints have also produced false cleavage, actually a fracture cleavage. On a small-scale a series of tension fractures occur on the summit of Sgorr a' Choise which has been healed subsequently by very narrow veinlets of white quartz (VB586, Appin Striped Transition Series). On a larger scale the closely-spaced joints in the shatter belt of Appin quartzite at the summit of Meall a' Chaolais are probably due to fracture cleavage.

(b) Relation of false cleavage to bedding, flow cleavage, and folding

False cleavage may cut bedding and flow cleavage at any angle; frequently the angle is greater than 55° . An exposure of Leven schist in the stream bed in upper Gleann Leac-na-muidhe (Loc.738,105543) shows

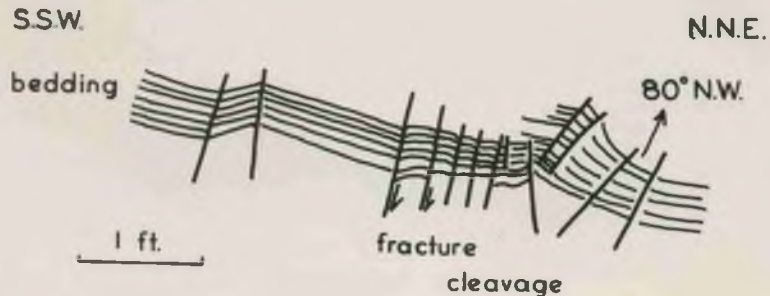
very well a series of fracture cleavage planes cutting the bedding at high angles (Text - fig. 3).

On the north spur of Sgorr Dhearg (Loc. 13,056572), for example, the bedding of Appin phyllite has been bent into a large, rather steeply-pitching isoclinal fold, with small crenulations on the limbs and around the nose marking the intersection of flow cleavage, parallel to the axial planes of these minor folds, and the bedding. Cross-cutting the whole structure at about 50° is a series of parallel lines marking the trace of false cleavage across the outcrop. (Text - fig. 4).

Another example appears in Pl. III, which shows a portion of the shore outcrop of Binnein schist west of Caolasnacon (130607). The influence of the type of rock upon cleavage and folding is well-illustrated. The axial planes of the folded quartzite bands are inclined 16° to the horizontal. The bands are openly folded and cut by cross-joints. The axial planes of the small drag folds, i.e., false cleavage, in the schistose layers are inclined 6° to the axial planes of the folded quartzite. The bedding is folded much more tightly.

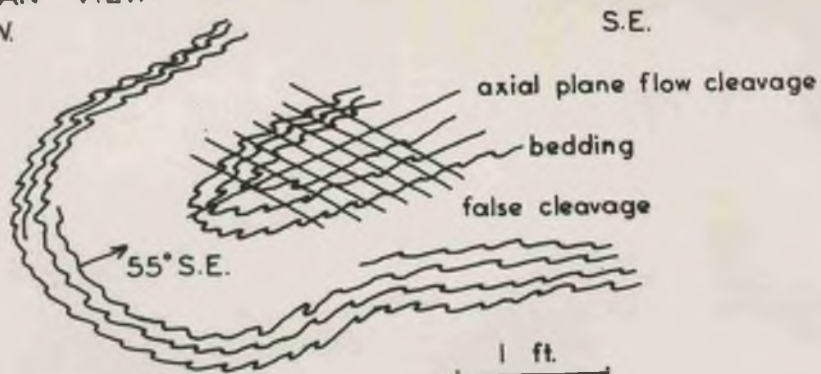
False cleavage coincident with the axial planes of small zig-zag folds in Leven schist and in phyllitic Ballachulish limestone is well-developed, (e.g., VB457 from Gleann Leac-na-muidhe (105543), VB533 from the south slope of Sgòr nam Fiannaidh (136569), and the numerous limestone outcrops on the southwest slope of Sgòr nam Fiannaidh (120585). Attenuated limbs of small folds are responsible for the definite, but irregularly spaced false cleavage cutting the folded bedding of the shore outcrop of Ballachulish phyllitic limestone at Cnocan Dubha (081584). These planes

PLAN VIEW:
S.S.W.



*Text-figure 3. Bedding of Leven schist, Glenn leac-na-muidhe (105543), cut by a series of nearly-vertical fracture cleavage planes which have dragged the bedding a few millimeters in the direction of movement.

PLAN VIEW:
N.W.



*Text-figure 4. Fold in quartzose Appin phyllite, north spur, Sgorr Dhearg (056572), with bedding drag-folded and cut by closely-spaced axial plane flow cleavage planes and by a series of less closely-spaced false cleavage planes.

are healed with narrow veinlets of white quartz.

Reverse faulting along some fracture cleavage planes is seen in thin-sections of Ballachulish slate (VB353) from the northwest slope of Sgorr a' Choise (081555) and of hornfelsed Ballachulish limestone (VB670) from the south slope of Sgòr nam Fiannaidh (136568).

It may be impossible to distinguish at times between flow cleavage and false cleavage; for example, when "post-tectonic crystallization... may transform the fracture cleavage of a phyllite or phyllonite into a crystallization schistosity indistinguishable from typical flow cleavage formed by paratectonic crystallization" (Turner, 1950, p. 561).

(c) Map III: Strike and dip of false cleavage

All measurements (164) of false cleavage strike and dip are plotted in black on Map III. There is no general strike pattern over the whole area as is the case of flow cleavage, although there seem to be two trends, one northwest-southeast, the other northeast-southwest. The directions of dip vary around the compass, and the amount of dip ranges from 14° to 90° .

(d) Origin of false cleavage

Unlike flow cleavage, false cleavage, particularly fracture cleavage may be a response to the growth of new minerals along shear planes due to movement, i.e., its origin may well be explained by the movement hypothesis of Sander, for an oriented fabric appears along certain, but not all, parallel planes. (Swanson, 1941, p. 1252).

3. Use of cleavage to determine superposition

The relative ages of strata may be determined in the field from the

relation of axial plane flow cleavage and axial plane false cleavage to the bedding. If the dip of the cleavage is greater than that of the bedding, the strata are right side up and are progressively younger down dip. If the dip of the cleavage is less than that of the bedding, the strata are upside down and are progressively older down dip (Wilson 1946, pp. 269-270).

The cleavage-bedding relationships have been studied in Ballachulish and Glen Coe, and are plotted on a sketch map of the area (Text - fig. 5). The arrows point in the direction in which the beds become younger. The arrows without an "o" refer to beds which are the right way up; those with an "o" refer to beds which are overturned. Disregarding for the moment those arrows with an "o", the data bear out the younging of the lithology as shown on Map III, i.e. from the upper right-hand corner towards Camas Calltuinn (from Binnein schist to Appin quartzite), from the upper left-hand corner towards Gleann an Fhiod (from Banded Passage Beds to Appin phyllite), northwestwards from the southeastern flanks of Sgorr a' Choise (from Leven schist to Appin quartzite), and generally westwards from the slopes of Am Meall and Meall Mor (from Leven schist to Appin phyllite).

The numerous cases of upside down strata indicate the propensity of Leven schist, Ballachulish limestone, Ballachulish slate, and Appin phyllite for recumbent folding; in this area the folds are generally overturned towards the east.



*Text-figure 5. The arrows point in the direction in which the strata become younger. An "o" signifies that the beds are overturned, otherwise they are right way up. Data obtained from the angular relationship between bedding axial plane cleavage.

The angle between bedding and flow cleavage varies with their positions in relation to the fold structure of which they are a part. On the limbs of a fold flow cleavage intersects the bedding at a very small angle (VB260). At the crest or trough the flow cleavage intersects the bedding at right angles (VB407). This is well-illustrated by a comparison of Maps II and III which shows that deviations between flow cleavage and bedding arise where the bedding bends around the nose of plunging fold structures, while the cleavage continues its north-northeast trend, e.g. around the Beinn Bhàn syncline. On specimens VB469 and 575 from Beinn Bhàn the bedding of the Appin Striped Transition Series intersects the flow cleavage in a succession of colored bands.

Using the criterion of the angular relationship between bedding and flow cleavage it is possible to predict at several localities on Map VII, particularly on Meall Mor, the position of the specimens examined with respect to the folded structures of which they are a part. The diagrams at localities 949, 849, and 1045 with the bedding and cleavage planes roughly parallel indicate that the rocks on the eastern side of Meall Mor are on the limb of a regional fold (the diagram at Loc. 1448 is not considered because the specimen contains a small fold). To the east the divergent planes in the diagram at Loc. 820 suggest that the centre of a regional fold has been reached. To the west, at Loc. 961 the planes begin to diverge until at Loc. 708 the center of another regional fold is reached. The diagram at Loc. 560 (072579) with its partially divergent planes is approaching the center of the Beinn Bhàn syncline.

Around Camas Calltuinn (102599) the diagrams at both Loc. 140 and Loc. 2 are parts of medium-scale fold structures (Pl. XXI, Fig. 2). They at least corroborate each other that the centre of a fold on some scale is very near. Unfortunately the examples at Loc. 132 (125604) and Loc. 625 (093583) are isolated, but the former indicates that the center of a fold is nearby and the latter that the specimen is on the limb of a fold.

c. Slickensides

Slickensides, the surfaces that result from friction along a fault plane, are sometimes smooth and even, such as the polished surfaces on Ballachulish slate in the abandoned quarries of West Ballachulish (075583; VB160). More commonly they exhibit a well-marked striation (VB43), which may often indicate the direction of movement along the plane. These surfaces may be coated with quartz crystals and subordinated epidote (VB204) or with mica and a red epidote (?) (VB43).

d. Shear zones

Shear zones are "narrow zones usually 0.5-3cm. thick along which movements have taken place without the formation of actual slickensides" (Kvale, 1948, p.23). Kvale differentiates between those shear zones in which mineral grains are arranged with their longest dimension parallel to a direction which is different from the direction of mineral lineation in the rock and those shear zones which cross the flow cleavage and along which the flow cleavage has been slightly bent, indicating movement along the zone (p. 23). No examples of the first case have been seen by the writer in Ballachulish and Glen Coe. The only instance similar to

the latter one occurs in one of the abandoned slate quarries of West Ballachulish (075583) where a medium-scale recumbent fold is exposed. A small fault approximately parallels the axial plane and is bordered by a gouge zone; the bedding has been bent nearly parallel with the plane of movement.

e. Joints

(1) Types

In Ballachulish and Glen Coe most of the joint surfaces examined are planar, with an occasional curved one (VB313). There are four main types:

- (a) cross-joints ("ac" - or tension joints), those occurring at nearly right angles to the dominant linear structure in the rock (VB100, Pl. I, Fig. 2; 115)
- (b) oblique joints, those forming roughly a 45° angle with the lineation (VB121)
- (c) longitudinal joints, those steeply-dipping ones which strike parallel to the lineation (VB18, Pl. XXX, Fig. 4; 47)
- (d) regional joints, those which can be traced over a mile or more; they are generally vertical or nearly so.

The degree of development of joints depends upon the character of the rock and the intensity of the tensile stress. Rocks containing much mica usually yield under tension by plastic flow until their elastic limit has been reached (see Table I, p.56). If analogy with sandstone is valid, then quartzites would be expected to have a low resistance to tensile stress. The majority of joints and those with the most regular

surfaces have developed in quartzite and quartzitic bands; these competent rocks commonly show variable angles of rupture between the planes of failure under stress. On the other hand, marble, limestone, slate, and schist have few, poorly-developed joint surfaces; strain rather than stress is more important and there is a limited number of possible angles between joint planes.

Small-scale joints are frequently healed with calcite (VB44, Pl. XIV. Fig. 2; VB91) or quartz (VB157, 264).

Many times in the field it was not possible to distinguish between the four types, particularly as the more massive quartzites frequently lack any linear structure. Probably the most common type, however, was the cross-joint. Of the 36 hand-specimens which contain a folded structure (Appendix V) 20 show "a-c" jointing, i.e. jointing perpendicular to the fold axes.

(2) Stereogram of joints

Poles to all measured joint planes (411) have been plotted on the lower hemisphere of a Schmidt stereonet, and the point diagram contoured for a 1%, 2%, 2.5%, and 3% concentration of poles. The resultant diagram (Text - fig. 9) shows that the joint planes have four general trends: north-northwest-south-southeast (the maximum concentration of poles), west-northwest-east-southeast (submaximum concentration), north-northeast-south-southwest (submaximum concentration), and east-northeast-west-southwest (submaximum concentration). The first two are predominant. The amount of

dip varies from horizontal to vertical, but by far the largest proportion of planes are vertical or nearly so. No field evidence was obtained for determining whether one set of joints is older than the others or whether they are contemporaneous.

(3) Origin of joint planes

According to Kvale (1948, p. 40), joints in metamorphic rocks may originate in two ways:

"They may have been produced by the same forces that imprinted upon the rocks their present planar and linear structures. The joints then represent the reaction upon these forces by the rocks when...under pressure-temperature conditions in which they could not yield by plastic deformation. We may expect the position in space of these joints to have a definite relation to the other structures of the rock provided the plan of deformation had not been changed. But some of the joints may also have been produced in a later phase of the same deformation or in a later period of deformation, which was not sufficient strong to leave its mark in the planar and linear structures of the rock. Joints of the latter kind cannot be expected to bear any definite relations to the other structures of the rock, although these structures may exercise some influence upon the positions of the new joints, in particular if the difference between the two plans of deformation are moderate".

f. Faults

(1) Regional

Both normal and thrust faults occur in Ballachulish and Glen Coe on both major and minor scales. The absence of Ballachulish limestone between Ballachulish slate and Leven Banded Passage Beds along the southwestern slopes of Sgòr na Ciche and Sgòr nam Fiannaidh (Map I) and the absence of Ballachulish slate between Ballachulish limestone and Appin Striped Transition Series in the shore section west of St. John's Church (Map I, 066588) are two examples of large-scale faulting between tectonic units which

occurs repeatedly in the area. From the relative straightness of the tectonic contacts it would seem that the faults are steeply-dipping.

Horizontal displacement has occurred in the slope south of Caolasnacan (140600) where Binnein schist has been laterally displaced northeastwards the width of its outcrop by a nearly-vertical fault.

Probably the most striking fault in the field is the nearly-vertical upthrust in the northwestern slope of Sgorr a' Choise which has carried Ballachulish slate higher in elevation than the younger Appin quartzite which forms the backbone of the ridge (Pl. XVI, Fig. 1).

When the faulting occurs within a tectonic unit, its attitude and extent are more difficult to estimate. The gash in the northeastern slope of Meall a' Chaolais in the upper reaches of Allt Bearnach (Pl. XXIX, Fig. 1) marks a shatter belt in Appin quartzite. The rocks are so jointed and fragmented that the direction and amount of displacement can not be determined in the field.

Bailey (Sheet 53, third edition, Ordnance Survey) has mapped another shatter belt in the upper wall of Allt a' Coire Riabhaich. One fault separates regularly-dipping Appin quartzite from contorted Striped Transition Series (F_1 , Pl. XXIX, Fig. 2). To the northwest a few tens of yards another fault displaces the folded Striped Transition Series (F_2 , Pl. XXIX, Fig. 2). These faults have not been studied in detail by the author because of the precarious nature of the corrie slopes.

(2) Medium-scale faults

Smaller-scale faults occur in the bed of the River Laroach (070549), where a dike cutting Appin quartzite has been displaced laterally four and

one-half feet to the southwest, and in the shore section west of St. John's Church (066588) where a series of en échelon normal faults cuts the Striped Transition Series near its contact with Ballachulish limestone (P1.XIII, Fig. 2).

(3) Small-scale faults

Of the 13 hand-specimens showing faulting (Appendix IV), eight faults are normal and five are thrust. Several typical examples appear on P1. XX. In addition, a low-angle thrusting acting along axial plane cleavage has cut out one limb of a small fold in quartzose Appin phyllite (VB687, P1. XXVII Fig. 2). Small-scale tension fractures frequently cross-cut the bedding in Ballachulish slate (P1. XVIII, Fig. 1) and Appin Striped Transition Series (VB586). Usually the fractures are healed with white quartz.

CHAPTER IV: TECTONICS -- FOLDED STRUCTURES

A. Folding

Folding has occurred in all of the lithologic formations in Ballachulish and Glen Coe -- from Binnein quartzite through Appin phyllite (Text-fig. 13). The intensity and scale of folding reflect the competence of the rock and the amount and type of stress to which it has been subjected.

1. Competence

Competence is a relative factor, for it is roughly an expression of the crushing strength and massiveness of one rock formation as compared with that of another. A competent rock transmits stress and at the same time supports its own weight, with the result that each layer retains its thickness during folding; the fold is a simple flexure. For example, the layers in Binnein quartzite show no appreciable thickening or thinning in the recumbent folds near Caol an Aonach (138607) (Pl. I, Fig. 2).

An incompetent rock neither transmits stress nor supports its own weight. "It is passively folded, the folding may be more or less replaced by shearing and the beds are thickened and thinned corresponding to the degree of pressure, material being moved from the limbs towards the crests of folds" (Kvale, 1948 p. 35). This is quite characteristic of folds in Binnein schist (Pl. II, Fig. 1), Ballachulish limestone (Pl. XI, Figs. 1, 3; Pl. XII, Fig. 3), and the like. "The difference in curvature [of a fold] between the top and bottom surfaces of the competent beds creates potential spaces on the crest, such spaces being occupied by incompetent material that has flowed in from the limbs". (Swanson 1941, p. 1258).

Details of the amount of thickening and thinning in hand-specimens containing folds are given in Appendix V, column six. Of 36 rocks, 24 show

thickening on the crests or in the troughs of folds with a corresponding thinning on the limbs; three show thinning on the crests or in the troughs with a corresponding thickening on the limbs. The crests may break up into series of smaller folds. This happens frequently in the schistose facies of Ballachulish limestone (Pl. XI, Fig. 2).

Folds in competent strata are open, bow-shaped, and large (Pl. XXII, Fig. 2), compared with the compressed, small concertina folds of incompetent strata (Pl. XI, Fig. 2). These features are well-illustrated side-by-side in Pl. III by the small asymmetric drag folds in the phyllitic bands between the larger, more open, isoclinal folds in the quartzitic bands of Binnein schist.

Variations in the competence of beds arise due to the combinations of thickness of competent and incompetent beds. For example, if the incompetent bands form relatively thin layers between competent beds, the deformation of the weaker strata is subject to a broad control imposed by the stronger ones. In the case of thick zones of incompetent material with a few thin competent bands, faulting and folding produce a great variety of local stresses. "With such zones, the minor folds and cleavage structure may have no direct relation to the major structure" (Swanson, 1941, p. 1260).

2. STRESS

A. Compressive stress

Flexure folds are the result of lateral compression or of a couple acting in the direction of the bedding plane and producing lateral shortening of the strata, e.g. the double fold in Pl. XXIII, Fig. 1. No compression folds have

been noted in the area which are the result of compression acting perpendicular to the bedding plane (i.e., doming), although there may be examples near the granite complexes and small plutons.

Flow folds are characteristic of incompetent strata. They have formed by compression in rocks which have been subjected to a sufficiently high temperature and pressure to become plastic or which are inherently plastic. Flow folds are asymmetric; their axial planes are irregular surfaces rather than planar. Their axial directions, however, may be fairly constant over small areas.

b. Tensile stress

Tensile stress produces radial tension joints in competent bands and corrugations in incompetent bands, but no folded structure as such. These features are well-shown in the Striped Transition Series specimen VB586, from the summit of Sgorr a'Choise (085551) where a series of small-scale joints have been healed with white quartz, and in Pl. XVIII, Fig. 1.

c. Shearing stress

Shear folds are formed by shearing stresses acting along closely-spaced fractures crosscutting the bedding of a rock and producing minute displacements along these parallel planes. "...The thickness of a layer is constant when measured parallel to the shear planes and consequently varies considerably when measured normal to the curvature of the fold....[Shear folds]... do not involve any lateral shortening of the rock and can not be straightened out" (Kvale, 1954, p. 38).

3. Relation of competence and stress

Table I gives the average resistance of various rocks to compressive

tensile, and shearing stresses. It shows that sandstone, quartzite,

TABLE I: AVERAGE STRENGTH OF ROCKS (in kg./cm.²) AND BULK DENSITY (in g./cm.³)

Rock	Compressive stress	Tensile stress	Shearing stress	Bulk density
Sandstone	500-1500	10-30	50-150	2200-2600
Quartzite	1100-2000 3345*	no data	no data	2640-2730
Conglomerate	1200-1300	no data	no data	no data
Limestone	400-1400 1685*	30-60	100-200	2300-2700
Marble	800-1500	30-90	100-300	2700-2850
Slate	700	250	150-250	2700-2800
Schist	2495*	no data	no data	2700-2950
Hornfels	3480*	no data	no data	no data

*

Data from Phemister et al (1946); all other data from Kessler (1927).

conglomerate, marble, schist, and hornfels stand up to compression much better than limestone and slate. On the other hand, slate is far more resistant to tensile stress than the others. Marble and slate withstand shearing better than limestone and sandstone, although the difference is not nearly so marked as in the cases of compression and tension. These figures are generally borne out by Ballachulish and Glen Coe by a lithologic evaluation of the folded structures (Text-fig.13).

B. Types of folds

1. Compression folds

a. Flexure folds

Most of the folds in the Ballachulish - Glen Coe area are the flexure type. The smallest number of folds is found in the quartzite -- Binnein (Text-fig. 13, D.1), Glencoe (D.3), and Appin (D.9), a

these are all large-scale. A relatively small number of folds occur in Leven schist (D.5), which is not surprising as schist as well as quartzite has a high resistance to compression. But there are as many small-scale folds as there are large-scale, mainly due to additional folding by shear.

b. Flexural-slip folds

Where schistose bands are intercalated with quartzite, as in the case of quartzose Binnein schist (D.2), Banded Passage Beds (D.4) and Striped Transition Series (D.8), the strata fold quite readily, due to the ease with which individual layers slip over the micaceous bedding foliation of the incompetent bands; the competent bands fold by flexure. These transitional formations contain three of the four largest concentrations of folds.

A fairly small number of folds in Ballachulish (D.6) and Appin (D.10) limestones would be anticipated from the experimental data. While this is true of the Appin, the largest concentration of folds in any formation occurs in the Ballachulish limestone. This apparent discrepancy is simply explained by the schistose nature of the Ballachulish limestone and by the fact that half of the folds are small-scale shear folds. The narrow bands of calcite have folded readily by slippage on and within the intercalated micaceous laminae. Ballachulish slate (D.7) and Appin phyllite (D.11) fold easily by compression, as would be expected from Table I, but, as in the case of Ballachulish limestone, shearing is also quite important.

c. Flow folds

Folds in Ballachulish and Appin limestones are characteristically of the flow type. An excellent example is VB693 (Pl. XXVI, Fig. 2), in which at the time of folding the white calcite became sufficiently plastic under pressure for the bedding to buckle and to flow along flow cleavage planes for short distances. Many larger scale examples may be seen along the Ballachulish limestone outcrop on the southeastern slope of Meall Mor.

2. Shear folds

None of the lithologic types in Table I for which data are available are particularly resistant to shearing. Unfortunately the record is incomplete for quartzite, schist, and hornfels. Every formation in Ballachulish and Glen Coe except the Binnein, Glencoe, and Appin quartzites is represented in Appendix V (description of the 36 hand-specimens showing folded structures) at least one rock in which thickening and thinning occurs across a fold. Differential thickness in the quartzites has not been noted in the field by author, perhaps because the scale of folding is so much larger than in the other formations.

3. Combinations of folds

Combinations of flexure folds and shear folds are more common than the pure types of folds. For example, the isoclinally-folded Banded Passage Bed in specimen VB448, Pl. V, Fig. 2, are certainly the result of compression, but close examination of the layers shows one band which thickens from 10 mm. on limb to 30 mm. in the trough, then thins to 15 mm. on the other limb. Obvious shearing has played a part, too. Similar examples occur in Leven schist (Pl. VIII, Figs. 1 and 2) and in the Striped Transition Series (Pl. XVIII, F

CHAPTER V: TECTONICS -- LINEAR STRUCTURES

There are two main categories of linear structures: lineations and fold axes.

A. Lineations

Lineation is any linear parallelism in a rock, and in metamorphic rocks is always a secondary feature. Of the 709 specimens collected in the field, 300 have only one lineation, 159 have two, 38 have three, 10 have four, and one has five.

1. Types

a. Lineations due to parallel orientation of prismatic and pinacoidal minerals

On the east slope of Meall Mor and around Signal Rock, Glen (VB410, Loc. 822, 122565) tremolite forms mats and even bands in thermally metamorphosed Ballachulish limestone. The individual crystals are sometimes aligned roughly parallel with the bedding strike, e.g., VB321, 404, 413. Sometimes they are inclined ca. with the strike, e.g., VB206, 544. At one locality on Meall Mor (Loc. 760, 117561) actinolite occurs instead of tremolite and roughly parallels the strike (VB381).

Along the shore west of Caolasnacon very thin cleavage sections of chlorite are aligned in Glencoe quartzite parallel with the fold axes in the area (VB370, 371, Loc. 751, 125606). In the same district secondary biotite porphyroblasts in Binnein schist are aligned almost parallel with the dip of the bedding (VB233, Loc. 378, 131607).

b. Lineations due to arrangements in streaks and rows of more or equidimensional minerals

Alignment of attenuated quartz grains is responsible for very fine lineation on the bedding of Ballachulish slate, e.g., VB592, Loc. 1356, 081554. This feature is well shown in the following thin-sections: VB24-2, 424-2, 473-2, 519-2, and 688-2, and in many others.

c. Lineations due to stretching of conglomerate fragments

The only example from Ballachulish and Glen Coe is Binne Schist near the contact with Glencoe quartzite south of Caolasnacon (VB216, Loc. 359, 141601). Here the schist contains small, flattened, and elongated quartz pebbles, oriented with their longest dimension at right angles to the strike of the foliation.

d. Lineations due to grooving and striation not caused by mineral orientation or stretching

These may occur on bedding, cleavage, joint, or fault planes and may or may not be related to tectonic axes. Frequently in Ballachulish and Glen Coe they pitch 90° from the strike of the planar surfaces upon which they occur in which case they mark the direction of slip of one lamina over another.

e. Lineations due to the intersection of planar surfaces

The intersection of bedding with flow cleavage, false cleavage, or jointing, or any combination of these four planar surfaces often produces a conspicuous lineation on at least one plane. The lineation may be color-banding, as is the case with

bedding transsecting flow cleavage (VB89, Pl. XXVII Fig. 1) or false cleavage (VB507), or it may occur as crenulations, varying in width across each pucker from 0.1-8 mm. (Pl. II, Fig. 1; V, Fig. 2; XV, Fig. 2; XXVI, Fig. 2; XXX, Figs. 1, 4), with occasional "pencil" rods 20 mm. across (Pl. IV, Fig. 2; XV Fig. 2). The narrow lineations tend to be parallel and continuous; the wider ones are frequently subparallel and discontinuous.

The more pelitic rocks tend to show at least two sets of lineations on one planar surface. Generally speaking, one lineation is coarser than the other, and in the majority of cases is due to false cleavage. The finer lineation is usually due to flow cleavage intersecting bedding or to slippage along certain planes.

More rarely there are three or more sets of lineation; for example, one specimen of slate (VB325) (Pl. XV, Fig. 2) from north slope of Am Meall (Loc. 629, 094580) has one fine lineation cross-cut at 61° and at 85° by two sets of coarse crenulations. The fine lineation is due to the intersection of a false cleavage on bedding.

2. Map IV: Direction and plunge of lineations

All lineations except those due to joint planes intersecting other planes have been plotted on Map IV. As the latter kind have no tectonic importance, they have been omitted. Wherever possible the types of lineation have been differentiated by symbols and colors. Lineation due to the elongation of minerals (Type a) is shown by a black line with a solid black circle at one end. Lineation due to streaks and rows of mineral grains (Type b) actually marks the intersection of bedding and flow

87

cleavage, and is shown by a black line with a solid black triangle at one end. Lineation which is the result of stretching of conglomerate fragments (Type c) is included in the category of differentiated lineation due to the intersection of bedding and false cleavage, as the one rock specimen showed both features. Lineation due to grooving and striation (Type d) has been included in the category of undifferentiated lineation due to the intersection of bedding and false cleavage, as the two can not be told apart in hand-specimen. The great majority of lineations are due to the intersections of planar surfaces (Type e), more particularly, to the intersection of bedding and flow cleavage and to the intersection of bedding and false cleavage, and are shown by black and red symbols. Those lineations due to the intersection of flow cleavage and false cleavage and to the intersection of false cleavages have been omitted because they have no pertinent structural significance.

As flow cleavage in Ballachulish and Glen Coe is generally the axial plane type, its trace on the bedding parallels the axis of the fold structure. This axis is conventionally called the "b"-axis or "b" - direction, and lineation which is parallel to it a "b" - lineation. All of the black symbols with a solid triangle on Map IV thus represent "b" - lineations.

False cleavage may or may not be the axial plane type. Where sufficient fold data are available to ascertain this, the lineations due to the trace of false cleavage on bedding have been differentiated as the "b"-type by a solid red triangle on a red bar. Where additional data are not available a red arrow has been used. Some of these arrows, by analogy with the red

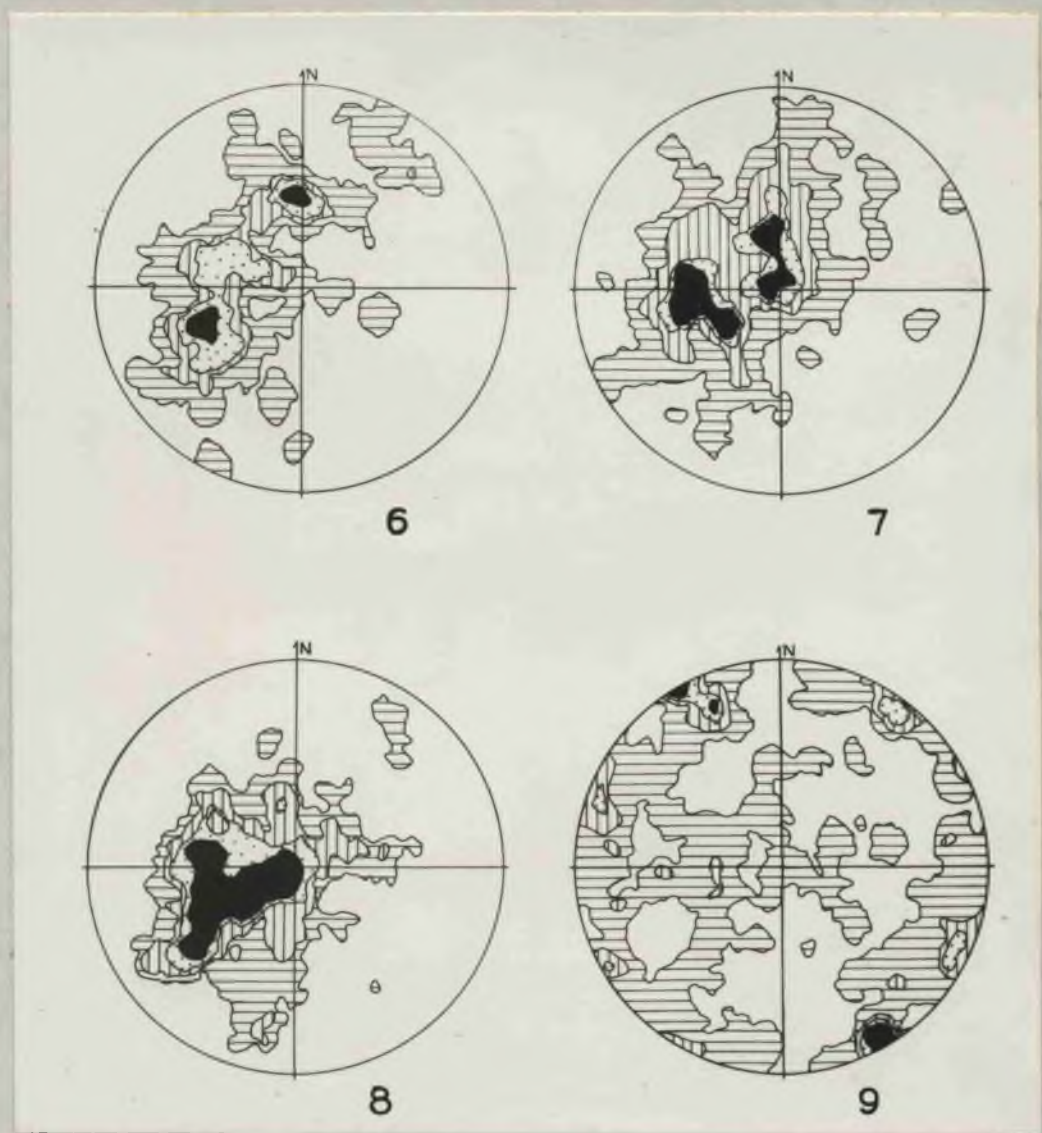
and black triangle symbols, are obviously "b"-lineations, too, e.g. around 061543 and 101580, but to designate these as such would inject a subject's note into the field information.

The pattern of symbols on Map IV is very complex; it will be discussed later in conjunction with Map V (fold axes).

3. Stereograms

The 166 lineations due to the intersection of bedding and flow cleavage have been plotted on the lower hemisphere of a Schmidt stereonet, and the resultant point diagram contoured at 1%, 3%, 4%, and 6% (Text - Fig. 6). In like manner, the 547 lineations due to the intersection of bedding and false cleavage have been plotted and contoured at 1%, 2%, 3%, and 3.5% (Text - Fig. 7).

A comparison of the two diagrams reveals two maxima in each and in roughly the same relative positions. From the "b"-lineations of Text - Fig. 6 it may be inferred that there are two trends of fold axes in Ballachulish and Glen Coe - one almost due north (176°) and another west-southwest (68°). The plunges vary between 48° - 58° N.W., averaging 52° N.W., in the former instance and between 40° - 55° S.W., averaging 45° S.W., in the latter. As the pattern in Text - Fig. 7 is so similar, it suggests that the majority of lineations due to false cleavage intersecting bedding are also approximately "b"-lineations. Again, two trends of folds may be inferred, one due north (0°), the other west-southwest (80°). The plunges vary between 60° - 94° N. (i.e., some folds have been overturned), averaging 77° N. in the first case and between 44° - 72° S.W., averaging 58° S.W. in the second. The greater variation in plunges in Text - Fig. 7 as compared with that of Text - Fig. 6 is due to the more random relation of false cleavage lineation to tectonic axes as compared with flow cleavage lineation.



Text-Figure 6. Plot on the lower hemisphere of a Schmidt stereonet of 166 lineations due to the intersection of bedding and flow cleavage; contoured at 1%, 3%, 4% and 6%.

Text-figure 7. Similar plot of 547 lineations due to the intersection of bedding and false cleavage; contoured at 1%, 2%, 3% and 3.5%.

Text-figure 8. Similar plot of 374 fold axes; contoured at 1%, 2%, 3% and 4%.

Text-figure 9. Similar plot of poles to 411 joint planes; contoured at 1%, 2%, 2.5% and 3%.

B. Fold axes

1. Definition

The axis of a fold is the direction which is parallel to the curved surface or mantle of the fold or is the best average of small variations in that curved surface (Wegmann, 1929, p. 102). In nature the direction and plunge of the axis frequently change within relatively short distances. For example, the fold in Banded Passage Beds, Pl. XXXI, Fig. 2, plunges 67° N. for a few inches, then flattens out to 55° N.W. In the road cut just west of the Glencoe boathouse on Loch Leven (Loc. 239, 102599) the axis of a fold in the Striped Transition Series may be traced for about five feet. In that distance the plunge varies from 58° to 61° to 54° to 44° to 64° to 76° S.W. The axis of the bifurcating small fold in Ballachulish slate, specimen VB2 changes its direction 6° within a few inches. But in many places the axes remain remarkably constant over considerable distances.

2. Measurement

Fold axes in Ballachulish and Glen Coe have been determined in three (1) by direct measurement, (2) by geometrical construction, and (3) by measurement of the lineation produced by the intersection of flow cleavage bedding.

a. Direct measurement

The direction and plunge of 213 fold axes were measured in the field with a Brunton compass. These data have been plotted on the lower hemisphere of a Wulff stereonet according to the size of the fold. Diagram 1 on Map V is the stereogram of fold axes of 110 small-scale structures^s, that is, those in which the width of the fold is less than one foot. Diagram 2 on Map V is the stereogram of fold axes of 103 larger-scale structures, that is, those in which the

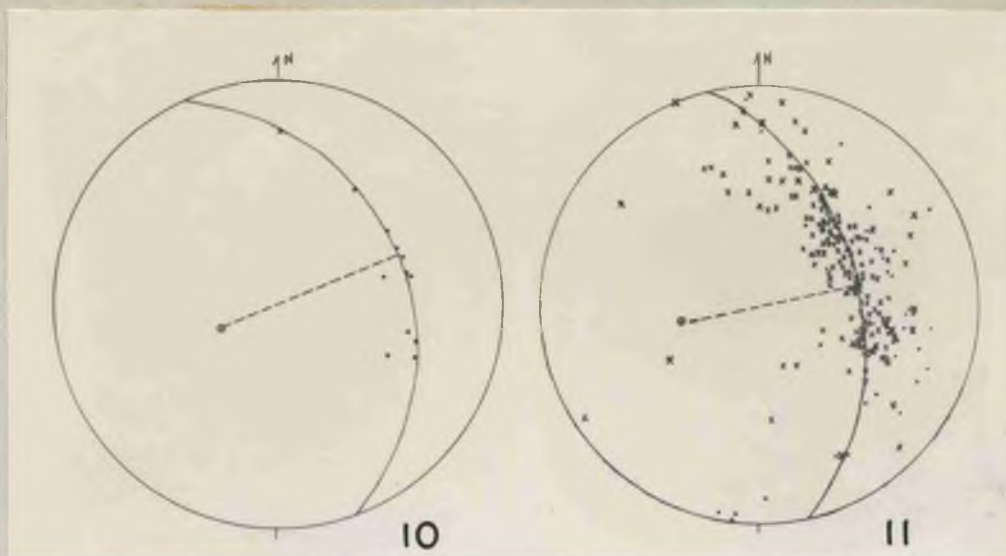
73

width of the fold is more than one foot and less than 50 feet. The data have been plotted in a similar manner on the basis of lithology (Text - Fig. 13) and geographic distribution (Text - Fig. 14); they have also been plotted on the lower hemisphere of a Schmidt stereonet (Text - Fig. 8) and on Map V as arrows showing trend and amount of plunge.

b. Geometrical construction

Sometimes the axis of a fold is not exposed in the field, and consequently cannot be measured directly. If sufficient areas of both limbs crop out and if the fold is cylindroidal, the fold axis can be constructed in the manner described by Wegmann (1929, p. 10). Briefly, a series of measurements of bedding strike and dip is made across both limbs of a cylindroidal fold. The pole to each measurement is plotted on the lower hemisphere of a Wulff stereonet and will be found to lie on the same plane or, where accurate readings are not possible, in the same zone across the net. The normal to this plane or zone is the direction of the fold axis, and its distance from the periphery of the net is the amount of plunge.

The method is illustrated in Text - Fig. 10. The strikes and dips measured at successive stages across a fold in a schistose facies of Glencoe quartzite are: 14° , 65° N.W.; 24° , 57° N.W.; 20° , 66° N.W.; 165° , 52° S.W.; 91° , 76° S.W.; 124° , 64° S.W.; 146° , 61° S.W.; 159° , 62° S.W.; 168° , 63° S.W.; 11° , 62° N.W.; 166° , 62° S.W.; 154° , 61° S.W. The normal to each of these readings is plotted on tracing paper over the lower hemisphere of a Wulff stereonet, the normal intersecting the hemisphere as a point. The



Text-fig. 10. Poles to bedding measurements across a fold in a schistose facies of Glencoe quartzite, Loc. 751 (130607), plotted on the lower hemisphere of a Wulff stereonet; fold axis trends 67° , plunges 59° S.W.

Text-fig. 11. Poles to all bedding measurements in the entire shore section west of Caolasnacon; axial strike 79° , axial plunge 51° S.W. Small cross, quartzite; dot, phyllite.



Text-fig. 12. Poles to all bedding planes; entire Ballachulish - Glen Coe area; axial strike ca. 58° , axial plunge ca. 50° S.W. Symbols same as above; open circle, limestone.

tracing paper is rotated until the narrow band of points coincides with a great circle on the stereonet. On the E.-W. great circle the pole of the axis (a point) is plotted 90° away from the plane. The tracing paper is again rotated, this time until the point falls on the N.-S. great circle. The co-ordinates of the point are then read off: the direction of the axis is the position of the north arrow on the periphery, and the amount of plunge is the distance along the N.-S. great circle from the periphery to the point. In the example cited the fold axis trends 67° and plunges 59° S.W.

The direction and plunge of 179 fold axes were constructed in this way, and the data added to all of the plots of directly-measured fold axes (Map V, with diagrams 1 and 2; Text - Figs. 13, and 14).

c. Measurement of "b"-lineations

Quite often fold axes are not apparent in the field. They can be inferred, however, where flow cleavage intersects bedding for the resultant lineation (a "b"-lineation) parallels the axis of the fold. The direction and plunge of 166 fold axes have been determined in this way. The size of the folds, unfortunately, has not been estimated; consequently the data are plotted separately on the lineation map (Map IV) and in Text- Fig. 6 instead of being added to Map V and to Text - Figs. 8, 13, and 14.

Lineations due to the intersection of bedding and false cleavage are much less dependable for determining fold axes. Sometimes they do roughly parallel the axis of a fold, but just as commonly they may be at right angles to it, i.e. an "a"-lineation or inclined at almost any angle to the axis. The somewhat random pattern of red symbols on Map IV compared with the pattern of black arrows makes this unreliability quite evident. Where the red arrows roughly parallel the black, it seems reasonable to assume that the false cleavage in these cases is approaching axial plane cleavage.

The relationship between fold axes and lineation is further illustrated by the detailed study of hand-specimens containing folded structure in Appendix V. Of these 36, 15 have one lineation parallel with the fold axis ("b"-type), five have one lineation perpendicular to the fold axis ("a"-type), 11 have both "a"- and "b"-lineations, and five show lineation inclined to the fold axis as well as a "b"-lineation.

Kvale (1948, pp. 32-33) summarizes the causes of an absence of parallelism between lineation and fold axes:

- "1. The lineation may be grooving on bedding planes produced by slippage of the individual beds over each other during the folding. The grooving may also, according to Cloos (1937, p. 55), be accompanied by stretching of minerals. This grooving or lineation may be at right angles with the axes of folds...."

"2. In shear folds, grooving or lineation may be formed on cleavage planes by the shearing that produces the folds. The linear structure is thus produced in the same way as in the first case, but it occurs on other planes. The linear structures must be at right angles with the axes of folds..."

"3. W. Schmidt (1932, p. 60 et seq.) deduced by theoretical considerations that during 'dreiaxiale Verformung' two systems of shear planes may be formed. Each system consists of two shear planes that intersect in a line which may appear as a linear structure in the rock. Two lines of intersection formed in this way must be at right angles with each other. This explanation of crossing linear structures may be used if they intersect at right angles and if evidence of two systems of shear planes can be found..."

This may explain the five lineations inclined to the fold axis noted above.

"4. The crossing linear structures are not formed simultaneously. They need not be formed in different periods of deformation but in different phases of the same period...."

This also may explain the five lineations inclined to the fold axis.

3. Map V: Trend and plunge of fold axes

The fold axes around Caolasnacon (138607), the Glencoe boathouse section (102599), and the southwestern slopes of the Pap of Glen Coe have in general a southwesterly plunge varying from 23° - 84° , with a mean of 54° whether the structures are large-scale or small-scale (Map IV). On the southwestern slopes of Sgòr nam Fiannaidh, however, the larger-scale folds have a pronounced northwesterly plunge, varying from 47° - 83° , with a mean of 64° , and the small-scale ones a southwesterly plunge, varying from 25° - 85° , with a mean of 71° . Further to the southeast both scale structures take on a westerly plunge varying from 37° - 72° , with a mean of 50° . The

arrows near the Glen Coe granite undoubtedly show local northwest-south trends rather than regional trends. Except for the southwesterly-plunging arrows on the east slope of Meall Mor (117560) there is no real pattern in the folds of Am Meall and Meall Mor. This is probably due to the nature of the lithology -- slate, limestone, and schist -- which would respond to all local stresses.

The arrows on Cnocan Dubha (079585), and westward along the shore of Loch Levan, on Sgorr a' Choise, in Gleann an Fhiod, and on Sgorr Dhean make up a heterogeneous scatter regardless of fold size. Again, it must be inferred that the absence of an orderly pattern is due to the lithology (Appin phyllite, Striped Transition Series, slate, and limestone) reacting differentially to local stresses.

Disregarding the size of the folds, a comparison of the plot of the "b" lineations on Map IV with the plot of fold axes on Map V provides strong corroboration of the pattern of plunging arrows on Map V. Apparent discrepancies on Map V appear also on Map IV; for example, the local deflection from the general trend near the Bridge of Coe (105588).

4. Stereograms

a. Based on the scale of folds

A comparison of the two diagrams on Map V both plotted on the lower hemisphere of a Wulff stereonet, shows the following details:

	115 small-scale folds	259 larger-scale folds
N. E. -S. W. trend	66%	60%
N. W.-S. E. trend	34%	40%
S. W. plunge	43%	47%
N. E. plunge	23%	13%
N. W. plunge	21%	29%
S. E. plunge	13%	11%

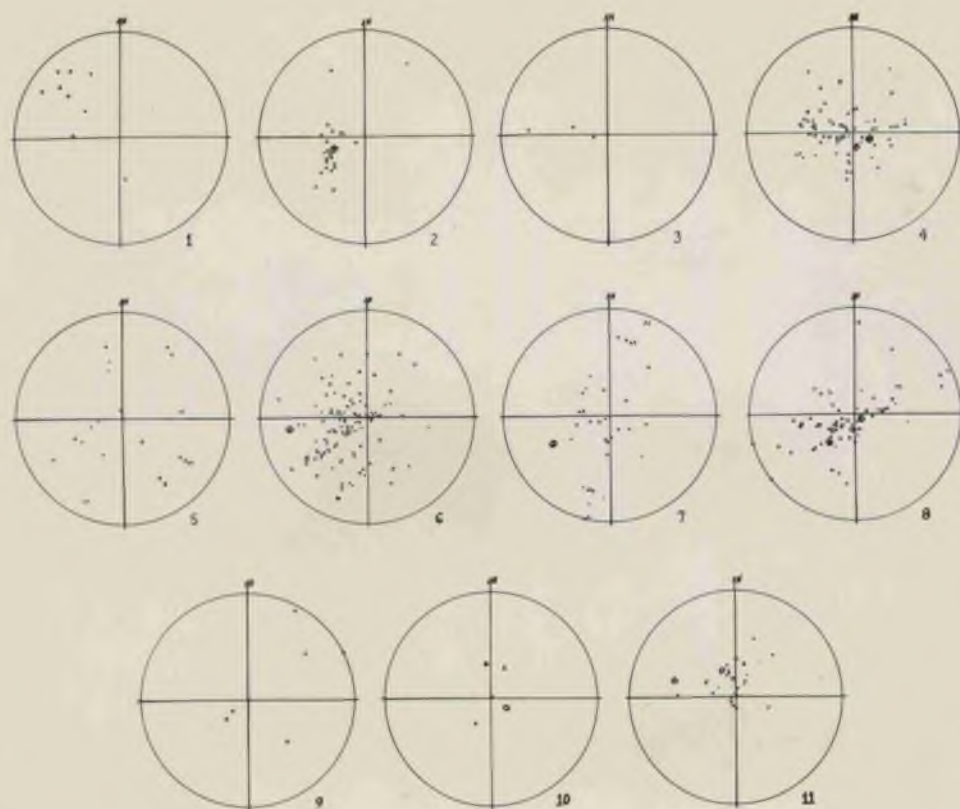
The number of northeast-southwest-trending small-scale folds is twice that of the northwest-southeast ones, while the number of northeast-southwest-trending larger-scale folds is one and one-half times that of the northwest-southeast ones. Folds with a southwesterly plunge account for nearly one-half of the total number: small-scale folds with this direction of plunge are double the number of those with a northeasterly plunge and also of those with a northwesterly plunge, and three times the number with a southeasterly plunge; larger-scale folds plunging southwest occur more than four times as often as those plunging southeast, three and one-half times as often as those plunging northeast, and one and one-half times as often as those plunging northwest. Proportionally more larger-scale folds than small-scale ones have gentler plunges.

The northwest direction of folding may have preceded the southwest direction and may have been partially obliterated by Caledonian movements, or it may post-date the southwest direction but may have been a much weaker folding. Whether the two trends are due to different deformations or to different stages in the same deformation can not be deduced from the above data.

b. Stereograms based on lithology

A All of the fold axes have been plotted on the lower hemisphere of a Wulff stereonet according to the size of the fold and on the basis of lithology (Text - Fig. 13). From a study of the 11 diagrams the following¹ observations can be made:

- (1) Folds are much more frequent in Binnein schist, Banded Passage Beds, Leven schist, Ballachulish slate, Ballachulish limestone, Striped Transition Series, and Appin phyllite than in the other more competent quartzose formations. Of these seven the majority of folds occur in the Banded Passage Beds, Ballachulish limestone, and Striped Transition Series.
- (2) Except for Binnein quartzite, no general direction of plunge is restricted to any particular formation. They all show both northwest-southeast and southwest-northeast trends as illustrated in the following table. T



Text-fig. 13. Fold axes plotted on the lower hemisphere of a Wulff stereonet on the basis of stratigraphic succession, from oldest to youngest: 1. Binnein quartzite, 2. Binnein schist, 3. Glencoe quartzite, 4. Banded Passage Beds, 5. Leven schist, 6. Ballachulish limestone, 7. Ballachulish slate, 8. Striped Transition Series, 9. Appin quartzite, 10. Appin limestone, 11. Appin phyllite. Solid circle, folds less than one foot in width; open circle, folds more than one foot and less than 50 ft. in width.

plunges are generally in northwesterly and southwest directions. The folding post-dates the deposition and consolidation of all of the 11 formations. (Five of fold axes plotted for Binnein quartzite were measured just east of Caolasnacon and are, therefore, not shown on Map V; even including these adjacent readings there are too few axes to be significant.)

Formation	N. E.-S. W. trend	N. W.-S. E. trend
Appin phyllite	45%	55%
Appin limestone	too few axes	too few axes
Appin quartzite	too few axes	too few axes
Striped Transition Series	81%	19%
Ballachulish slate	64%	36%
Ballachulish slate	62%	38%
Leven schist	53%	47%
Banded Passage Beds	52%	48%
Glencoe quartzite	too few axes	too few axes
Binnein schist	78%	22%
Binnein quartzite	too few axes	too few axes

(3) There is no relationship necessarily between the size and the direction of plunge in any particular formation.

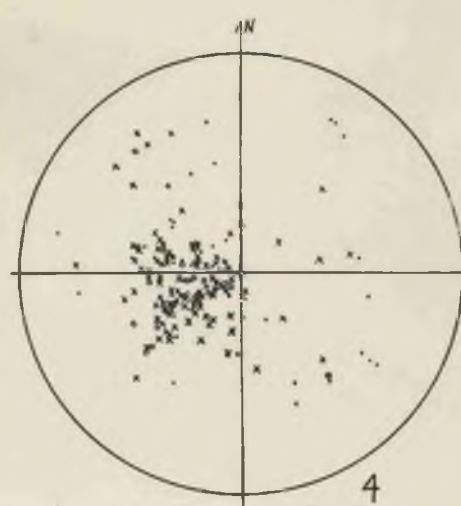
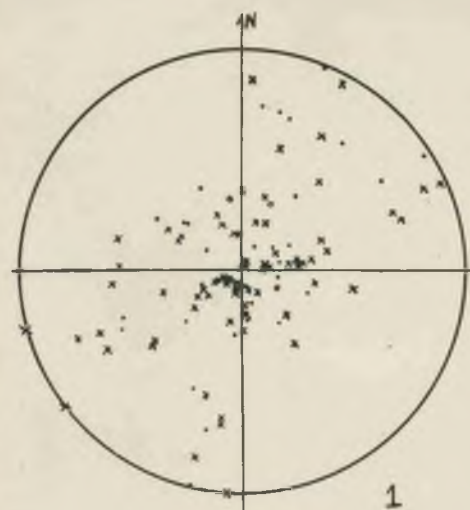
c. Stereograms based on geographic distribution of fold axes

Besides the general considerations of the distribution of fold axes on Map V, the fold axes have also been investigated from the point of view of areal distribution and rock type. For convenience Ballachulish and Glen Coe have been divided into major divisions.

II, III, and IV, as outlined on Map VI. In Text - Fig. 14 the folds are plotted on the lower hemisphere of a Wulff stereonet, an "o" for limestone, an "x" for quartzite and quartzose schist and a dot for slate, phyllite, and schist. The trends and plunges together with the prominent rock type and its plunges, are summarized in the following table.

	I	II	III	IV	Total Area	
Number of axes	107	33	73	161	374	
N.E.-S.W. trend	69%	62%	70%	52%	62%	
N.W.-S.E. trend	31%	38%	30%	48%	38%	
S.W. plunge	33%	41%	55%	47%	46%	
N.E. plunge	36%	21%	15%	6%	16%	
N.W. plunge	16%	29%	26%	38%	27%	
S.E. plunge	15%	9%	4%	9%	11%	
Prominent rock type	qtzte. & qtz. sch.	sl.	qtzte.	ls.	qtzte. & qtz. sch.	qtzte. & qtz. sch.
S.W. plunge	39%	38%	50%	56%	53%	48%
N.E. plunge	35%	23%	25%	16%	4%	18%
N.W. plunge	14%	31%	25%	26%	38%	25%
S.E. plunge	12%	8%	0%	2%	5%	9%

From these data it can be seen that there is a rough pattern in the heterogeneous scatter of arrows exclusive of the Sgòr na Ciche-Sgòr nam Fiannaigh-Caolasnacon section (Division from which a pattern has already been described. About two-th



Text-figure 14. Fold axes plotted on the lower hemisphere of a Wulff stereonet on the basis of geographic distribution and rock type;

1. Division I
2. Division II
3. Division III
4. Division IV
5. Total area



of the fold axes have a northeast-southwest trend and one-third northwest-southeast trend, and the southwesterly plunges are about twice as numerous as the northwesterly ones. Only in the Sgorr Dhearg-Meall a' Chaolais-Beinn Bhan section (Division I) are the northeasterly plunges as significant as the southwesterly ones; that is due to the structural control exercised by Appin quartzite and the Striped Transition Series.

In Division IV an almost equal number of folds have a northwest-southeast trend as have a northeast-southwest one, and the number of northwesterly plunges compares relatively closely with the number of southwesterly ones. However, the prominent rock types (Glencoe quartzite and Banded Passage Beds) tend to have a substantially larger number of southwesterly plunges than northwesterly ones. These rocks differ from their younger counterparts in Division I by having very few northeasterly plunges.

The plots for I, II, III, and IV have been put onto one stereogram to give the total area distribution. The picture, in general, is the same as that for I, II, and III. The folds occur mainly in the quartzites and quartzose transitional strata, in which the southwesterly plunges predominate substantially over the northwesterly plunges.

All of the fold axes have also been plotted on the lower hemisphere of a Schmidt stereonet, and the point diagram contour at 1%, 2%, 3%, and 4% (Text - Fig. 8). The double trend of the

axes shown by "b"-lineations (Text - Fig. 6) is less evident. one, and very pronounced, maximum has a west-southwest trend (6 with extremely variable plunges (between 34° - 92°), averaging 62° S.W. This compares quite favorably with the 68° , 45° S.W. plunge of the "b"-lineations. A small submaximum indicates a second trend of 168° , with plunges varying between 62° - 68° N.W. averaging 65° N.W. Again, this is similar to the 176° , 52° N. plunge of the "b"-lineations.

5. Axial direction

a. Construction

"Axial direction" involves the concept of "fold rhythm" (Wegmann, 1929, p. 104). It is a compilation of all fold axes within a given region, and is determined, not by averaging the individual fold axes themselves, but by plotting normals to all bedding planes in the area on tracing paper over the lower hemisphere of a Wulff stereonet. As in the geometrical construction of fold axes, the normals appear as points on the hemisphere and form a zone corresponding to a great circle if a large enough number are plotted. The axis of this great circle gives the axial strike and axial dip, which together are the axial direction (Text - Fig. 11). Owing to errors in measurement in the field to local modifications of structure a certain amount of scatter in points can be expected, and the zone frequently becomes a more or less broad girdle (compare Text - Figs. 10 and 11).

b. Stereograms and Map VI: Axial strikes and plunges

Wegmann, (1929, p. 105) suggests that a large area to be studied from the point of view of axial direction should be divided into quarters, and these portions treated statistically and separately -- the variations from one region to another then stand out clearer. He also recommends differentiating between rock types, because individual rocks have different deformation styles and rhythms.

Ballachulish and Glen Coe have been studied along these lines: (1) as a whole, (2) in four major divisions, and (3) in smaller subdivisions. The axial directions and boundaries of divisions and subdivisions are plotted on Map VI. The division boundaries are topographic: I includes Sgorr Dhearg, Beinn Fhàr, Beinn Bhàn, and Meall a' Chaolais; II includes Sgorr a' Choise, Gleann an Fhiod, and Cnocan Dubha; III includes Am Meall and Meall Mor; and IV includes Sgòr na Ciche, Sgòr nam Fiannaich, and An t-Sron. The subdivision boundaries are largely arbitrary for they necessarily depend a great deal upon the amount and density of field data, but topography has been used as far as possible as a basis of division.

(1) Total area

In Text - Fig. 12 all of the normals to bedding (ca. 1600) in the Ballachulish-Glen Coe area have been plotted on the lower hemisphere of a Wulff stereonet on the basis of rock type. There is a very broad scatter of points; the great circle drawn in

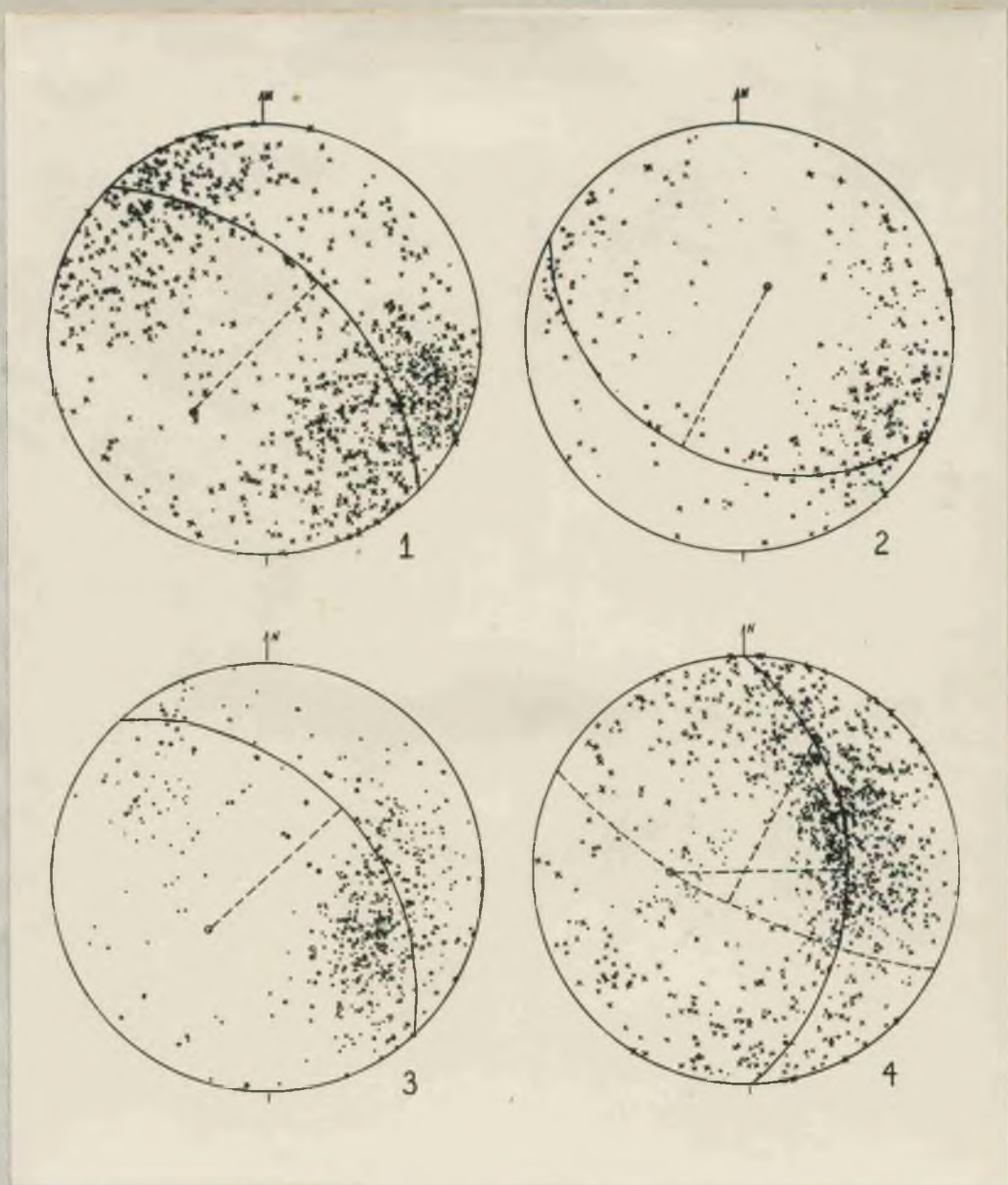
seems the best approximation to a girdle. The resultant axial strike is ca. 58° and the axial plunge ca. 50° S.W. Admittedly this axial direction is rather subjective. However, it comes quite close to the obvious trend of individual fold axes in the total compilation in Text- Fig. 14, D. 5, where the axial strike is roughly 54° and the axial plunge ca. 60° S.W. The lithology does not seem to have any marked control over the girdle pattern.

(2) Major divisions

The 1600 or so bedding normals have also been plotted according to their geographic distribution and rock type. In Text - Fig. 15 are the stereograms for the four major divisions outlined on Map VI. The axial strikes and plunges are tabulated below together with the general strikes and plunges to be inferred from the individual fold axis stereograms in Text - Fig. 14:

Division	Axial direction	General fold direction
I	44° , 40° S.W.	ca. 53° , 70° S.W.
II	29° , 60° N.E.	ca. 20° , 70° S.W. (too few data to be significant)
III	48° , 50° S.W.	ca. 56° , 45° S.W.
IV	90° , 50° W.	ca. 80° , 65° S.W.

The lithology seems important only in Division IV. In Text - Fig. 15, D. 4, the schist, phyllite, and slate have an axial strike of ca. 29° and an axial plunge of ca. 20° N.E. which is quite a deviation from the general axial strike of 90° and axial plunge of ca. 50° W. The pelitic strata seem to carry over the deformation style of Division II.



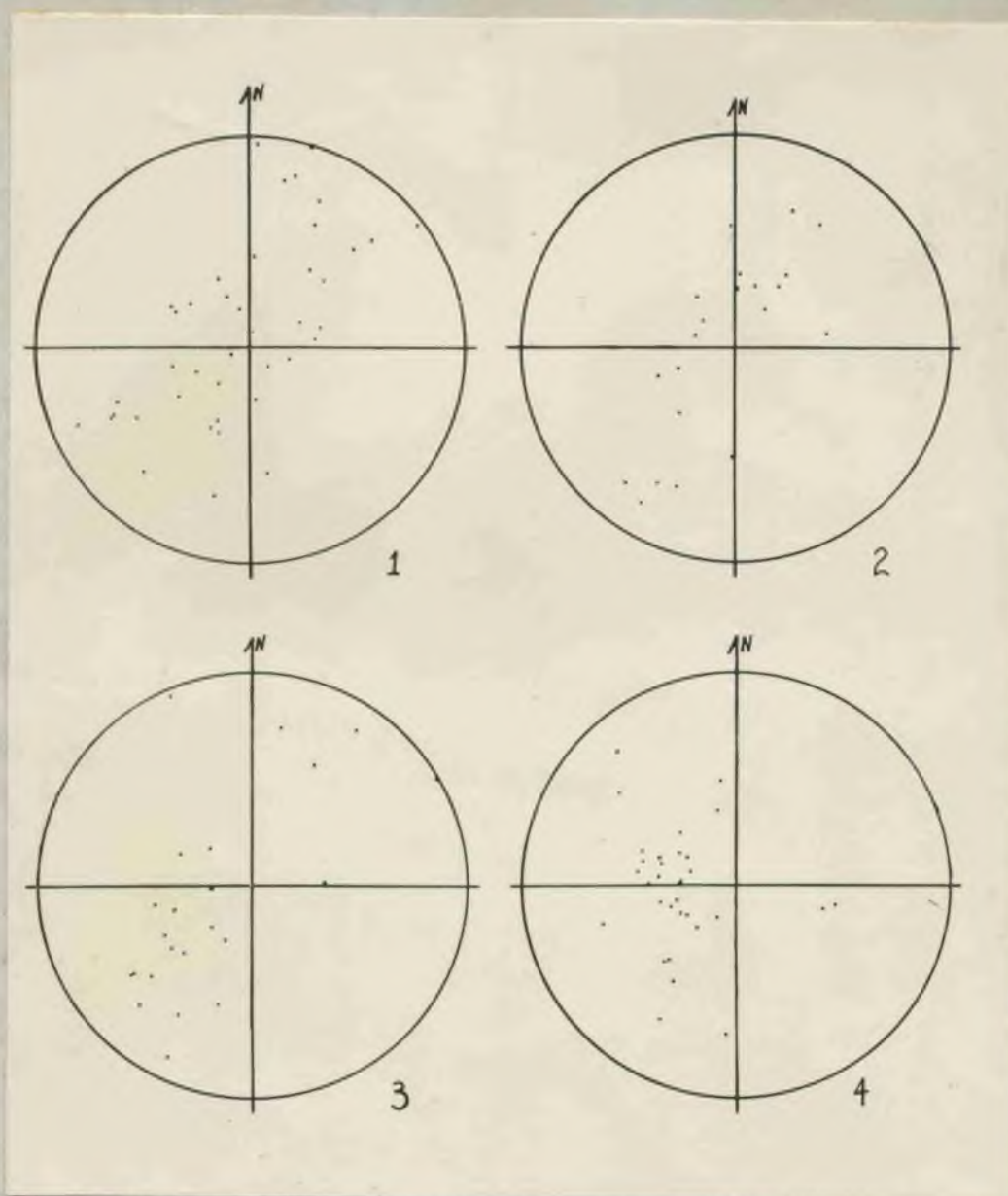
Text-figure 15. Poles to bedding planes plotted on the lower hemisphere of Wulff stereonet on the basis of geographic distribution and rock type:

1. Division I. Axial strike ca. 44° , axial plunge ca. 40° S.W.
2. Division II. Axial strike ca. 29° , axial plunge ca. 60° N.E.
3. Division III. Axial strike ca. 48° , axial plunge ca. 50° S.W.
4. Division IV. Axial strike in general ca. 90° , axial plunge ca. 50° axial strike for schist, phyllite and slate ca. 29° , axial plunge ca. 20° N.E.

(3) Subdivisions

The four divisions have been further subdivided in order to break down their axial directions into their component parts. For example, compare Text - Figs. 10, 11, and 15, D. 4. One of the typical individual folds in the shore section west of Caolasnaid farm has a trend of 67° and a plunge of 59° S.W. The axial direction for the subdivision of which the fold is a part is $79^{\circ}, 51^{\circ}$ S.W. -- a deflection to the west. The axial direction for the major division, IV, is $90^{\circ}, 50^{\circ}$ W. -- a further deflection towards the west.

Over Map VI as a whole the subdivision brings out the diversity of the axial directions which is otherwise masked to a large degree. The stereogram on Map VI is a plot of all of the subdivision axial directions. The distinct tendency for a northeast-southwest axial strike reflects the axial strike constructed in Text - Fig. 12 for all of Ballachulish and Glen Coe. In Text - Fig. 16 are plotted the axial directions within the four major divisions. There is certainly a pronounced tendency for northeast-southwest strike in divisions I, II, and III (D. 1-3) which compares favorably with the constructed divisional axial strikes in Text - Fig. 15, D. 1-3. The westerly tendency in Division IV (Text - Fig. 16, D. 4) corroborates the divisional axial strike constructed in Text - Fig. 15, D. 4, but there is a suggestion of the subsidiary northeast-southwest trend, too.



Text-figure 16. Axial directions plotted on the lower hemisphere of a Wulff stereonet on the basis of geographic distribution.

1. Division I
2. Division II
3. Division III
4. Division IV

CHAPTER VI: PETROFABRIC STRUCTURES

A. General principles of petrofabric analysis

The structural and textural features of a metamorphic rock are a response to the stress to which that rock has been subjected, and comprise its fabric. Petrofabrics is the study of these features and their spatial relations. When a rock is deformed without destroying the cohesion between the grains, it is called a tectonite. The metamorphic rocks in Ballachulish and Glen Coe fall into this category. Grain rotation, intragranular lattice displacement, and ionic migration may all give rise to a preferred orientation of the mineral constituents, and the resultant pattern is termed a deformation fabric. The pattern of the deformation fabric can be used to deduce the location of planes of weakness in the rock and to deduce directions of deformation in the area. 59 oriented thin-sections from 10 formations have been prepared and examined statistically for these purposes.

A statistical study of mineral orientation was not possible until 1925 when Schmidt improved the Federov Universal Stage, whereby a thin-section may be rotated into any position in space. The Universal Stage is fixed to the stage of a polarizing microscope so that the Universal Stage axes and the microscope axis intersect in a point lying in the plane of the thin-section centered in the field of view. A low-power objective is used.

Twenty-two minerals have been studied in this manner by structural petrologists, the most frequently used minerals being quartz, mica, and calcite. In this thesis 62 petrofabric analyses of quartz have been made from 59 hand specimens (Pl. XXXIV, D. 1-62). The lithologic representation is as follows:

Binnein quartzite, 4 diagrams; Glencoe quartzite, 13; Banded Passage Beds, Leven schist, 5; Ballachulish limestone, 7; Ballachulish slate, 1; Striped Transition Series, 9; Appin quartzite, 9; Appin phyllite, 1; Glenc granite, 1.

Preparation for petrofabric work begins in the field, for all rocks to be analysed statistically must be orientated geographically. The procedure has already been discussed in the comments on field work in the Introduction, Chapter I. As stated previously, hand-specimens are described in terms of three reference axes: "b", the direction of lineation, "a", at right angles to "b" and in the same foliation plane, and "c", normal to the "ab" plane. Tectonically, "a" is the direction of transport in a rock, and may be a direction of shearing or a direction of compression; "b" is normal to the direction of transport, lies in the plane of slippage, and coincides with the tectonic axis.

Inhomogeneities in grain fabric are greatly exaggerated in petrofabric analyses of thin-sections cut normal to the "a" and "c" megascopic reference axes. The "b" sections, cut normal to the tectonic axes, give the most reliable data; wherever possible, the thin-sections analysed in this thesis are perpendicular to linear features.

Fairbairn (1937, pp. 68-69) explains the differences in the value of the sections as follows:

"Superindividuals [i.e., aggregates of crystals acting as a single element] commonly break down to lens-shaped masses whose long axes are parallel to 'b' of the fabric. Study of separate lenses indicates their probable origin from a superindividual. The granulation of such a grain results in a group of smaller grains whose orientation is essentially the same as that of the parent superindividual. The best statistical measure of the fabric is therefore obtained from that section which includes the maximum number of the

lenses. Due to the arrangement of the long axes parallel to 'b', the 'b'-section shows the best profile, and is the one to be measured wherever possible.

"The same explanation holds for folds and ^faults. Their axes are parallel to the tectonic axis 'b' and as a result the most complete profile is seen in a 'b'-section. Measurement of this section gives the best statistical picture of the orientation and most reliable indication of the position of the 's' structural-surfaces".

B. Procedure for preparation and orientation of petrofabric diagrams

Only quartz, the most abundant tectonite mineral, has been studied petrofabrically for this thesis. "Its lattice orientation is determined through measurement of its vertical crystal axis ' c_v '.....No constant relation holds between lattice and dimensional orientations" (Fairbairn, 1949, p. 8). The geographic co-ordinates of the optic axis in a quartz grain are measured by rotation of the thin-section on the Universal Stage until the grain is at extinction, and noting the azimuth and inclination of the section on the A_1 and A_2 scales of the stage (See Haff, 1938 and 1942, for detailed procedure). These co-ordinates are plotted on the lower hemisphere of a Schmidt equal-area stereonet. The same procedure is carried out for each quartz grain in successive traverses across the thin-section until about 300 optic axes have been measured. The upper glass hemisphere mount should be the type with a Schmidt sledge attached so as to provide a common starting point for each traverse. The upper and lower glass hemispheres must have the same index of refraction. If the index of refraction is not the same as that of quartz, the readings must be corrected by using Plate I in A. Winchell's Principles of optical mineralogy which gives the graphical correction of Universal Stage angles necessary for differences in indices of refraction of the mineral crystal and hemisphere glass. The resultant point diagrams are then contoured to bring out the areas of density (Haff, 1938, pp. 558-565).

The petrofabric diagram is oriented geographically by the arrow which is on both the thin-section and the plane of the thin-section on the hand-specimen. The angle between the normal to the base of the thin-section (the 0° position A_1 of the Universal Stage) and the arrow shaft is measured and plotted to the right or left of the zero (Λ) position on the periphery of the diagram. A small geographically oriented sketch of the structural data of the rock being studied (bedding, cleavage, lineation, fold axis, axial direction, plane of thin-section and position of the arrowhead) is drawn on tracing paper over the lower hemisphere of a stereonet. The distance on the plane of thin-section (P_T) between the arrowhead (A) and the intersection of P_T with the bedding (P_B) is plotted on the periphery of the petrofabric diagram. The distance between the normal to P_T and the normal to P_B is measured by rotating the tracing paper until both points lie on the same great circle. This distance is then plotted on the petrofabric diagram by rotating the paper until the intersection of P_T and P_B lies on the horizontal axis of the net and both normals lie on the same great circle, i.e., the vertical axis of the net. The paper is then rotated until the intersection of P_T and P_B lies on the vertical axis; the trace of P_B is drawn 90° away from the pole to P_B . The same procedure is followed in plotting the geographic horizontal (P_H), flow cleavage (P_{FL}), false cleavage (P_{FR}) and joint planes (P_J).

C. Analysis of the Ballachulish-Glen Coe petrofabric diagrams

1. Relation of quartz orientation to maxima

Sander's fracture hypothesis has become the basis of petrofabric studies. According to him, quartz grains under deformation are first fractured into needles whose dimensional axes are parallel to the

crystallographic axes. These needles then become rotated roughly into the planes of shear with their dimensional axes parallel to the direction of movement. Subsequent recrystallization may destroy the distinctive needle shape but the orientation of the crystal axes remains the same. (Fairbairn 1949, p. 117). It is the orientation of the "c" crystal axis which is measured for quartz petrofabric diagrams. The areas of maximum concentration of this "c"-axis are significant in determining the type of lattice orientation in a rock fabric.

Hietanen (1938, pp. 35-36) describes quite clearly the detailed mechanism of quartz deformation as far as it is understood:

"When strain first acts upon an undeformed quartz lattice, gliding along (0001) takes place, but only to a limited extent, as the translations in the quartz lattice are slight. This gliding is connected with glide-folding and unruptural strain shadows. In the continued deformation there appear Böhm striations or ruptural strain shadows, or both together. In the case of Böhm striations the gliding causes a feeble breaking of the crystal lattice.....

"When the mechanical strain...grows stronger, fractures appear perpendicular to the Böhm lamellae and gliding along the prism faces begins. In other cases the gliding along (0001) has taken place in the beginning of deformation only to so limited an extent that Böhm striations do not appear at all. During the continuation of the deformation the quartz lattice breaks also in this case into needles parallel to the c-axis.

"This breaking seems to be the process in which the quartz lattice is able to 'turn its front'. This turning of front may take place in such a way that one or another of the three preferred translation directions turns parallel to the glide direction caused by a shear... The Si-atoms build the lattice planes of the closest packing parallel to the gliding and one or another of the gliding surfaces is formed, subparallel to the shear surface.

"The characters of the gliding parallel to (0001) and parallel to the prism planes are different. In the former case the gliding at first seems to proceed smoothly and to be accompanied by glide folding (undulose extinction) but soon it causes broad streaks of twinning along rhombohedral faces or broken zones in the quartz lattice (Böhm striations), whereas in the latter case breaks appear as fine ruptures parallel to the c-axis. The friction in the translation along (0001) seems to increase to such an extent as to set a limit to gliding in this plane, and it is probably at this stage that breaking takes place instead of continued glide-folding... Besides immediate breaking of the lattice, gliding along the prism faces in the direction [0001] must be assumed".

It has been discovered experimentally that there are eight possible positions of maximum concentrations in relation to the "b" direction, which is the direction of the tectonic axis, and to the "a" direction, which is the direction of transport. Fairbairn (1949) has plotted the distribution of maxima types on a stereonet in Fig. 9-2 (p. 119).

In order to determine the patterns of maximum quartz concentrations in Ballachulish and Glen Coe, the 62 petrofabric diagrams were rotated in terms of "b" and "a", that is, so that "b" and "a" in turn became the centre of the diagram (see Pl. XXXV, D. 1-62). The resultant schematic distribution of maxima (solid circles) and submaxima (open circles) in each case were then compared with Fairbairn's Fig. 9-2, and classified in the explanation of D. 1-62, Pl. XXXIV.

Fairbairn lists the abundance of types of maxima as follows: most common, I, IV, and VI; less common, III; still less common, II; and least common, V, VII, and VIII (p. 120). In Ballachulish and Glen Coe the maxima on 47 diagrams are either type IV or VI or transitional between the two, three diagrams have type II, and the remainder are indecisive.

2. Relation of quartz orientation to girdles

As deformation is not a static thing, minor changes in the direction of stress are reflected in minor changes in the direction of the quartz optic axes in the deformed strata. The resultant pattern of optic axis concentrations is a girdle associated with the maxima.

Girdles, like maxima, have been classified into several types, significant tectonically. The patterns are shown diagrammatically by Fairbairn (1949, p. 10 Fig. 2-1), and have been compared with the diagrams in Pl. XXXV to determine the kinds of girdles in Ballachulish and Glen Coe. According to Fairbairn (p. 122) the "ac" girdle is the most common. This is certainly true in this area. A count of the various patterns listed in the plate explanations for D. 1-62, Pl. X reveals 52 "ac" girdles, 26 "bc", 10 "ab", and eight others.

The "ac" girdle is thought to be due to forward movement parallel with "a" plus a rotational movement about "b". There are three hypotheses about the latter rotation: (a) it could be due to grain rotation relative to fixed strain axes, which would make maxima I, IV, and VI the controlling orientations for the development of a girdle parallel to "ac"; (b) it could be due to rotation of strain axes around "b" relative to a fixed grain position; thus, "ac" girdles could form through successive changes of the movement direction without any necessary rotation of grains; "b" would...be the intersection line of an unlimited number of 's' [structural] -surfaces" (Fairbairn, p. 122); (c) it could be due to the formation of microfolds, for a complete "ac" girdle is formed by the flexing of a structural surface in which the quartz axes have developed only incomplete girdles.

Usually, where there is rotation about "b", the rock is a B-tectonite that is, the axis of the fabric girdle (B) is coincident with the "b" tectonic axis. This applies to all of the metamorphic rocks analysed from Ballachulish and Glen Coe. Whether "b" in any particular instance is an axis of external or internal rotation can not be determined from the contour pattern, for an "ac" girdle is equally characteristic of both types. However, when this can be determined from field evidence, the rocks whose fabrics are predominantly the result of flexure or flexure-slip are termed R-tectonites (Sander, 1930, pp. 220-222). Examples are found in D.10, 13, 15-20, 24, 26, 27, 29-32, and 38 of Pl. XXXIV.

Sometimes there are two girdles present in the same quartz fabric (Pl. XXXIV, D. 1, 2, 4-9, 13, 16, 17, 21-23, 27, 28, 36, 41-48, 51, 53, 55, 56, 59, 61), in which case the rocks are called B \wedge B'-tectonites (Sander, 1930, pp. 239-243). The normal to the more complete girdle is taken as "B" and the normal to the other one as "B'". A B \wedge B'-tectonite is caused by the superposition of two deformation patterns which may be unrelated or which may be two phases of the same general movement.

In most cases the two girdles intersect at approximately right angles; these rocks are termed B \perp B'-tectonites (all diagrams listed above except 5, 23, 27 and 45). Turner [1948, (1), p. 220] states that B \perp B'-tectonites are the most widely distributed class of B \wedge B'-tectonites, a fact borne out by the Ballachulish-Glen Coe diagrams, and "the B \perp B' pattern therefore seems to be a stable pattern rather than an unstable transitional type of fabric".

Over half (18) of the 31 diagrams cited above have an "ac" girdle (i.e., normal to the $b=B$ of the megascopic fabric) accompanied by a partial "bc" girdle (i.e., normal to the $a=B'$ of the megascopic fabric) (D. 4, 6-8, 17, 22, 36, 41-44, 46, 51, 53, 55, 56, 59, 61).

"Girdles parallel to 'bc' are conventionally interpreted as resulting from some degree of rotation about 'a' $\angle=B'$..., during a deformation in which the main axis of rotation was still 'b' $\angle=B$... Possible rotations about 'a' include external rotation of individual mineral grains and internal rotation of slip planes, both of which are pictured as movements that accompany a general elongation of the deformed mass parallel to 'b', such as certainly occurs when a complex strain ('crossed strain') develops as a result of rotational kneading transverse to 'b' $\angle=B'$." Turner, 1948, (1), pp. 221-227.

Seven of the 31 diagrams have an "ac" girdle accompanied by a partial "ab" girdle (i.e. normal to the $c=B'$ of the megascopic fabric) (D. 1, 2, 9, 13, 16, 21, 48). This combination is virtually ignored by Turner and Fairbairn. Hietanen (1938), however, describes several "ab" girdles from the Karelidic quartzites of Finland. In these cases "prism planes have acted as gliding surfaces and ruptural grain deformation has been dominant" (p. 111).

Different combinations of quartz planes parallel to shearing planes and glide directions parallel with "a" explain the "b'c" and "a'b" girdle combination of D.47, the four BAB' diagrams -- D.5 ("ac" girdle plus one extending from "b3" between "a3" and "c"), D.23 ("ac" girdle plus one extending from "b" between "a" and "c"), D.28 (two girdles passing through "c" and symmetrically inclined to "a" and "b"), and D. 45 ("b'c" girdle plus one extending from "a'" between "b'" and "c") -- and the one example of three girdles, D. 27 ("bc" and "ac" girdles plus one inclined to "ab"

3. Relation of girdle patterns to linear structures

Many of the diagrams on Pl. XXV show an interesting relation between girdle patterns and linear structures. If a lineation on a foliation surface is conventionally selected as the "b" direction, structurally direction of the tectonic axis what happens in the cases where there more than one lineation? Which lineation is "b"? Take as an example D. 2a, b, c, and d on Pl. XXXV. The petrofabric diagram D. 2 on Pl. XX has been rotated in terms of the four lineations L_1 , L_2 , L_3 , and L_4 , in each instance assuming that $L = "b"$. "a" has been located 90° away from "b" and in the same foliation plane, and the petrofabric diagram been rotated also in terms of a_1 , a_2 , a_3 , and a_4 . The resultant patterns are : one girdle symmetrical about b_3 (L_3), one girdle slightly distorted about b_1 (L_1), and two girdles unsymmetrical with respect to b_2 (L_2) and b_4 (L_4). From these sketches the dominant structural control seems to be exercised by b_3 . Whether this control was stronger than the others or whether it was later and thus not partially obliterated can not be deduced. Now compare these data with the causes of lineation stated in the plate explanation for D. 2, Pl. XXXIV. L_3 is due to bedding intersecting flow cleavage. As seen in Chapter V, this intersection gives direction and plunge of the fold axis. Thus the girdle pattern in D. is due to rotation about the tectonic axis. L_1 is due to slippage on flow cleavage foliation. This direction happens to be near to L_3 , and so the girdle pattern is only slightly distorted. The other two lineations

are due to false cleavage intersecting flow cleavage. Unlike the case of L_3 , these intersections do not parallel fold axes. As the patterns are unsymmetrical but roughly the mirror-image of each other, it may suggest that the false cleavages are actually a pair of shear planes which developed approximately 45° to the direction of compression.

Similar reasoning may be applied to the girdle patterns in D. 1, 7, 10, 11, 14, 15, 16, 18, 19, 20, and 21, Pl. XXV. In D. 14 a and b for example, the patterns are the reverse of one another, i.e., " b_1 " " a_2 " are the same, " b_2 " and " a_1 " are the same. L_2 , taken to equal " b_1 " on the diagram, is due to the trace of axial plane flow cleavage on bedding foliation and thus marks the direction of the fold axis. This justifies the assumption that $L_2 = b_2$. L_1 , taken to equal b_1 , is due to the trace of false cleavage on bedding foliation. From field data it is known to be nearly normal to the fold axis, thus, it is an "a"-lineation. As "a"- and "b"-lineations are perpendicular to each other, it is to be expected to find two symmetrical sets of girdles, the one with the fold as the tectonic axis the centre of rotation and consequently having an "ac" deformation plane, the other one with "bc" the deformation plane.

4. Symmetry of fabric

Symmetry of the lattice orientation in metamorphosed strata is closely linked to the patterns of movements which deformed the rock. Orthorhombic symmetry results from simultaneous movement on two sets of structural planes which are symmetrical with respect to the compressive force; "ab", "bc", and "ac" are symmetry planes [Turner, 1948, (1), p. 192]. Monoclinic symmetry is produced by laminar slip in one direction on a single set of structural planes (p. 189); the deformation plane "ac" is the one plane of symmetry. Triclinic symmetry develops when external rotation about "b" occurs together with rotation of sl

about "a" or "c" or when one monoclinic deformation is superposed on another, and the axis of the two movements do not coincide (BAB'); there are consequently no planes of symmetry.

Only monoclinic and triclinic symmetry have been observed in the petrofabric diagrams for Ballachulish and Glen Coe. By far the greater proportion have a triclinic pattern (see plate explanations for D. 1-4 Pl. XXXIV). As Turner says (p. 191), this does not necessarily imply more than one period of metamorphism. Minor changes in the orientation of tectonic axis during a single major deformation would also change the direction of slip.

5. Homogeneity of fabric

Petrofabric diagrams from the same locality, e.g. from adjacent limbs (D. 30, VB117, and D. 31, VB118, Pl. XXXIV) or from opposite limbs of a folded band (D. 13, VB101, and D. 27, VB100) may show some variation of data because of imperfections in method and because of minor differences in the rocks themselves. A comparison of D. 30 and D. 31 from the same limb of a plunging fold shows general agreement but not down to the last detail. In both cases "ac" is the deformation plane, the type of tectonism is $R=F(b)$, the type of lattice orientation is "h", with maximum IV, and the fabric symmetry is triclinic. But D. 31 also has a maximum II, and D. 30 suggests that the lineation is due to axial plane cleavage, a fact which is borne out in the field.

A comparison of D. 13 and D. 27, which are the fabrics of the upper and lower limbs respectively of a horizontal recumbent fold in Binnear quartzite (Pl. I, Fig. 2), together with their plate explanation,

indicates that the quartz in both cases has a crystallographic orientation parallel to the flow cleavage and roughly to the bedding (the "ab" plane). In other words, the predeformational pattern has only been partially obliterated. In both cases $R=F(b)$ and the girdle and maxima patterns are indecisive, and there is a suggestion of a possible pair of shear planes inclined with respect to the fold axis $F(b)$. However, D. 13 is a $B \perp B'$ -tectonite, whereas D. 27 is a $B \wedge B'$ one. Obviously in reality they should be, and are, the same. Petrofabric diagrams studied collectively from one area should, therefore, be used in a general way, and not too specifically.

6. Map VII: Geographic orientation of quartz optic axes

Over the entire Ballachulish-Glen Coe section the metamorphic rocks obviously have a heterogeneous pattern. This is evident from Map VII on which are plotted 56 petrofabric diagrams geographically oriented. The heterogeneity is not unexpected, however for "the fabric of a rock that has been affected by pure flexure or by flexural-slip is obviously inhomogeneous within the field of a complete fold, although within a small field, one of the limbs for instance, it may be substantially homogeneous" [Turner, 1948, (1), p. 193]. As seen in Chapter IV, flexure and flexural-slip folds are quite common in Ballachulish and Glen Coe.

As "ac" girdles are normal to tectonic axes the trend and plunge of "b" (=B) axes can be deduced from the orientation of these girdles. With the exception of the 11 diagrams at localities 23, 73, 76, 90, 158, 300, 395, 403, 406, 431, and 563, the girdles shown on Map VII are all, at least in part, the "ac" type. Their "b"-axes have the following geographic distribution:

Direction of plunge	Division I	Division II	Division III	Division IV	Total deduced fold axes	Total measured fold axes
N.W.	3	2	5	3	13 (29%)	27%
N.E.	2	1	0	3	6 (13%)	16%
S.W.	3	2	1	10	16 (36%)	46%
S.E.	1	0	3	2	6 (13%)	11%
Vertical	1	1	0	2	4 (9%)	

Unfortunately the data for the major divisions are too sparse to make a valid comparison with the geographic distribution of fold axes discussed in Chapter V, B., 4c. The figures for the total area, however, are more significant, and are given in percentages for comparison with the percentages for measured fold axes over the total area. In general, the two kinds of data tally quite well, but there is a greater preponderance of measured fold axes with a southwesterly plunge.

A closer correspondence of the data can not really be expected.

"As the mechanism of orientation of quartz is imperfectly known, its use in regional problems is at best a 'fingerprint' method by which consistent differences in orientation from place to place can be observed. The 'fingerprint' application is useful, however, in an empirical way...Each areal investigation of orientation in tectonites provides an additional link in the chain of data which, if not immediately comprehensible, nevertheless, adds to our factual reserve" (Fairbairn, 1949, pp. 191, 194).

SUMMARY AND CONCLUSIONS

The Ballachulish and Glen Coe area has been examined in detail in an attempt to deduce its tectonic pattern and history. For this purpose field and laboratory data have been collected and analysed, embracing all scales of structures from large-scale regional folds to the microscopic structures and fabric orientations shown in thin-section. The features of particular value have been the alignment of planar structures (bedding, flow cleavage, and false cleavage), the alignment of linear structures (lineations, fold axes, and axial directions), and petrofabric structures. Petrofabric analysis is a relatively new approach to tectonics and has only been applied to a limited degree to tectonic problems, especially in Great Britain. Determination of the crystallographic orientation of mineral constituents has been found by the author not only to help a great deal in correlating and explaining the megascopic and microscopic structures but also to supplement these data in the synoptic study of the whole area under consideration.

The various lines of examination enumerated above corroborate each other to a significant degree, and indicate that there is no one simple, uniform regional pattern, but rather two main structural directions, the predominant one trending in general northeast-southwest and plunging southwest, and a subsidiary one trending in general northwest-southeast and plunging northwest. The former is illustrated by the following data:

- (1) the northeast-southwest alignment of the lithologic contacts exclusive of those on Sgòr na Ciche and Sgòr nam Fiannaidh
- (2) the northeast-southwest alignment of bedding strikes
- (3) the general northeast-southwest pattern of flow cleavage strikes

- (4) the roughly northeast-southwest pattern of one of the two trends of false cleavage strikes
- (5) the southwesterly plunge of most of the lineations
- (6) the southwesterly plunge of the majority of fold axes and axial directions
- (7) the southwesterly plunge of the largest proportion of tectonic axes deduced from petrofabric girdles.

The subsidiary direction is shown by the following data:

- (1) the northwest-southeast alignment of the lithologic contacts on Sgòr na Ciche and Sgòr nam Fiannaidh
- (2) the roughly northwest-southeast pattern of the second of the two trends of false cleavage strikes
- (3) the northwesterly plunge of a substantial minority of lineations
- (4) the northwesterly plunge of a substantial minority of fold axes and axial directions
- (5) the northwesterly plunge of a significant proportion of tectonic axes deduced from petrofabric girdles.

From the field and laboratory data it can not be ascertained definitely whether the subsidiary structural direction preceded, accompanied, or followed the development of the major trend. Certainly both directions post-date the deposition and consolidation of Appin phyllite, the youngest formation studied in the area. Intermediate directions are probably due to local modifications of the deformation movement or movements which caused the northeast-southwest and northwest-southeast trends.

The structural pattern of a dynamically metamorphosed area can be constructed by using the types of data described in this thesis, but the elucidation of the tectonic history is not usually possible from the examination of only one limited area. The determination of the tectonic history of Ballachulish and Glen Coe must await the results of similar structural studies in adjoining areas of the Scottish Highlands.

BIBLIOGRAPHY

- AGRON, S. L. 1950. "Structure and petrology of the Peach Bottom slate, Pennsylvania and Maryland, and its environment". Geol. Soc. Am., Bull., v. 61, pp. 1265-1306.
- _____. 1950. "Deformation in the Peach Bottom syncline". Am. Geophys. Union, Trans., v. 31, pp. 262-266.
- ANDERSON, E. M. 1948. "On lineation and petrofabric structure and the shear movement by which they have been produced". Geol. Soc., Quart. Jour., v. 104, pp. 99-132.
- ANDERSON, J. G. C. 1945. "High-grade silica rocks of the Scottish Highlands islands". Geol. Surv. Gt. Brit., Wartime Pamphlet, n. 7, pp. 7-10, 24.
- _____. 1945. "Limestones of Scotland. Area IV. South-west Highlands and islands". Geol. Surv. Gt. Brit., Wartime Pamphlet, n. 1, pp. 14, 16, 20.
- BAILEY, E. B. 1910. "Recumbent folds in the schists of the Scottish Highlands". Geol. Soc., Quart. Jour., v. 66, pp. 586-618.
- _____. 1914. "The Ballachulish fold near the head of Loch Creran (Argyllshire)". Geol. Soc., Quart. Jour., v. 70, pp. 321-327.
- _____. 1916. "The geology of Ben Nevis and Glen Coe (Explanation of Sheet 53)". Geol. Surv. Gt. Brit., Memoir, n. 53, esp. pp. 188-203.
- _____. 1922. "The structure of the South-west Highlands of Scotland". Geol. Soc., Quart. Jour., v. 78, pp. 82-131.
- _____. 1930. "New light on sedimentation and tectonics". Geol. Mag., v. 67, pp. 77-92.
- _____. 1934. "West Highlands tectonics: Loch Leven to Glen Roy". Geol. Soc., Quart. Jour., v. 90, pp. 462-525.
- _____. 1936. "The Ballachulish lag at Callert, Loch Leven". Geol. Mag., v. 73, pp. 412-414.
- _____. 1938. "Eddies in mountain structure". Geol. Soc., Quart. Jour., v. 94, pp. 607-625.
- _____. 1953. "Facies changes versus sliding: Loch Leven, Argyll". Geol. Mag., v. 90, pp. 111-113.
- BALK, R. 1936. "Structural and petrologic studies in Dutchess County, New York. Part I: Geologic structure of sedimentary rocks". Geol. Soc. Am., Bull., v. 47, esp. pp. 699-753.

BIBLIOGRAPHY (continued)

- _____. 1952. "Fabric of quartzites near thrust faults". Jour. Geol., v. 60, pp. 415-435.
- _____. 1953. "Faltenachsen in Überschiebungszonen". Geol. Rund., B. 41 pp. 90-103.
- BILLINGS, M. P. 1942. Structural geology. New York: Prentice-Hall, Inc., esp. pp. 12-98.
- BIRCH, F. and BANKCROFT, D. 1940. "New measurements of the rigidity of rock at high pressure". Jour. Geol., v. 48, pp. 752-766.
- BOSWELL, P. G. H. 1918. British resources of sands and rocks used in glass making. London: Ministry of Munitions of War, 2nd ed., p. 155.
- BROUGHTON, J. G. 1946. "An example of the development of cleavages". Jour. Geol., v. 54, pp. 1-18.
- CH'IH, C. 1950. "Structural petrology of the Wissahickon schist near Philadelphia, Pennsylvania". Geol. Soc. Am., Bull., v. 61, pp. 923-955.
- CLARK, R. H. and MCINTYRE, D. B. 1951. "The use of the terms pitch and plunge". Am. Jour. Sci., v. 249, pp. 591-599.
- CLOOS, E. 1946. "Lineation; a critical review and annotated bibliography". Geol. Soc. Am., Memoir, n. 18, 122 pp.
- _____. et al. 1949. New list of map symbols. Washington: U. S. Geological Survey, 6 pp.
- _____. 1953. "Lineation; review of literature 1942-1952". Geol. Soc. Memoir, supplement to n. 18, 14 pp.
- FAIRBAIRN, H. W. 1935. "Notes on the mechanics of rock foliation". Jour. Geol., v. 43, pp. 591-608.
- _____. 1937. Structural petrology. Kingston, Canada: Queen's University, esp. pp. 56-69.
- _____. 1949. Structural petrology of deformed rocks. Cambridge Mass.: Addison-Wesley Press, 344 pp.
- FELLOWS, R. E. 1943. "Recrystallization and flowage in Appalachian quartzites". Geol. Soc. Am., Bull., v. 54, pp. 1399-1432.
- FISHER, D. J. 1952. "Crystallographic projections nomenclature dilemma". Am. Min., v. 37, pp. 857-860.

BIBLIOGRAPHY (continued)

- GREEN, J. F. N. 1931. "The South-west Highland sequence". Geol. Soc., Quart. Jour., v. 87, esp. pp. 517-521, 526-529.
- GUPPY, E. M. 1931. "Chemical analyses of igneous rocks, metamorphic rocks and minerals". Geol. Surv. Gt. Brit., Memoir, pp. 126, 129.
- HAFF, J. C. 1938. "Preparation of petrofabric diagrams". Am. Min., v. 23, pp. 543-574.
- _____. 1942. "Federow method (universal stage) of indicatrix orientation". Colorado School of Mines, Quarterly, v. 37, pp. 3-28.
- HARDIE, W. G. 1952. "The Lochaber series south of Loch Leven, Argyllshire". Geol. Mag., v. 89, pp. 273-285.
- _____. 1953. "Facies changes versus sliding - a reply". Geol. Mag., v. 90, pp. 114-116.
- HARKER, A. 1939. Metamorphism. London: Methuen & Co., esp. pp. 152-271, 323-331.
- HIETANEN, A. 1938. "On the petrology of Finnish quartzites". Comm. géol. Finlande, Bull., v. 122, 118 pp.
- HILLS, E. S. 1943. Outlines of structural geology. New York: Nordeman Publishing Co., Inc., pp. 69-125.
- HOLMES, A. 1930. Petrographic methods and calculations. London: Thomas Murby & Co., pp. 372-383.
- KESSLER, D. W. 1927. "Building stones". International Critical Tables. New York: McGraw-Hill Book Co., v. 2, pp. 47-49.
- KNOPF, E. B. 1933. "Petrotectonics". Am. Jour. Sci., s. 5, v. 25, pp. 433-454.
- _____. and INGERSON, E. 1938. "Structural petrology". Geol. Soc. Am. Memoir, n. 6, 270 pp.
- KVALE, A. 1945. "Petrofabric analysis of a quartzite from the Bergsdalen quadrangle, western Norway". Norsk Geol. Tidssk., v. 25, pp. 193-215.
- _____. 1948. "Petrologic and structural studies in the Bergsdalen quadrangle, western Norway. Pt. II. Structural geology". Bergens Museums Arbok 1946 og 1947, Natur. rekke, n. 1, esp. pp. 11-64.
- _____. 1953. "Linear structures and their relation to movement in the Caledonides of Scandinavia and Scotland". Geol. Soc., Quart. Jour., v. 190, pp. 51-73.

BIBLIOGRAPHY (continued)

- LADURNER, J. 1950. "Beiträge zur Typisierung von Quarzfalten". Tscher. und petrog. Mitt., s. 3, b. 2, pp. 47-66.
- LEITH, C. K. 1905. "Rock cleavage". U. S. Geol. Surv., Bull., n. 239, 2.
- LOVERING, T. S. 1928. "The fracturing of incompetent beds". Jour. Geol. v. 36, pp. 709-717.
- MCINTYRE, D. B. 1950. "Note on two lineated tectonites from Strathavon, Banffshire". Geol. Mag., v. 87, pp. 331-336.
- _____. 1950. "Note on lineation, boudinage, and recumbent folds the Struan flags (Moine), near Dalnacardoch, Perthshire". Geol. Mag. v. 87, pp. 427-432.
- _____. 1951. "Note on the tectonic style of the Ord Ban quartzite mid-Strathspey". Geol. Mag., v. 88, pp. 50-54.
- _____. 1951. "The tectonics of the area between Grantown and Tomintoul (mid-Strathspey)". Geol. Soc., Quart. Jour., v. 107, pp. 1.
- MCKEE, E. D. and WEIR, G. W. 1953. "Terminology for stratification and of stratification in sedimentary rocks". Geol. Soc. Am., Bull., v. 64, pp. 381-390.
- MCKINSTRY, H. E. 1953. "Shears of the second order". Am. Jour. Sci., v. pp. 401-414.
- MEAD, W. J. 1940. "Folding, rock flowage, and foliate structures". Jour. Geol., v. 48, pp. 1007-1021.
- MUIR, I. D. 1953. "A local potassic modification of the Ballachulish granodiorite". Geol. Mag., v. 90, pp. 182-192.
- OFTEDAHL, C. 1950. "Petrology and geology of the Rondane area". Norsk Geol. Tidssk., v. 28, pp. 210-219 (chapter on tectonics).
- PHEMISTER, J. et al. 1946. "Roadstone: geological aspects and physical Dept. Scientific and Industrial Research, Road Research, Special Report n. 3, pp. 25-31.
- PHEMISTER, T. C. 1952. "The use of quartz as an index of movement in tectonites of metamorphic origin". 19th International Geol. Congress Compt. Rend., Sect. III, Mécanique de la déformation des roches, pp. 1.
- PHILLIPS, F. C. 1937. "A fabric study of some Moine schists and associated rocks". Geol. Soc., Quart. Jour., v. 93, pp. 581-620.

BIBLIOGRAPHY (continued)

- _____. 1954. "The micro-fabric of the Moine schists". Geol. Mag.
v. 82, pp. 205-220.
- _____. 1949. "Lineation in Moinian and Lewisian rocks of the
Northern Highlands of Scotland". Geol. Mag., v. 86, pp. 279-287.
- _____. 1951. "Lineation in schists southeast of the Great Glen".
Geol. Mag., v. 88, pp. 71-72.
- PINCUS, H. J. 1951. "Statistical methods applied to the study of rock
fractures". Geol. Soc. Am., Bull., v. 62, pp. 81-130.
- _____. 1952. "Some methods for operating on orientation data". Geol.
Soc. Am., Bull., v. 63, pp. 431-434.
- RAMSAUER, H. 1941. "Achsenverteilungsanalysen an Quarztektoniten". Inst.
Min. Pet., Deut. Alpen-Universität Innsbruck, Bibliotheks, n. 304, pp.
- READ, H. H. and MACGREGOR, A. G. 1948. "The Grampian Highlands". Geol. S.
Gt. Brit., Regional Guide, esp. pp. 25-27, 30-34.
- RICHEY, J. E. 1948. "Pre-metamorphism cleavage in the Moine schists of Mo
western Inverness-shire". Edinburgh Geol. Soc., Trans., v. 14, pp. 200
- RODGERS, J. 1952. "Use of equal-area or other projections in the statisti
treatment of joints". Geol. Soc. Am., Bull., v. 63, pp. 427-430.
- SANDER, B. 1930. Gefügekunde der Gesteine. Vienna: J. Springer, 358 pp.
- _____. 1942. "Über Flächen und Achsengefüge (Westende der Hohen Tauern
III. Bericht.)." Mitt. Reichsamts für Bodenforschung, v. 4, pp. 1-94
- _____. 1948. Einführung in die Gefügekunde der geologischen Körper.
Pt. I. Allgemeine Gefügekunde und Arbeiten im Bereich Handstück bis
Profil. Vienna: Springer-Verlag, 215 pp.
- _____. 1950. Einführung in die Gefügekunde der geologischen Körper.
Pt. II. Die Korngefüge. Vienna: Springer-Verlag, 409 pp.
- STRAND, T. 1945. "Structural petrology of the Bygdin conglomerate". Norsk
Geol. Tidssk., v. 24, pp. 14-31.
- _____. 1951. "The Sel and Vågå map areas: geology and petrology of a
part of the Caledonides of central southern Norway". Norges Geol.
Undersøkelse, n. 178, pp. 26-37 (chapter on tectonics).
- SWANSON, C. O. 1927. "Notes on stress, strain, and joints". Jour. Geol.,
v. 35, pp. 193-223.

BIBLIOGRAPHY (continued)

- _____. 1941. "Flow cleavage in folded beds". Geol. Soc. Am., Bull., v. 52, pp. 1245-1264.
- TANTON, T. L. 1930. "Determination of age-relations in folded rocks". Geol. Mag., v. 67, pp. 73-77.
- TILLEY, C. E. 1925. "Metamorphic zones in the Southern Highlands of Scotland". Geol. Soc., Quart. Jour., v. 81, pp. 100-110.
- TURNER, F. J. 1948. "Mineralogical and structural evolution of the metamorphic rocks". Geol. Soc. Am., Memoir, n. 30, 342 pp., esp. pp. 149-282.
- _____. 1948. "Review of current hypotheses of origin and tectonic significance of schistosity (foliation) in metamorphic rocks". Am. Geophys. Union, Trans., v. 29, pp. 558-564.
- _____. 1948. "Note on the tectonic significance of deformation lamellae in quartz and calcite". Am. Geophys. Union, Trans., v. 29, pp. 565, 569.
- VOGT, T. 1930. "On the chronological order of deposition of the Highland Schists". Geol. Mag., v. 67, pp. 68-73.
- WEGMANN, C. E. 1929. "Beispiele tektonischer Analysen des Grundgebirges in Finnland". Comm. géol. Finlande, Bull., v. 87, pp. 98-127.
- WILSON, G. 1946. "The relationship of slaty cleavage and kindred structures to tectonics". Geol. Assoc., Proc., v. 57, pp. 263-302.
- _____. 1953. "Mullion and rodding structures in the Moine series of Scotland". Geol. Assoc., Proc., v. 64, pp. 118-151.
- WINCHELL, A. N. Elements of optical mineralogy, Part I. New York: John Wiley & Sons, Inc., 1937, plate I.

LIST OF TEXT-FIGURES

1.	Physiographic provinces of Scotland	3
2.	Bedding trends in Ballachulish and Glen Coe	30
3.	Fracture cleavage cross-cutting bedding	4
4.	Axial plane flow cleavage and false cleavage intersecting bedding	4
5.	"Younging"	5
6.	Contoured diagram of lineations due to intersection of bedding and flow cleavage	71
7.	Contoured diagram of lineations due to intersection of bedding and false cleavage	71
8.	Contoured diagram of fold axes	71
9.	Contoured diagram of poles to joint planes	71
10.	Fold axis constructed on a Wulff stereonet	74
11.	Axial direction constructed on a Wulff stereonet	74
12.	Axial direction constructed for entire Ballachulish-Glen Coe area	74
13.	Fold axes plotted on the basis of lithology and size of fold	81
14.	Fold axes plotted on the basis of geography	84
15.	Axial directions constructed on the basis of geography	85
16.	Axial directions plotted on the basis of geography	91

LIST OF PLATES

- I. Fig. 1. Current-bedding in Binnein quartzite.
Fig. 2. Recumbent folding in Binnein quartzite.
- II. Fig. 1. Competence of Binnein schist.
Fig. 2. Steeply-dipping Glencoe quartzite.
- III. Folding in Binnein schist.
- IV. Fig. 1. Slightly overturned fold in Banded Passage Beds.
Fig. 2. Rodding in Banded Passage Beds.
- V. Fig. 1. Augen in Banded Passage Beds.
Fig. 2. Isoclinal folding in Banded Passage Beds.
- VI. Fig. 1. Biotite porphyroblasts in Banded Passage Beds.
Fig. 2. Böhm lamellae and strain shadows in Banded Passage Beds.
- VII. Fig. 1. Sgòr na Ciche and Sgòr nam Fiannaich.
Fig. 2. Glen Coe.
- VIII. Fig. 1. Chevron folding in Leven schist.
Fig. 2. Isoclinal folding in Leven schist.
- IX. Fig. 1. Bedding intersecting flow cleavage in Leven schist.
Fig. 2. Garnets in Leven schist.
- X. Fig. 1. Bedding and cleavage in Leven schist.
Fig. 2. Flow cleavage cross-cutting bedding in Ballachulish limestone.
- XI. Fig. 1. Symmetrical small-scale folding in Ballachulish limestone.
Fig. 2. Contorted small-scale folding in Ballachulish limestone.
Fig. 3. False cleavage cross-cutting bedding in quartzose Ballachulish limestone.
- XII. Fig. 1. Ptygmatic folding of quartz vein in Ballachulish limestone.
Fig. 2. False cleavage cross-cutting bedding in schistose Ballachulish limestone.
Fig. 3. Competence of Ballachulish limestone.
- XIII. Fig. 1. Contact between Ballachulish limestone and Banded Passage Beds.
Fig. 2. Contact between Ballachulish limestone and Striped Transition Series.
- XIV. Fig. 1. Contact between Ballachulish limestone and Glencoe quartzite.
Fig. 2. Impure nature of Ballachulish limestone.
- XV. Fig. 1. Rodding in Ballachulish slate.
Fig. 2. Lineation in Ballachulish slate.

LIST OF PLATES (Continued)

- XVI. Fig. 1. Contact between Ballachulish slate and Striped Transition Series.
Fig. 2. Small-scale folding in Ballachulish slate.
- XVII. The Ballachulish slate quarry.
- XVIII. Fig. 1. Folded quartzite band cross-cutting bedding of Ballachulish slate.
Fig. 2. Chevron folding in Appin Striped Transition Series.
- XIX. Fig. 1. Fragmentation of bedding in Striped Transition Series.
Fig. 2. Recrystallization in Striped Transition Series.
- XX. Fig. 1. Ratio of quartz to feldspar in Striped Transition Series (with polarizer).
Fig. 2. Same (with crossed nicols).
- XXI. Fig. 1. False cleavage intersecting bedding of Striped Transition Series.
Fig. 2. Steeply-plunging fold in Striped Transition Series.
- XXII. Fig. 1. Syncline in Striped Transition Series.
Fig. 2. Anticline in Striped Transition Series.
- XXIII. Fig. 1. Double fold in Striped Transition Series.
Fig. 2. Recumbent fold in Striped Transition Series.
- XXIV. Fig. 1. Regularly-dipping Appin quartzite.
Fig. 2. Graded bedding in Appin quartzite.
- XXV. Western portion of the Beinn Bhàn syncline.
- XXVI. Fig. 1. Folded micaceous bands in Appin limestone.
Fig. 2. Flow folding in Appin limestone.
- XXVII. Fig. 1. Color banding on flow cleavage in Appin phyllite.
Fig. 2. Folding in quartzose Appin phyllite.
- XXVIII. Fig. 1. Crenulate quartz and strain shadows in Appin phyllite.
Fig. 2. Thrusting in Appin phyllite.
- XXIX. Fig. 1. Beinn Bheithen range, with fault zone in Appin quartzite.
Fig. 2. Shatter belt in Upper Coire Riabhaich.
- XXX. Fig. 1. Normal faulting in Banded Passage Beds.
Fig. 2. Low-angle reverse faulting in Appin quartzite.
Fig. 3. High-angle reverse faulting in Appin quartzite.
Fig. 4. Normal faulting in Appin phyllite.

LIST OF PLATES (Concluded)

- XXXI. Structural trends on Sgòr nam Fiannaidh.
- XXXII. Structural trends on Sgerr a' Choise.
- XXXIII. Structure of Beinn Bhan and Beim Fhiodha.
- XXXIV. Petrofabric diagrams.
- XXXV. Rotated quartz maxima.

LIST OF MAPS

- I. Geology.
- II. Strike and dip of bedding.
- III. Strike and dip of cleavage.
- IV. Trend and plunge of lineation.
- V. Trend and plunge of fold axes.
- VI. Trend and plunge of axial directions.
- VII. Geographic orientation of quartz optic axes.

APPENDIX I

Thin-section number	Special Interest
VB7-1	Poikilitic orthoclase and albite
VB9	Contact between Appin phyllite and Ballachulish granite
VB24-2	Attenuation of quartz parallel to lineation; tourmaline
VB40	False cleavage intersecting bedding foliation
VB44	Impure nature of Ballachulish limestone; calcite healing microjoints
VB57-1	False cleavage cross-cutting mica bands
VB75-1	Cataclasis; strain shadows
VB125	Series of small faults
VB131-1, -2 -3, -4	Four sections cut through a small fold and normal to the foliation axis
VB148A	Large feldspar porphyroblasts
VB180	Contact between Glencoe quartzite and Ballachulish limestone
VB204	Pockets of quartz in hornfelsed limestone
VB206	Tremolite, albiclasts
VB224	Pleochroic halos in biotite porphyroblasts
VB229-1	Relict structure; chlorite pseudomorphous after garnet
VB263A	Poikilitic texture
VB268	Telescoped fragments of quartz and mica matrix
VB338	Crenulate quartz boundaries
VB353-1	Asymmetric folding of slate and quartz bands
VB376-1	False cleavage cutting chlorite bands; calcite porphyroblasts Fe-free zoisite, sphene
VB378	Actinolite, diopside
VB407-1	Relict structure; garnets
VB410-1	Tremolite, β -zoisite, large crystals of calcite and muscovite
VB445	Graded bedding; feldspathization; zircons
VB447	Slate with quartz bands; false cleavage; garnets being replaced by chlorite
VB455	Flow cleavage intersecting bedding; chlorite porphyroblasts
VB458	Epidote, calcite, biotite, completely recrystallized quartz
VB462-1	Relict bedding
VB486	"Ghost" cubes of pyrite
VB493	Sphene
VB531	Isoclinal relict folding
VB541	False cleavage cutting mica bands; chloritoid
VB542	Graphic structure of mica (after feldspar) and quartz
VB543	Barrel-shaped crystals of β -zoisite
VB556	Thermally metamorphosed Appin phyllite, with cordierite and andalusite
VB560	Thermally metamorphosed Appin phyllite, with cordierite, sphene, albite, tourmaline, sillimanite, corundum, and andalusite

APPENDIX I (Continued)

Thin-section number	Special Interest
VB565	Large biotite porphyroblasts
VB569	Tourmaline
VB623	Böhm lamellae
VB629	Scapolite and diopside
VB644	False cleavage cutting bedding; chlorite, garnet, rutile
VB686	Thrust fault
VB690	Retrograde metamorphism

A P P E N D I X I I

CHEMICAL ANALYSES OF BALLACHULISH AND GLEN COE ROCKS

	Binnein quartzite					Appin qtzite.		Ball. ls.	Appin limestone			
	1	2	3	4	5	6	7	8	9	10	11	
SiO ₂	98.40	99.10	98.50	97.80	96.21	93.69	96.40	12.70	1.90	25.38	3.70	
Al ₂ O ₃	-	-	-	-	1.20	2.07	2.06	4.10	1.82	5.01	1.66	
Fe ₂ O ₃	0.16	0.08	0.09	0.09	0.59	0.87	0.07	2.44	1.26	1.82		
MgO	-	-	-	-	0.16	0.09	0.11	1.98	18.53	5.45	20.85	1
CaO	-	-	-	-	1.30	1.26	0.20	42.21	31.67	28.93	28.90	3
Na ₂ O	0.02	0.02	Nil	Nil	0.28	0.45	0.10	-	-	1.95	-	
K ₂ O	0.25	0.11	0.23	0.49	0.29	1.38	1.03	-	-	1.00	-	
H ₂ O	0.03	0.01	0.04	0.02	0.01	0.01	-	} 0.91	} 0.90	} 0.10	}	
H ₂ O+	-	-	-	-	0.08	0.15	-					
TiO ₂	-	-	-	-	0.08	0.08	-	-	-	0.47	-	
P ₂ O ₅	-	-	-	-	Nil	Nil	-	-	-	0.19	-	
MnO	-	-	-	-	0.02	0.04	-	-	-	0.06	0.17	
ZrO ₂	-	-	-	-	0.01	0.03	-	-	-	-	-	
Li ₂ O	-	-	-	-	Nil	Nil	-	-	-	-	-	
FeS ₂	-	-	-	-	Nil	0.06	-	-	-	0.33	-	
CO ₂	-	-	-	-	0.06	0.08	-	35.98	44.60	29.26	44.80	4
C	-	-	-	-	Nil	trace	-	-	-	-	-	
Insoluble residue										35.50		
Loss on Ignition	-	-	-	-	-	-	0.27					
TOTAL	98.86	99.32	98.86	98.40	100.29	100.26	100.24	100.32	100.68	100.45	100.08	10
CaCO ₃								75.39	56.51	51.66	51.62	6
MgCO ₃								4.16	38.73	10.58	42.78	3

1. Geol. Surv. Lab. Analysis 1393
2. " " " " 1394
3. " " " " 1392
4. " " " " 1391
5. " " " " 498
6. " " " " 499

7. Analysis quoted from Boswell (1918, p.15)
8. Geol. Surv. Lab. Analysis 497
9. " " " " 508
10. A. Muir, Macaulay Institute for Soil Research.
11. Analysis quoted from Bailey (1916, p.233)
12. " " " " (" ")

APPENDIX III

<u>Type of bedding</u>	<u>Locality No.</u>	<u>National Grid Reference</u>	<u>Specimen No.</u>
Graded bedding	428	056564	VB264
	457	081575	VB277
	563	068576	VB303
	912	127570	VB445
<hr/>			
Current bedding right way up	37	024595	VB31
" " "	88	059550	-
upside down	123	137607	-
right way up	133	123605	-
" " "	135	122604	-
" " "	141	102599	VB117, 118
" " "	243	108600	VB146
" " "	244	109600	VB147
" " "	381	134605	VB237
" " "	410	134581	VB256
" " "	550	115601	-
" " "	1055	109599	-
" " "	1071	123592	VB521

APPENDIX IV: FAULTS.

A. Small-scale faults (in hand-specimen)

Rock type	Specimen No.	National Grid Reference	Fault type	Amount of displacement
Appin phyllite	VB18	062545	Normal	8 mm.
	VB686	067545	Low-angle thrust	Not measured (cuts out limb of small fold)
	VB687	067546	Low-angle thrust	"
Appin quartzite	VB264	056564	Low-angle thrust	10 mm.
	VB307	064570	High-angle thrust	11 mm.
Appin Striped	VB268	063569	High-angle thrust	1 mm.
Transition Series	VB588	085550	Normal	2 mm.
Ballachulish limestone	VB331	103584	Normal	1 mm.
	VB506	102579	Normal	2.5 mm.
	VB670	138569	High-angle thrust	7 mm.
Leven schist	VB534	139566	Normal	10 mm.
Leven Banded	VB69	127567	High-angle thrust.	2 mm.
Passage Beds	VB624	103598	Normal	1 mm.

B. Medium-scale faults (in the field)

Rock type	Locality No.	National Grid Reference	Fault type	Amount of displacement
Appin quartzite	686	070549	Dip	4.5 ft.
Appin Striped Transition Series	43	066588	Series of en échelon normal faults	Not measured
	87	078574	Dip	Not measured
Ballachulish limestone	1038	102580	Normal	6 mm.

APPENDIX V: FOLDS IN HAND-SPECIMEN

Specimen number	Rock formation	Attitude of fold	Axial trend	Axial plunge	Thickening of bands; "as" jointing
VB22	Ballachulish slate	Asymmetrical; non-cylindrical; anticlinal	154°	45° N. W.	One band thickens from 8 mm. on limbs to 30 mm. towards crest, then thins to 25 mm. at crest; no "as" jointing
VB22x	Apin phyllite	Symmetrical; synclinal	30°	18° N. E.	None; no "as" jointing
VB22	Apin phyllite	Asymmetrical; synclinal	61°	85° N. W.	One band thickens from 4 mm. on limbs to 8 mm. in trough; no "as" jointing
VB100x	Binnin quartzite	Symmetrical; horizontally recumbent	129°	26° N. W.	None apparent; "as" jointing
VB115	Apin striped Transition Series	Non-cylindrical; synclinal	67°	40° N. W.	None; no "as" jointing
VB131x	Ballachulish limestone	Non-cylindrical; synclinal	169°	25° N. W.	One band thickens from 4 mm. on limbs to 10 mm. towards trough, then thins to 3 mm. in trough; no "as" jointing
VB161x	Quartzite band in Ballachulish slate	Roughly symmetrical; recumbent	4°	0°	One band thickens from 22 mm. on limbs to 30 mm. at crest; "as" jointing
VB219	Binnin schist	Asymmetrical	Not measurable		One band thickens from 7 mm. on limb to 20 mm. at crest and to 21 mm. on other limb; "as" jointing
VB286	Ballachulish limestone	Symmetrical; synclinal	4°	44° N. E.	None visible; no "as" jointing
VB328x	Binnin schist	Asymmetrical; anticlinal	Not measurable		One band thickens from 17 mm. on one limb to 30 mm. at crest and to 15 mm. towards other limb, then thins to 27 mm. "as" jointing

photographed in thesis

Specimen number	Rock formation	Attitude of fold	Axial trend	Axial plunge	Thickening of bands; "ac" jointing	Lamination		
						Relation to fold axis	Type	Width
VB329	Bimstein schist	Symmetrical; anticlinal	63°	50° S.W.	One band thickens from 31 mm. on limbs to 38 mm. at crest; no "ac" jointing	Parallel	b	Fine
VB330	Quartz vein in Ballechulish limestone	Non-cylindrical; synclinal	76°	86° N.E. changing to 35° S.E.	One band 2 mm. thick on one limb, 10 mm. thick on other limb, 17 mm. in trough; rough "ac" jointing	Perpendicular	a	Coarse
VB382	Ballechulish limestone	Asymmetrical; synclinal	21°	13° S.W.	One band thickens from 2 mm. on limbs to 10 mm. at crest; rough "ac" jointing	Roughly parallel	b	Fine
VB384	Ballechulish limestone	Symmetrical; anticlinal; chevron	49°	46° S.W.	None visible; "ac" jointing	Parallel	b	Very fine
VB385	Ballechulish limestone	Asymmetrical; non-cylindrical; recumbent	14°	35° S.W.	One band thickens from 17 mm. on limbs to 22 mm. at crest; rough "ac" jointing	Roughly perpendicular (inclined ca. 70°)	a	Very fine
VB386	Ballechulish limestone	Roughly asymmetrical; recumbent; chevron	52°	33° S.W.	One band thickens from 17 mm. on one limb and 15 mm. on the other to 12 mm. at crest; "ac" jointing	Parallel	b	Coarse
VB387	Ballechulish limestone	Asymmetrical; anticlinal	57°	31° S.W.	One band thickens from 9 mm. on limbs to 19 mm. at crest; rough "ac" jointing	Parallel	b	Coarse
VB403a	Quartz band in Banded Passage Beds	Roughly asymmetrical; anticlinal and synclinal	Not measurable		One band thickens from 0.5 mm. in trough to 5 mm. on one limb to 6 mm. at crest; no "ac" jointing	Parallel	b	Coarse

* photographed in thesis

Specimen number	Rock formation	Attitude of fold	Axial trend	Axial plunge	Thickening of beds; "ae" jointing
V1446E	Banded Passage Beds	Asymmetrical (almost isoclinal); synclinal	115°	44° N.W.	One band thickens from 10 mm. on one limb to 30 mm. in trough, then thins to 15 mm. on other limb; "ae" jointing
V1449	Banded Passage limestone	Asymmetrical; synclinal	104°	39° N.W.	Beds thicken in trough, amount not measurable; no "ae" jointing
V1453	Banded Passage Beds	Symmetrical; anticlinal	Not measurable		One band thickens from 12 mm. on limbs to 14 mm. at crest; rough "ae" jointing
V1475	Appl. striped Transition Series.	Slightly asymmetrical; Pseudo chevron	75°	0°	One band thickens from 9 mm. on one limb to 18 mm. at crest, then thins to 12 mm. on other limb; "ae" jointing
V1493	Quartzite band in Appl. limestone	Asymmetrical; synclinal; chevron	56°	88° N.E.	Band thickens from 10 mm. on limbs to 16 mm. in trough; "ae" jointing
V1531E	Lavan schist	Symmetrical; anticlinal and synclinal	157°	25° N.E.	One band thickens from 0.5 mm. on limbs to 1 mm. on crest and in trough; no "ae" jointing
V1533	Lavan schist	Symmetrical; synclinal	127°	48° N.W.	One band thins from 23 mm. on limbs to 20.5 mm. in trough; rough "ae" jointing
V1567E	Banded Passage slate	Symmetrical; synclinal	60°	43° N.W.	None visible; "ae" jointing

* photographed in thesis

Lamination				Relation to fold axis	Type	Width	Cause
Parallel	Perpendicular	Parallel	Parallel				
					b	Coarse	Axial plane flow cleavage
					a	Fine	Slippage on bedding foliation
					b	Coarse	Flow cleavage intersecting bedding
					b	Coarse	Axial plane flow cleavage
				Inclined ca. 45°		Very fine	False cleavage intersecting bedding
				Slightly perpendicular	a	Fine	Slippage on bedding foliation
					b	Fine	Axial plane flow cleavage
				Side visible			
				Nearly parallel	b	Fine	Axial plane false cleavage
				Perpendicular	a	Fine	Slippage bedding foliation
				Parallel	b	Medium	Axial plane flow cleavage



Fig. 1. Current bedding in Binnein quartzite (VB237), west of Caolasnaon (134605), indicates that the strata are right way up.



Scale
1 in. = 2

Fig. 2. A horizontal recumbent fold in Binnein quartzite (VB100, 101), west of Caolasnaon (138607); the fold axis trends 129° and plunges 26° N. W.; a fine "b" lineation parallels the axis. For the quartz crystallographic orientation see petrofabric diagrams 13 and 27, Pl. XXXIV.



Fig. 1. Asymmetric folding in quartzose Binnein schist (VB328 shore section, west of Caolasnacon (130607), accompanied by thickening of layers towards the crest and thinning on the limbs; a coarse lineation roughly normal to the fold axis is due to slippage of the layers along the bedding foliation away from the crest.



Fig. 2. Steeply-dipping Glencoe quartzite at 2100 ft. elevation on the northwest slope of Sgor na Ciche (127595); the general strike of the bedding is 133° and the dip 70° N. W.- 90° .



Scale
1 in. = 1

Differential competence of Binnein schist along its shore outcrop west of Caolasnacon (130607); the quartzite bands have folded isoclinally, while the phyllitic layers have flowed into the troughs and crests and have responded to drag folding.

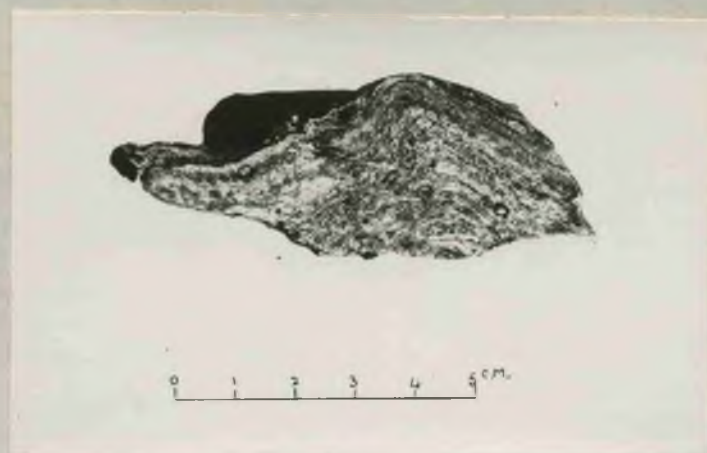


Fig. 1. A slightly overturned fold in Banded Passage Beds (VB647), south slope, Tom Breac, Glen Coe (115580); the fold axis trends 43° and plunges 79° S. W.; a medium-fine "b" lineation parallels the axis. For the quartz crystallographic orientation see petrofabric diagram 38, Pl. XXXIV.



Fig. 2. Rodding in Banded Passage Beds, southeast slope, Tom Breac, Glen Coe (117580), trends 119° and plunges 76° N. W.



Fig. 1. West of Clachaig Hotel, Glen Coe (126567), thin pegmatitic veins roughly concordant with the bedding of Banded Passage Beds (VB400) occasionally widen to form augen.



Fig. 2. Isoclinal folding in Banded Passage Beds (VB448) on the southwest slope of Sgòr nam Fiannaich (128567); the fold axis trends 143° and plunges 67° N. W.; a coarse "b" lineation parallels the fold axis, a fine "a" lineation is normal to it.

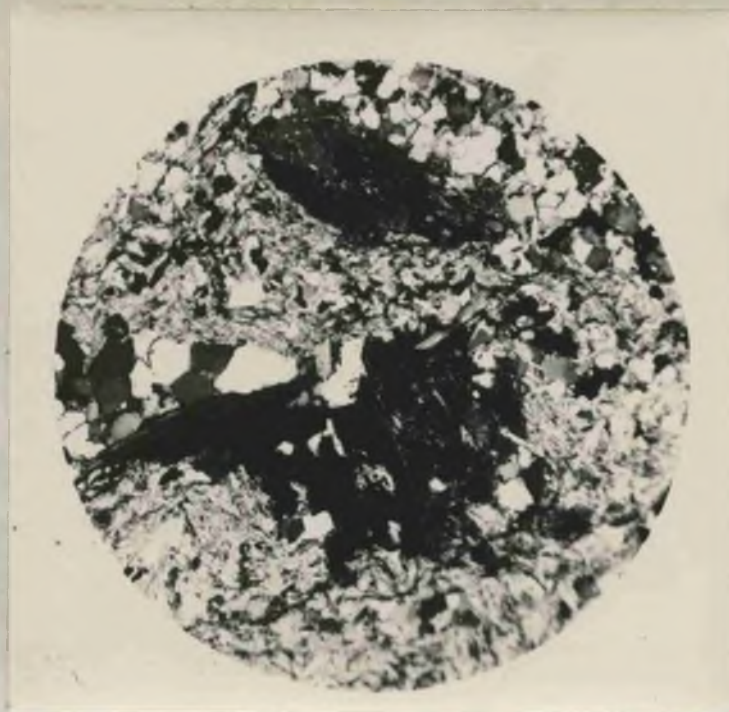


Fig. 1. Photomicrograph (x30) of a biotite porphyroblast inclined 16° (P_{PB}) to the bedding foliation (P_B) in Banded Passage Beds (VB565) on the Glencoe Estate (101597).

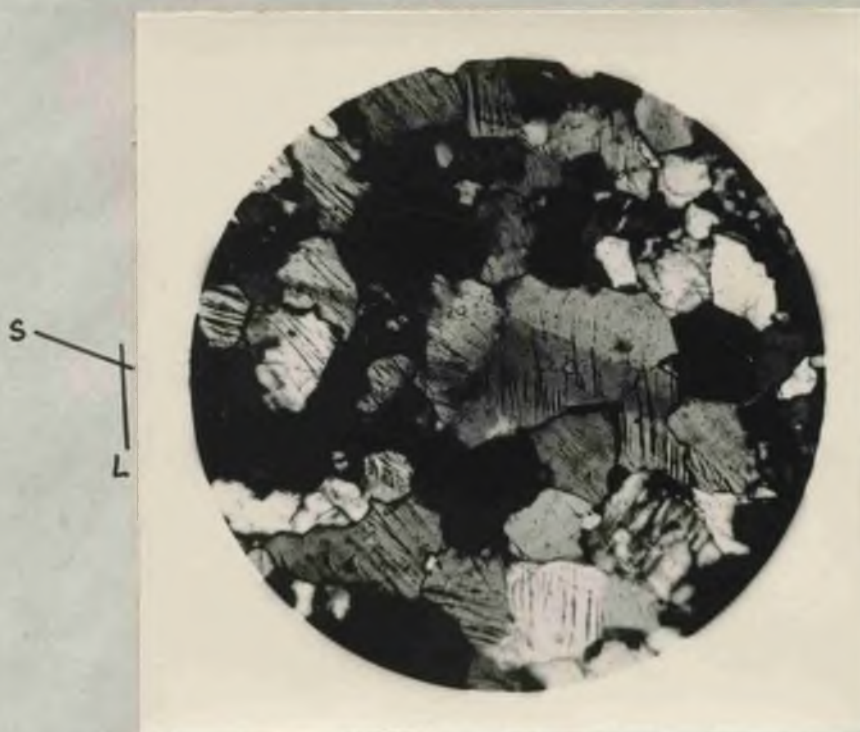


Fig. 2. Photomicrograph (x53) of lamellae (L) and strain shadows (S) in quartz in one limb of a northeasterly-plunging fold in Banded Passage Beds (VB623) on the Glencoe Estate (103598).



Fig. 1. Looking north towards the southwestern slopes of Sgòr na Cìche, on the left, and of Sgòr nam Fiannaidh, on the right. From the ridge crest downslope to the lower limit of the heather (blackish) Glencoe quartzite outcrops; below this it interdigitates with Banded Passage Beds.



Fig. 2. Looking east up the glaciated trough of Glen Coe at the threshold of the cauldron subsidence. On the left is the southern slope of Sgòr nam Fiannaidh, a continuance of Fig. 1; its general structure is roughly synclinal, with Glencoe quartzite surrounding Leven schist and Ballachulish limestone, and with Glencoe granite penetrating along and across contacts. In the right foreground is An t-Sron, mainly of Glencoe granite. In the right background are the lavas of Bidean nam Bian. (See Map I).



Fig. 1. Chevron folding due to compression in Leven schist (VB705) on the south slope of Sgorr a' Choise (081543); the fold axis trends 61° and plunges 42° S. W.; a fine lineation crosses the crests at about 45° to the fold axis.

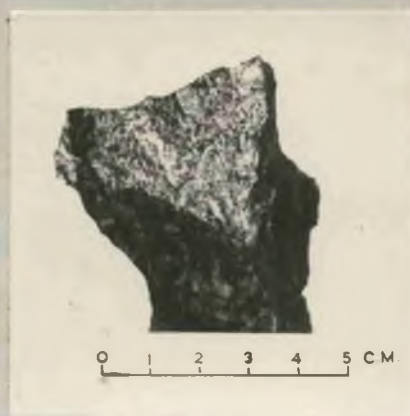


Fig. 2. Symmetrical isoclinal folding due to compression of relict bedding in hornfelsed Leven schist (VB531) on the south slope of Sgòr nam Fiannaigh (139570); the surface in the shadow on the right-hand side marks the axial plane flow cleavage.

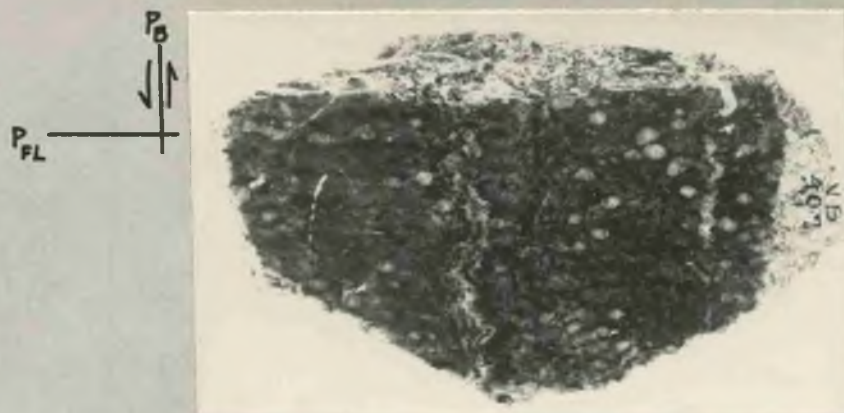


Fig. 1. A polished section (natural size) cut perpendicular to the flow cleavage (P_{FL}) of Leven schist (VB407-1) from the River Coe (121565); crumpling is due to a couple acting parallel with the original bedding (P_B), which is roughly normal to the axial plane flow cleavage; light-colored, rounded grains are garnets.

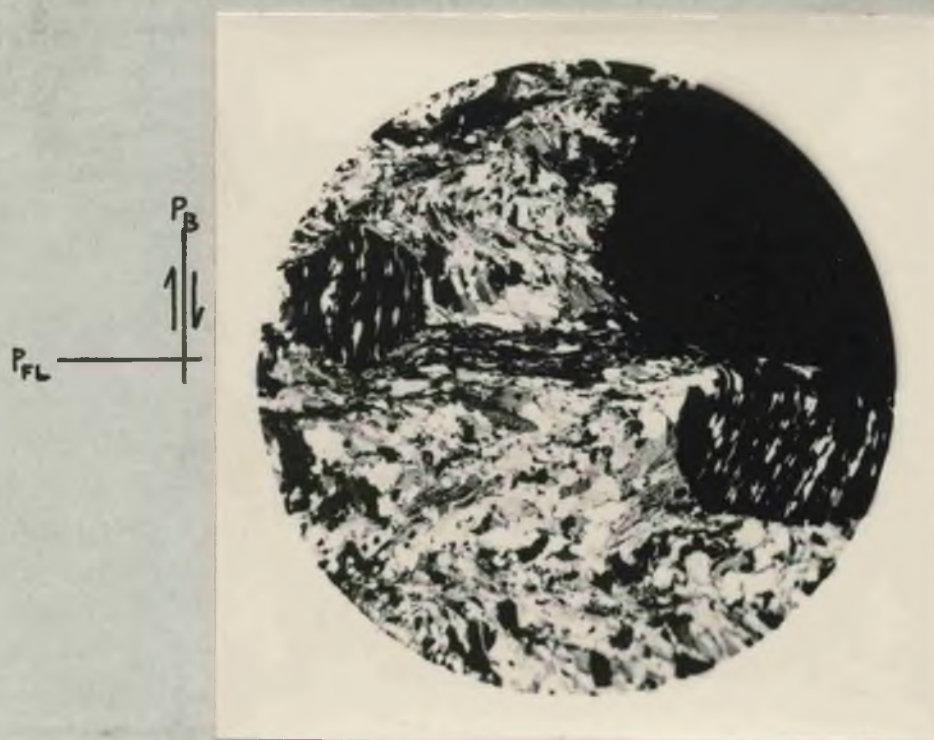


Fig. 2. Photomicrograph (xl7) of the same specimen of Leven schist (VB407-1); the trend of the small attenuated quartz grains (white) in the garnets (black) marks the original bedding (P_B), which is normal to the horizontal bands of mica marking flow cleavage (P_{FL}); the trend of the larger attenuated quartz grains in the matrix reflects somewhat asymmetric folds in the bedding, i. e., the crumpling in Fig. 1, with their axial planes parallel with the flow cleavage. For the quartz crystallographic orientation see petrofabric diagrams 5-7, Pl. XXXIV.

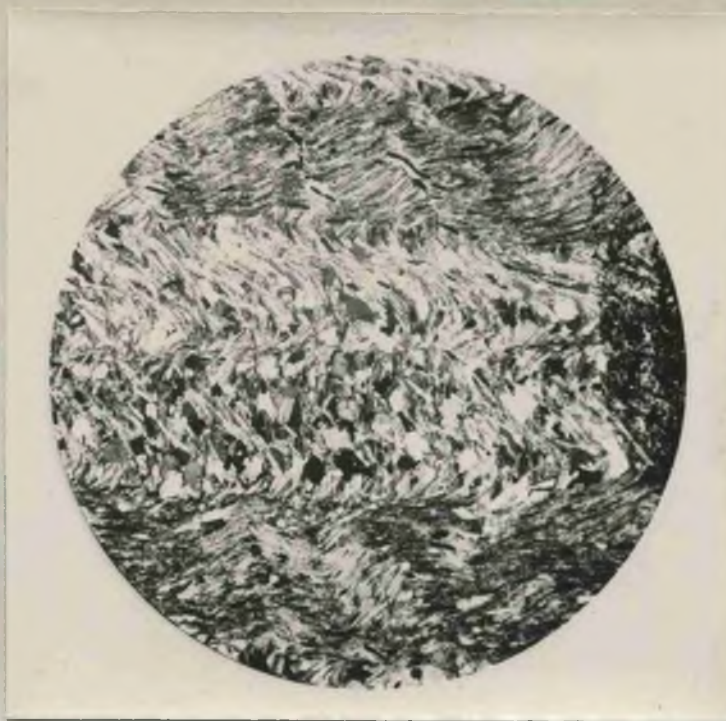
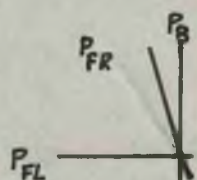


Fig. 1. Photomicrograph (x35) of Leven schist (VB462-1) from the southeast slope of Sgorr a' Choise (087544); the horizontal bands of mica laths mark the trace of flow cleavage (P_{FL}); corrugations in these bands are due to false cleavage (P_{FR}) intersecting flow cleavage at ca. 59° ; normal to the flow cleavage is the original bedding (P_B) in isoclinal fold whose axial planes are parallel with the flow cleavage. For the quartz crystallographic orientation see petrofabric diagram 2, Pl. XXXIV.

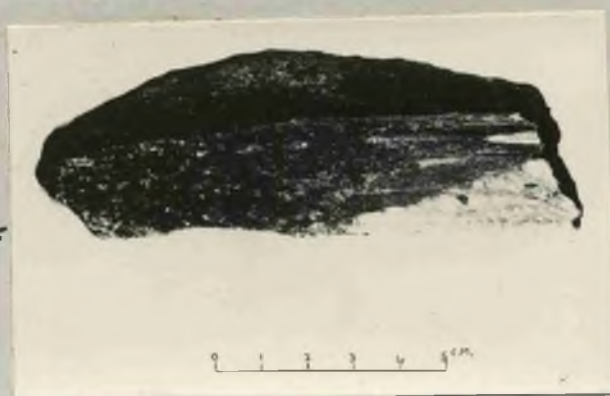


Fig. 2. Schistose Ballachulish limestone (VB383) near its contact with Leven schist on the east slope of Meall Mor (115561); the bedding (P_B), marked by the junction between the white calcite facies and the black biotite-muscovite-tremolite facies, is crosscut at ca. 17° by flow cleavage (P_{FL}).

EXPLANATION OF PLATE XI

- Fig. 1. Polished surface of Ballachulish limestone (VB643), from the north slope of Meall Mor (099567), shows quite uniform thickening of layers from 2 mm. on limbs of the small fold to 10 mm. at the crest; the fold axis trends 5° , plunges 57° S.W.; a medium ("b") lineation parallels the axis, a fine ("a") lineation is roughly normal to it.
- Fig. 2. Polished surface of Ballachulish limestone (VB664) from the northeast slope of Am Meall (099577) reveals a small chevron fold within which the alternating bands of mica (dark) and calcite (light) are contorted and generally thin on the limbs of subsidiary folds; the main fold axis trends 40° , plunges 83° S.W.; a medium ("b") lineation parallels the axis, a very fine ("a") lineation is approximately normal to it.
- Fig. 3. A larger fold in more quartzose Ballachulish limestone (VB644), near its contact with Leven schist on the north slope of Meall Mor (099567), trends 44° , plunges 76° S.W.; there has been a subsidiary movement of layers along a series of fracture cleavage planes (P_{F}) which cross-cut the bedding foliation (P_{B}) at 24° ; a coarse ("b") lineation parallels the fold axis, a medium ("a") lineation is normal to it, another coarse lineation is oblique to it. For quartz crystallographic orientation, see petrofabric diagram 10, Plate XXXIV.



Fig. 1.



Fig. 2.



P_B
P_{FR}

Fig. 3.

EXPLANATION OF PLATE XII

- Fig. 1. Ptygmatic vein of white quartz cross-cutting bedding foliation of schistose Ballachulish limestone (VB 403), west of Clachaig, Glen Coe (127566); vein thickens on crests and in troughs.
- Fig. 2. A series of closely-spaced false cleavage planes (P_{FR}) transects^s the bedding foliation (P_B) of schistose Ballachulish limestone (VB416) at an angle of 30° ; differential weathering has produced^c ribs of mica schist which stand out from depressions of almost pure calcite. Typical of limestone outcrops on Am Meall and Meall Mor.
- Fig. 3. A fold in the more calcitic Ballachulish limestone (VB131), north-east of Meall Mor (115573), trends 16° , plunges 25° S.W.; a fine ("b") lineation parallels the fold axis, a fine ("a") lineation is roughly perpendicular to it; a band of almost pure calcite (dark grey) thickens greatly in trough, a band of almost pure quartz (white) and a band of calcite and quartz (light grey) thin in the troughs.



Fig. 1.

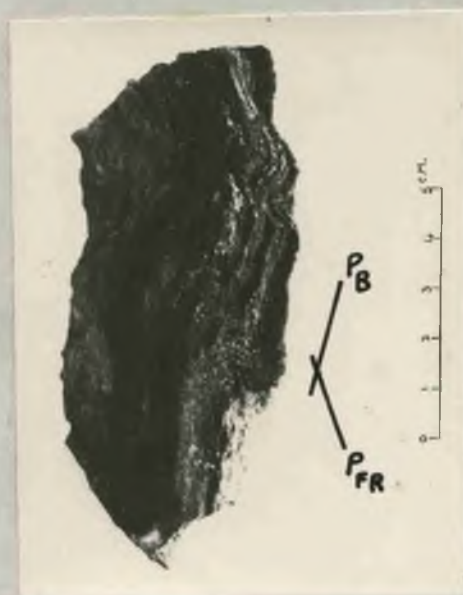


Fig. 2.



Fig. 3.



Fig. 1. Part of the shore section west of Ballachulish (06658) in the middle foreground is the undulating, near-vertical contact (note hammer) between Ballachulish limestone (light gray) and the quartzose Banded Passage Beds (darker gray); the general trend of the contact is 43° .

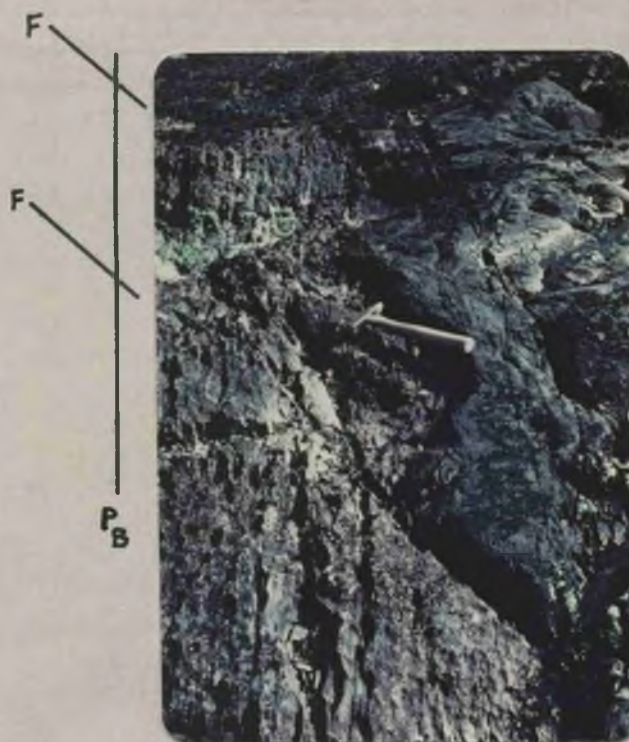


Fig. 2. Part of the shore section west of Ballachulish (06658) showing the folded contact between pitted Ballachulish limestone on the left and a 10-inch thick black phyllitic band of Appin Striped Transition Series on the right; the lighter band on the extreme right is a porphyrite dike; a series of small en échelon faults (F), striking between 175° and 5° , cuts the contact; the effects of weathering and erosion on different lithologies are well-illustrated by these three rock types; the general trend of the bedding and of the contact varies between 43° and 52° .

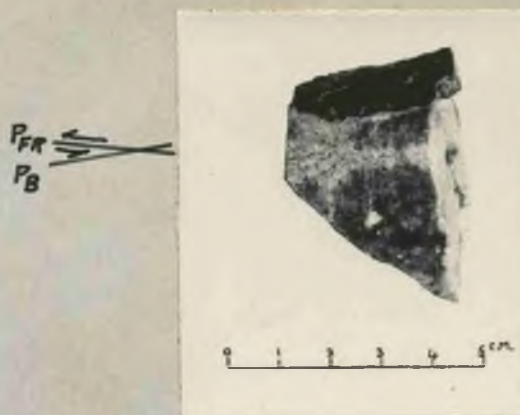


Fig. 1. The slightly irregular contact between schistose Ballachulish limestone and Glencoe quartzite (VB180), Allt an t-Sithein (140572), is due to false cleavage (P_{FR}) intersecting the bedding (P_B) at a low angle.



Fig. 2. Photomicrograph (x25) of Ballachulish limestone (VB44) taken near its contact with the Appin Striped Transition Series, in the shore section west of Ballachulish (066588) -- at the hammerhead in Pl. XIII, fig. 2; the impurity of the rock, as shown by the alternating bands of mica and quartz, is typical of much of the Ballachulish limestone formation; microjoints crosscutting the bedding are healed with calcite.



Fig. 1. Rodding and the finer lineation mark the intersection of axial plane flow cleavage on the bedding foliation in Ballachulish slate (VB567), west-northwest of Sgòr na Cìche (102598).

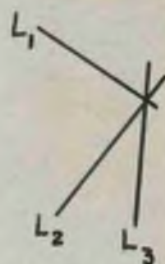


Fig. 2. Strongly lineated Ballachulish slate (VB325) from the north slope of Am Meall (094580); L₁ marks the trace of flow cleavage on the bedding foliation, L₂ and L₃ the trace of false cleavages on bedding.



Fig. 1. Looking east toward Sgorr a' Choise, with Bidean nam Bian in the background. The backbone (right foreground) of Sgorr a' Choise is Appin quartzite, while the north slope and summit are Ballachulish slate; the near-vertical whitish line downslope from the summit marks the trace of an upthrust (F).

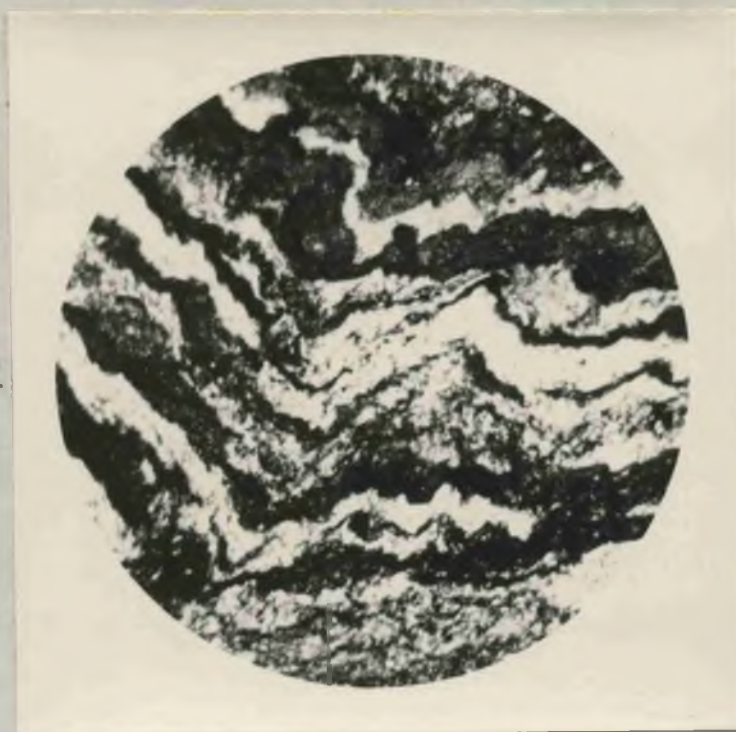
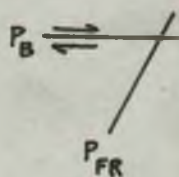


Fig. 2. Photomicrograph (x25) of asymmetric small-scale folds of bedding (P_B) in strongly lineated Ballachulish slate (VB35 1) on the northwestern slope of Sgorr a' Choise (081555); the white bands are quartz, the blackish bands slate; a series of false cleavage planes (P_{FR}) has developed across the bedding as a result of a couple acting along the bedding foliation. For the quartz crystallographic orientation see petrofabric diagram 21, Pl. XXXIV.



Fig. 1. On the right is Ballachulish slate quarry, cut into the northwestern slope of Am Meall; in the center is the glaciated trough of Glen Coe, and to the left Sgor nam Fiannaich and Sgor na Ciche.



Fig. 2. Looking into the Ballachulish slate quarry from its southern rim (086580); the general strike of the bedding is 127° and the dip 72° S. W.; two nearly horizontal joint planes provide convenient platforms for working the slate.



Fig. 1. A folded band of quartzite cuts across the bedding of Ballachulish slate in an abandoned quarry, West Ballachulish (074582); its fold axis trends 14° and plunges 9° S. W.; a coarse "b" lineation parallels the axis, a fine lineation is inclined to it; the band is out by a series of tension joints nearly normal to the bedding and healed with white quartz; the general bedding strike is 10° and the dip 65° N. W.



Fig. 2. A horizontal chevron fold in the Appin Striped Transition Series (VB475), north spur, Beinn Fhiodha (063569); the fold axis trends 75° and plunges 0° ; a fine "a" lineation is normal to the axis.

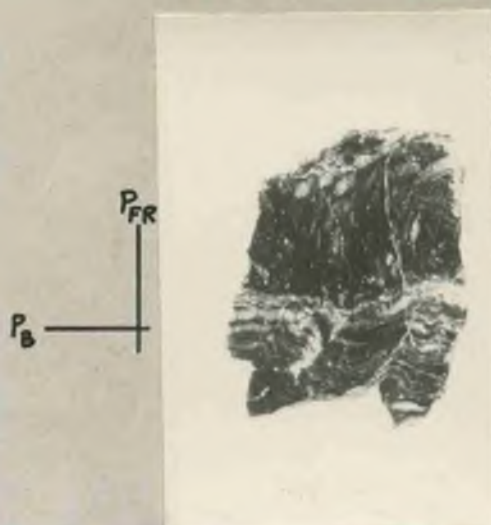


Fig. 1. A polished section (natural size) of a slaty portion of Appin Striped Transition Series (VB268), Coire Riabhaich (063567), shows crumpled bedding foliation (P_B) in the lower part of the specimen and an upper band of telescoped layers, in which fragments (P_{FR}) lie approximately perpendicular to the bedding.



Fig. 2. Photomicrograph (x64) of a quartzose portion of the Appin Striped Transition Series (VB75-1), Allt a' Coire Riabhaich (078573), showing the outline of one large quartz grain which has recrystallized into smaller grains with straight boundaries (mosaic structure); the surrounding small, angular quartz grains have recrystallized similarly from larger grains.

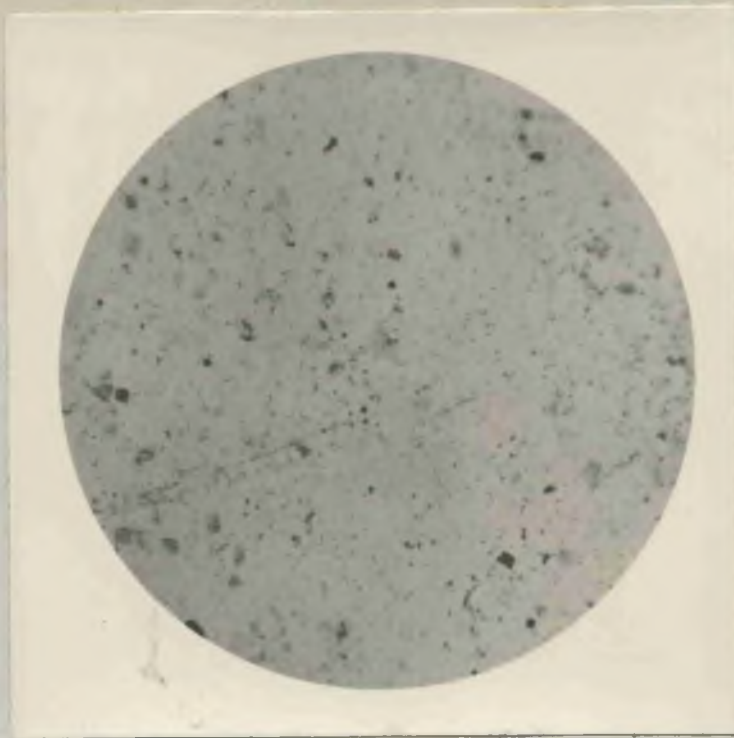


Fig. 1. Photomicrograph (x25) of Appin Striped Transition Series (VB75-1), Allt a' Coire Riabhaich, with only the polarizer shows the approximate 1:1 ratio of quartz (light gray) and feldspar (darker gray).



Fig. 2. Photomicrograph (x25) of the same thin-section with crossed nicols.

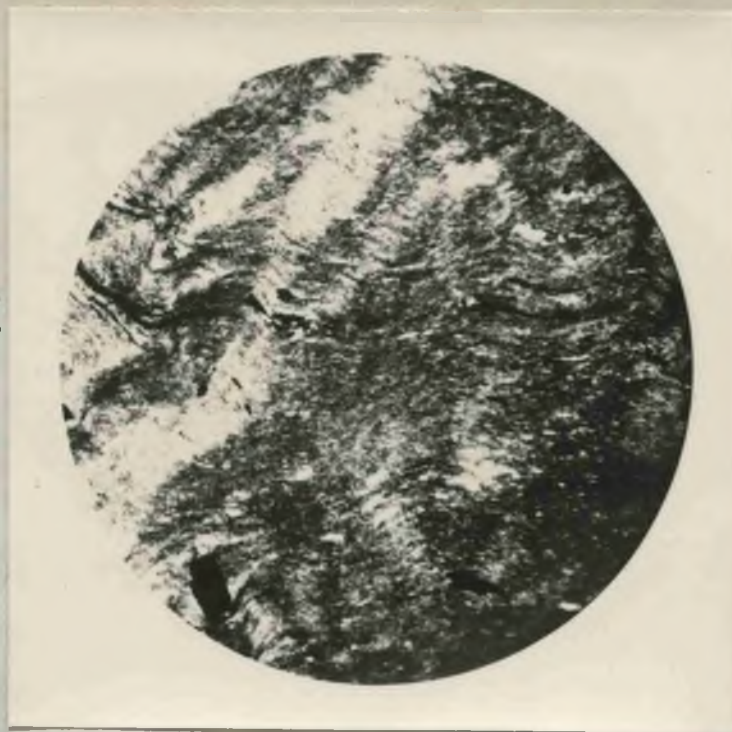
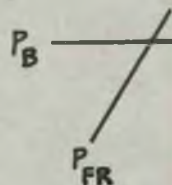


Fig. 1. Photomicrograph (x33) of false cleavage (P_{FR}) intersecting bedding foliation (P_B) in a slaty portion of Appin Striped Transition Series (VB40), shore section, West Ballachulish (067586).



Scale:
1 in. = 5ft.

Fig. 2. A fold in the Appin Striped Transition Series. Camas Caltuinn (102599); the axis trends 67° and plunges 59° S. W.; the strata are cut by a series of joints normal to the bedding.



Fig. 1. A large synclinal fold in the Appin Striped Transition Series is exposed in the bed of the River Laroch at Brecklet, South Ballachulish (092577); the fold axis trends 74° and plunges 52° S. W. (toward the upper left-hand corner); the trace of a joint plane (P_J) cuts across the bedding near the nose of the fold.



Fig. 2. The nose of a broad, open fold in the Striped Transition Series, Coire Riabhaich (066568); the fold axis trends 85° and plunges 30° S. W. (towards the upper left-hand corner, a series of cross-joints has developed normal to the bedding.



Fig. 1. A double fold in the Appin Striped Transition Series, upper Coire Riabhaich (066566); the axis of the crest on the left trends 68° and plunges 14° S. W., the axis of the trough on the right trends 66° and plunges 7° N. E.



Fig. 2. To the north of the same outcrop shown in Fig. 1 a large recumbent fold has an axis trending 72° and plunging 17° N. E.; there is conspicuous jointing perpendicular to the bedding.



Fig. 1. A close-up view of the upper portion of Coire Riabhaich (065566); the general strike of the Appin quartzite is 60° and the dip 20° N. W.; the grassy slope is Striped Transition Series, thrown into fairly large-scale folds (see Pl. XXI, XXII); the contact between the two formations is marked by an upthrust (F_1 in Fig. 2, Pl. XXIX).

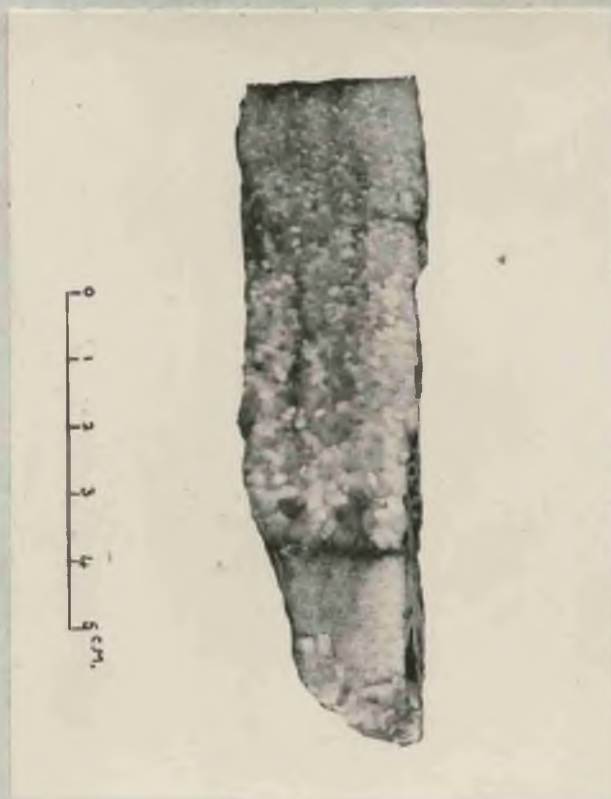


Fig. 2. Graded bedding in Appin quartzite (VB303), Beinn Bhan (068576); the opaque grains are feldspar, the translucent grains are quartz. For the quartz crystallographic orientation see petrofabric diagram 56, Pl. XXXIV.



View of the western slopes of Beinn Bhàn and Beinn Fhiodha. The large light-colored patch in the center is a bedding plane of Appin quartzite dipping northwest; downslope and to the left is the trend of a long outcrop of the same quartzite dipping southeast. From the aerial photograph on Pl. XXXIII it will be seen that these two outcrops are the two limbs of the Beinn Bhàn syncline, whose fold axis plunges toward the southwest (the right-hand margin of the photograph).



Fig. 1. Narrow, folded micaceous bands crosscutting the flow cleavage (P_{FL}) of Appin marble (VB617), on the southeast slope of Sgorr a' Choise (082548), mark an earlier foliation, probably bedding (P_B ?); one limb of each plication is parallel to the flow cleavage.



Fig. 2. Flow folding along flow cleavage (P_{FL}) in Appin marble (VB693), southeast slope, Beinn Fhiodha (069550); the bedding (P_B) shows as minor ridges on the upper surface of the specimen; the fold axis trends 23° and plunges 53° N. E.; the lineation parallels the axis; there is a thickening of the layers on the crest.



Fig. 1. Bedding (P_B) appears as color banding on flow cleavage in Appin phyllite (VB89) from Gleann an Fhìod (078565); the small fold (F. A.) at the top trends 35° and plunges 18° N. there is no thickening of layers at its crest; a fine "a" lineation (L), perpendicular to the axis, is due to slippage of laminae away from the crest.



Fig. 2. Small-scale parallel folding in quartzose Appin phyllite (VB692), Ailt Sheilach (069560); the polished surface shows every gradation from undisturbed bedding (P_B) to bands folded asymmetrically with respect to the false cleavage plane (P_{FR}) in response to a couple acting along the bedding foliation.



Fig. 1. Photomicrograph (xl7) of crenulate boundaries between quartz grains and of strain shadows in the larger quartz grains in quartzose Appin phyllite (VB338), upper Gleann an Fhiod (065546), features typical of quartzitic rocks which have only undergone incipient recrystallization.



Fig. 2. Thrusting along false cleavage (P_{FR}) has cut out one limb of a steeply-plunging fold in quartzose Appin phyllite (VB686), southeastern slope, Sgorr Dhearg (067546).



Fig. 1. The Beinn Bheithir range, southwest of Ballachulish; Beinn Bhàn in center foreground, Allt a' Coire Riabhaich and Beinn Fhiodha to the left, the snow-capped peak is Sgorr Dhearg, and its northern spur (to the right) Meall a' Chaolais; the gash (F) between the trees on the latter slope marks a fault zone in Appin quartzite.



Fig. 2. Looking southwest up Allt a' Coire Riabhaich from Gleann an Fhiodha; quartzite float in foreground; glacial deposits obscure rock exposures on the lower valley slopes, above them rises a massive wall of well-bedded, jointed Appin quartzite; F_1 and F_2 mark two fault zones in the west face of the corrie.

EXPLANATION OF PLATE XXX

- Fig. 1. Surface normal to the coarse lineation of Banded Passage Beds, Glencoe Estate (103598), showing small-scale normal fault with a displacement of 1.5 mm.
- Fig. 2. Surface showing low-angle thrust fault in Appin quartzite, Sgorr Dhearg (056564), which has displaced a coarse-grained quartz vein 10 mm. (quartz, white; feldspar, black).
- Fig. 3. High-angle reverse fault in Appin quartzite (VB307), Sgorr Dhearg (064570), has displaced 11 mm. a joint plane healed with white quartz.
- Fig. 4. Surface normal to the rodding in quartzose Appin phyllite, southeast slope, Sgorr Dhearg (062545), shows small joints normal to the bedding and a normal fault, displacing the layers 8 mm. For quartz crystallographic orientation see petrofabric diagram 11, Plate XXXIV.

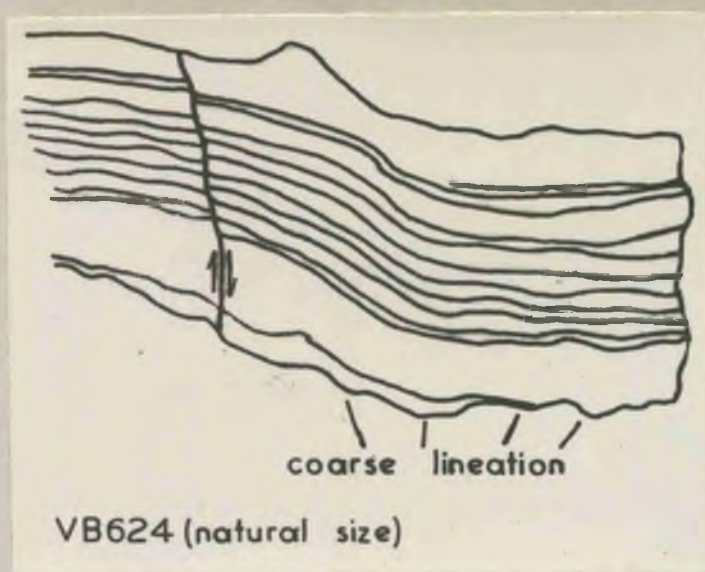


Fig. 1.

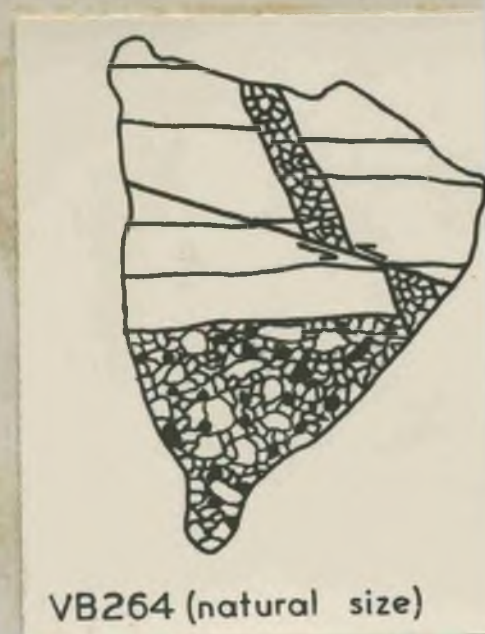


Fig. 2.



Fig. 3.

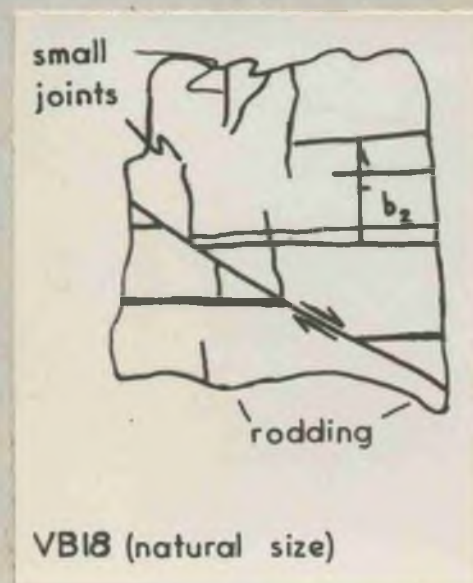
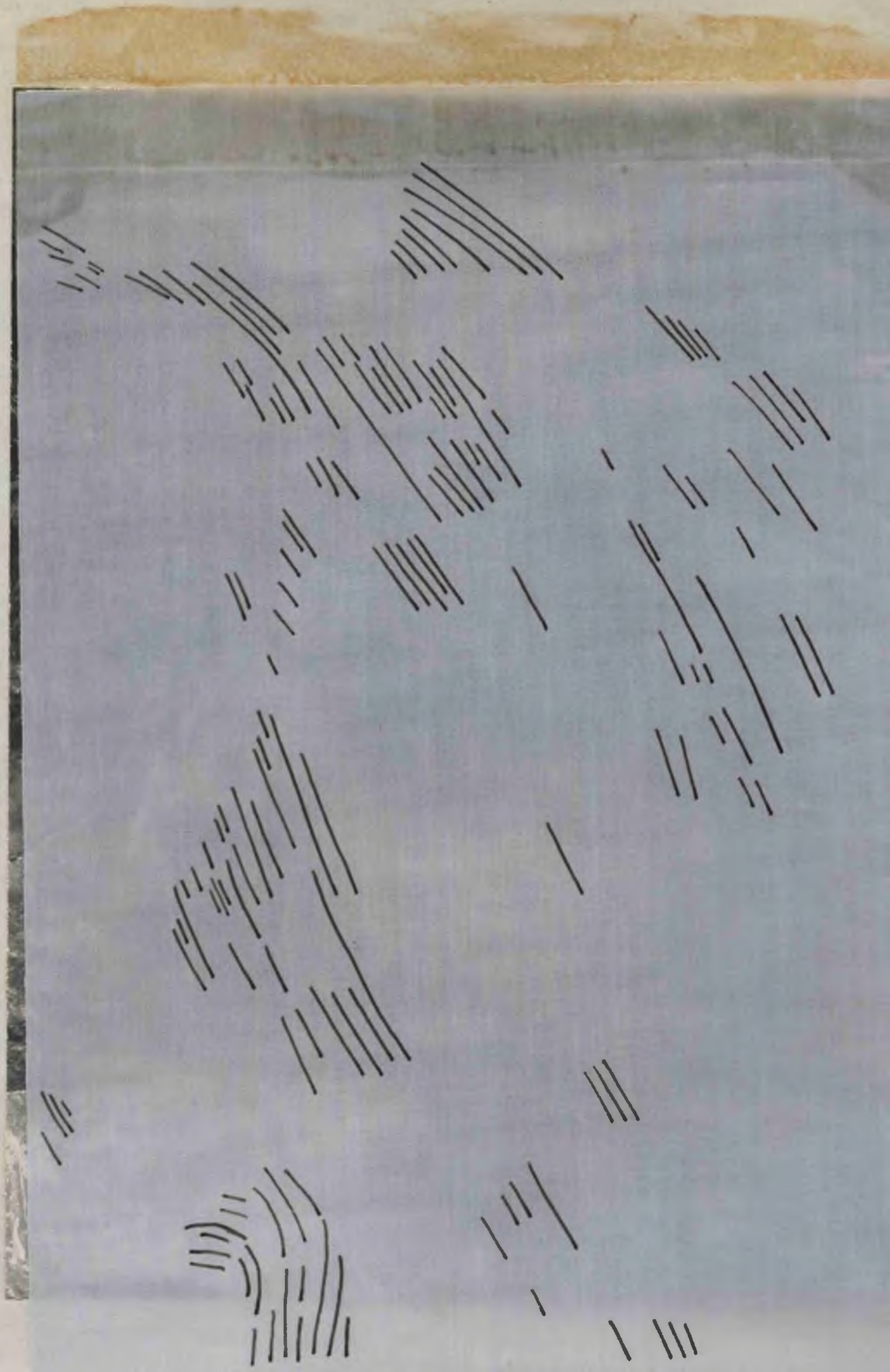


Fig. 4.

EXPLANATION OF PLATE XXXI

The lines on the overlay trace structural trends in Glencoe quartzite from the summit of Sgòr nam Fiannaigh (upper left-hand corner) to the summit of Cnap Glas (left-centre) and to the south-east slope of Sgòr na Ciche (lower left-hand corner), as shown by stereopairs of aerial photographs, scale 1:10,000. Compare with strikes of bedding and cleavage for this area on maps II and III.
(Crown copyright reserved; not to be reproduced without permission of the Air Ministry.)

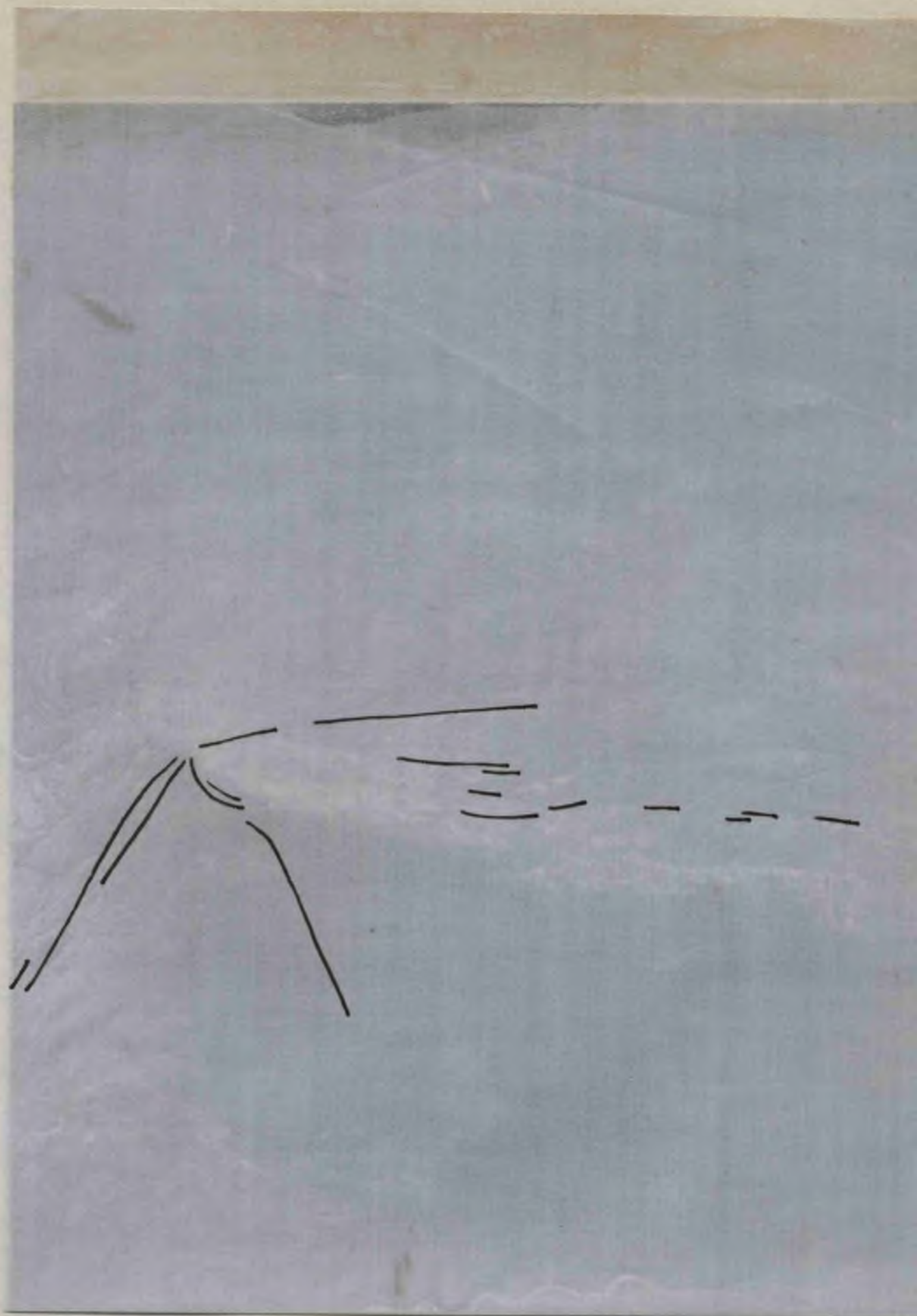


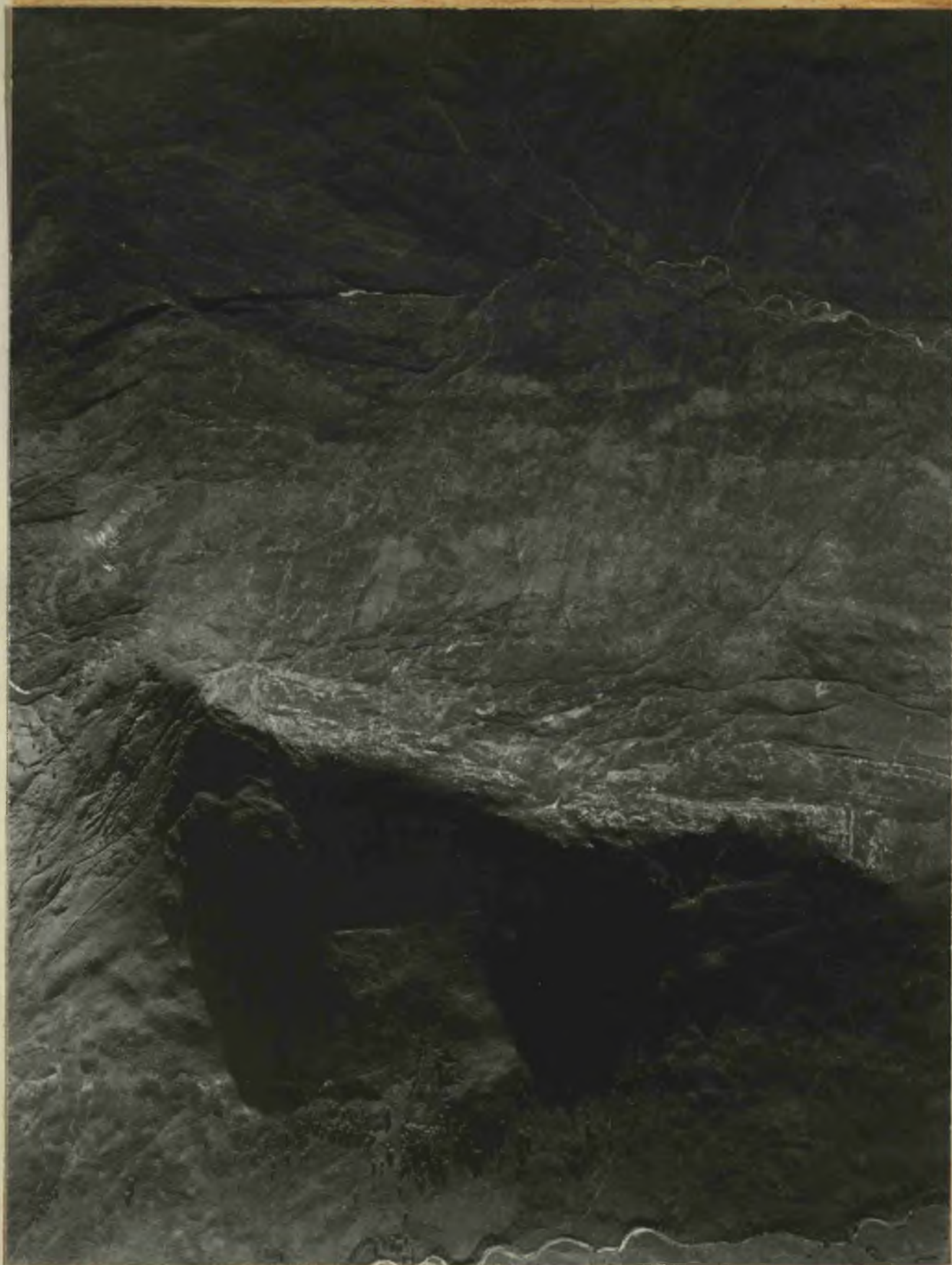


EXPLANATION OF PLATE XXXII

The lines on the overlay trace structural trends on Sgorr a' Choise as revealed by stereopairs of aerial photographs, scale 1: 10,000. Compare with strikes of bedding and cleavage for this area on maps II and III.

(Crown copyright reserved; not to be reproduced without permission of the Air Ministry.)





EXPLANATION OF PLATE XXXIII

The lines on the overlay trace structural trends across Beinn Fhiodha, Ailt a' Coire Riabhaich, and Beinn Bhan from top centre to lower left hand side respectively, as shown by stereopairs of aerial photographs, scale 1:10,000. Compare with strikes of bedding and cleavage for this area on maps II and III.

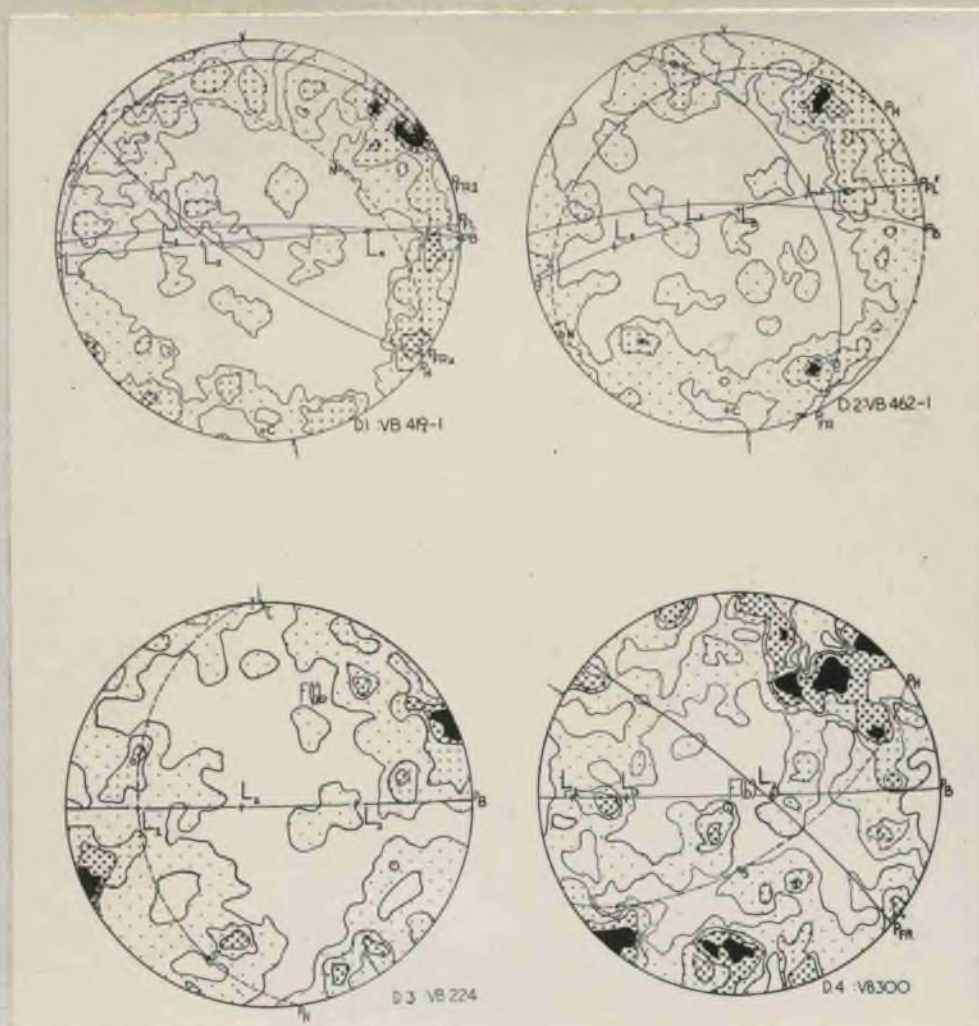
(Crown copyright reserved; not to be reproduced without permission of the Air Ministry.)





Diagram No.	1	2
Specimen No. and locality	VB419; Loc. 849, S. slope, Meall Mor	VB462; Loc. 961, S. E. slope, Sgorr a' Choise
Formation; specimen description	<u>Leven schist</u> : very thin alternating bands of mica and of quartz, with garnet porphyroblasts; 3 fine lineations: L_1 may be due to slippage on flow cleavage, L_2 and L_3 due to false cleavages intersecting flow cleavage, one coarse lineation (L_4), due to trace of bedding on flow cleavage	<u>Leven schist</u> : alternate bands 2-3 mm. thick of mica and of mica and quartz; 4 lineations: very fine (L_1), due to slippage on flow cleavage, fine (L_2) and medium-fine (L_4), due to trace of false cleavage on flow cleavage, medium-coarse (L_3), due to trace of bedding on flow cleavage
Position of thin-section	Roughly $\perp L_2$; inclined to $F(b')$	$\perp L_1$; inclined to $F(b')$
Thin-section no. and description	VB419-1: Small mica lath traces arranged in a herringbone pattern, those \perp arrow mark trace of flow cleavage, those inclined mark traces of false cleavages and relict bedding; predominantly medium to small, subangular quartz grains fill in mica matrix and occasionally form discontinuous bands parallel with flow cleavage	VB462-1: Narrow bands of mica laths, sometimes parallel with flow cleavage, sometimes inclined (due to intersection of false cleavage intersecting flow cleavage), alternate with narrow bands of medium to small, subangular to subrounded, quartz grains and small mica laths attenuated parallel to flow cleavage and in undulating pattern normal to flow cleavage (folded relict bedding). (Pl. X, Fig. 1)
No. optic axes	329	292
Contours	1, 2, 3, 3.5	1, 2, 3, 3.5
General contour pattern	Peripheral (a_2c) girdle + tendency for central girdle (just off ab); pair of shear planes parallel but inclined to bedding foliation; second pair inclined to $F(b')$	Peripheral (a_1c , a_3c) girdle + slight tendency for central girdle (just off ab); pair of shear planes parallel but inclined to bedding foliation; second pair inclined to L_1 ; third pair also inclined to L_1
Type of tectonite	$B \perp L_1 = b_1$ $B = L_4 = b_4 = F(b) = \text{roughly } F(b')$ $B \perp B'$	$B = L_1 = b_1 = F(b)$ $F(b') = L_3 = b_3$ $B \perp B'$
Type of lattice orientation	J(?), with Max. VI	J(?), with Max. VI
Fabric symmetry	Triclinic	Monoclinic
Remarks	Central girdle may be due to quartz orientation along false cleavage (PFR1)	Central girdle may be due to quartz orientation along false cleavage (PFR)

Diagram No.	2	4
Specimen No. and locality	VB224; Loc. 370, Craighannoch, W. Ballachulish	VB300; Loc. 560, N. slope, Beinn Bhàn
Formation: specimen description	<u>Banded Passage Beds:</u> quartzose schist, thermally metamorphosed, with 3 fine lineations: L_1 , L_2 , and L_3 , all due to false cleavage intersecting bedding foliation	<u>Striped Transition Series:</u> flaggy quartzite, with 3 fine lineations: L_1 , an "a" type, L_2 , approaching a "b" type, and L_3 , all due to false cleavage intersecting bedding foliation
Position of thin-section	$\perp L_2$; inclined to $F(b')$	$\perp L_2$; \perp interpolated fold axis of Beinn Bhàn syncline
Thin-section no. and description	VB224: narrow bands of medium to small quartz grains, angular to sub-rounded, alternate with narrow bands of small mica laths and fine, attenuated quartz grains; individual mica laths inclined 24° , 43° , and 63° to bedding; some large biotite porphyroblasts inclined 19° , 36° , 56° , and 68° to bedding	VB300: bands of small, sub-rounded quartz grains, individually separated by narrow bands of tiny mica lath aggregates; bedding not disturbed; individual laths not inclined
No. optic axes	418	247
Contours	1, 2, 2.5, 3%	1, 1.5, 2, 3%
General contour pattern	Peripheral (a_2c) girdle; pair of shear planes inclined to L_2 and responsible for L_1 and L_3 ; second pair parallel but inclined to bedding foliation	Peripheral (a_2c) girdle + central (b_2c) girdle; pair of shear planes inclined to $F(b')$ and responsible for L_3 ; second pair inclined to $F(b')$; third pair parallel but inclined to bedding foliation and responsible for L_1
Type of tectonite	$B = L_2 = b_2$ $B \neq F(b')$	$B = F(b')$; approximately $= L_2 = b_2$ $B \perp B'$
Type of lattice orientation	h, with Max. IV	j, with Max. IV
Fabric symmetry	Monoclinic	Triclinic
Remarks		



- P_B - bedding foliation plane
- P_{FL} - flow cleavage foliation plane
- P_{FR} - false cleavage foliation plane
- P_H - plane of the geographic horizontal
- c - pole to bedding
- L - lineation on foliation plane
- N or S - true north or south
- $F(b)$ - fold axis intersecting thin-section
- $F(b')$ - axial direction intersecting thin-section
- \uparrow - orientation arrow on thin-section
- \wedge - 0° point on A_1 of the Universal Stage

Specimen No. and locality	VB407; Loc. 820, River Coe	Same as D. 5
Formation: specimen description	Leven schist: contorted relict bedding approximately normal to conspicuous flow cleavage; biotite and garnet porphyroblasts throughout; 3 lineations: 1 very fine (L_1), due to false cleavage intersecting flow cleavage, 2 fine, L_2 also due to trace of false cleavage on flow cleavage and L_3 due to trace of bedding on flow cleavage (Pl. IX, Fig. 1)	Same as D. 5
Position of thin-section	$\perp L_3$; $\perp F(b)$; $\perp F(b')$	Same as D. 5
Thin-section No. and description	VB407-1: Small mica laths form narrow, rather discontinuous bands marking flow cleavage and narrow bands of similar folds whose axial plane parallels flow cleavage; quartz occurs in tiny grains where mica is most abundant, in small grains in garnet porphyroblasts, and in larger grains in the more quartzose bands; grains usually subangular to subrounded; large garnet porphyroblasts have preserved relict bedding (Pl. IX, Fig. 2)	Same as D. 5
No. optic axes	314 (in matrix only)	300 (in garnets only)
Contours	1, 2, 2.5, 3.25%	1, 1.75, 2.25, 3%
General contour pattern	Peripheral (a_1c , a_2c , a_3c) girdle + slight tendency for central girdle (b_3 and between a_3 and c); pair of shear planes parallel but inclined to bedding; second pair inclined to L_2	Peripheral (a_3c) girdle + a rough central (bc) girdle
Type of tectonite	$B = L_3 = b_3 = F(b) = F(b')$ $B \wedge B'$	$B = L_3 = b_3 = F(b) = F(b')$ $B \perp B'$
Type of lattice orientation	j, with Max. IV	j, with Max. IV
Fabric symmetry	Monoclinic	Triclinic
Remarks		Central girdle marks quartz orientation due to relict bedding

Diagram No.	7	8
Specimen No. and locality	Same as D. 5	VB458; Loc. 949, S. slope, Meall Mor
Formation: specimen description	Same as D. 5	<u>Leven schist</u> : biotite schist near contact with Ballachulish limestone; porphyroblasts of pink calcite; 3 lineations: fine (L_1), due to bedding intersecting flow cleavage, coarse (L_2) and fine (L_3), due to trace of false cleavages on flow cleavage
Position of thin-section	Same as D. 5	$\perp L_1, F(b)$ and L_3 ; axial direction lies practically in thin-section plane
Thin-section No. and description	Same as D. 5	VB458-1: long lath traces of biotite in more or less continuous bands marking flow cleavage; medium to small, angular quartz grains attenuated parallel with flow cleavage; epidote and calcite porphyroblasts conspicuous, mica does not bend around them
No. optic axes	614 (in matrix and garnets)	358
Contours	1, 1.5, 2, 2.5%	1, 2, 2.5, 3%
General contour pattern	Peripheral (a_2c, a_3c) girdle + tendency towards a central (bc) girdle; pair of shear planes inclined to L_2 ; second pair inclined to L_3	Irregular peripheral (a_3c) girdle + rough central (b_1c, b_3c) girdle
Type of tectonite	$B = L_3 = F(b) = F(b')$ $B \perp B'$	$B = L_1 = b_1 = F(b); F(b') = a_3$ $B \perp B'$
Type of lattice orientation	j, with Max. IV	j, with Max. IV(?)
Fabric symmetry	Triclinic	Triclinic
Remarks		Central girdle marks quartz orientation due to relict bedding

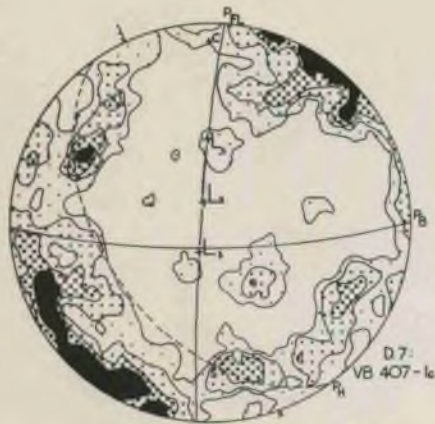
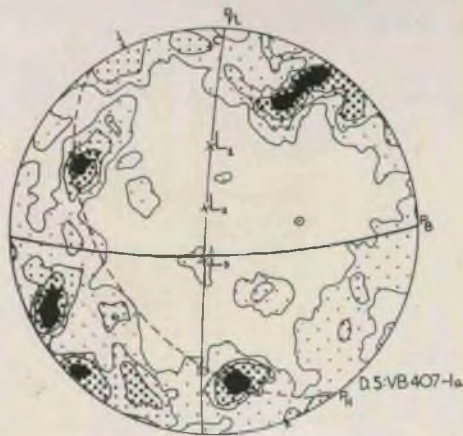


Diagram no.		10	
Specimen no. and locality	VB509; Loc. 1045, N. E. slope. Am Meall	VB644; Loc. 1448, N. slope, Meall Mor	
Formation: specimen description	<u>Ballachulish limestone</u> : folded bands of bluish-white quartz 3 mm. thick alternate with folded bands of gray calcite and mica 1-2 mm. thick; 3 lineations: 2 fine (L_1, L_2), both due to trace of false cleavages on flow cleavage, 1 coarse (L_3), due to intersection of bedding and flow cleavage	<u>Ballachulish limestone</u> : near contact with Leven schist; alternate bands 1-3 mm. thick of quartz, of calcite, and of mica, folded into a small synform trending 69° , plunging 78° N. E.; 3 lineations: 1 medium (L_1), due to trace of false cleavage on bedding, 2 coarse (L_2, L_3), also due to intersection of false cleavage and bedding (Pl. XI, Fig. 3)	
Position of thin-section	Roughly $\perp b_1$; almost $\perp b_3$ and $F(b)$	$\perp b_2$; inclined to b_3 and $F(b)$	
Thin-section no. and description	VB509-1: bands of small calcite grains and small mica laths alternate with bands of medium-sized, angular quartz with minor calcite and mica; thickness of individual bands varies due to minor small-scale folding; mica laths inclined ca. 14° to 20° , 90° to flow cleavage	VB644: folded bands of medium to small, subangular to sub-rounded quartz and weathered feldspar alternate with folded mica and quartz bands containing some porphyroblasts of chlorite, garnet, and calcite; undulations in bedding mark traces of false cleavages	
No. optic axes 339		335	
Contours	1, 1.5, 2, 2.5	1, 2, 3, 4	
General contour pattern	Peripheral (a_1c, a_3c) girdle + rough central (ab) girdle; one set of shear planes possibly responsible for L_1 & L_2 ; second pair inclined ca. $16^\circ - 21^\circ$ to bedding foliation; third pair normal to bedding foliation and inclined ca. 70° with respect to each other	Distinct peripheral (a_2c) girdle; pair of shear planes inclined ca. 30° to L_2 ; second pair unsymmetrically inclined to bedding foliation	
Type of tectonite	$B = L_3 = b_3 = F(b) = a_2; \neq F(b')$ $B \perp B'$	$R = L_3 = b_3 = F(b) = a_1 \neq F(b')$	
Type of lattice orientation	j (?), with Max. IV (?)	h, with Max. IV	
Fabric symmetry	Triclinic	Triclinic	
Remarks	Central girdle marks quartz orientation due to bedding; peripheral girdle marks quartz orientation due to flow cleavage		

Diagram No.	11	12
Specimen No. and locality	VB18; Loc. 26. upper Gleann an Fhiad	VB31, Loc. 37, Rudh' a Shaid Ineithe
Formation: Specimen description	Appin phyllite: flaggy quartzite, jointed into small blocks, with one fine (L_1) and one very coarse (L_2) lineation; L_1 due to trace of false cleavage on flow cleavage, L_2 due to rodding on flow cleavage and probably parallels direction of transport (a)	Appin quartzite: flaggy quartzite, with one very coarse (L_1) and one fine (L_2) lineation; L_1 may be due to current-bedding intersecting bedding foliation and represent direction of transport (a), L_2 due to trace of false cleavage on bedding
Position of thin-section	$\perp L_1$; $F(b')$ lies in thin-section plane	$\perp L_1$; inclined to $F(b')$
Thin-section no. and description	VB18-1: General attenuation of medium to very fine quartz grains marks flow cleavage, occasional pockets of coarser grains; folded relict bedding flow cleavage; discontinuous bands and isolated patches of mica laths, narrow, coarse-grained veinlets of calcite cross-cut cleavage	VB31: Large to medium quartz grains, subangular to embayed, some attenuated parallel to bedding foliation; tiny mica laths scattered poikilitically through quartz and inclined 22° to foliation
No. optic axes	314	438
Contours	1, 2, 3, 4	1, 2, 3, 3.5
General contour pattern	Peripheral (a, c) girdle; pair of shear planes inclined to L_1 ; second pair of shear planes inclined to flow cleavage	Peripheral (a, c) girdle; pair of shear planes parallel but inclined to bedding foliation
Type of tectonite	$B \perp L_1, \perp b_1$ $B = F(b') = L_2 = b_2$	$B = L_1 = b_1$ $B \neq F(b')$
Type of lattice orientation	n, with Max. II	n, with Max. II
Fabric Symmetry	Monoclinic	Triclinic
Remarks	Attenuation of quartz in thin section shows folded relict bedding roughly normal to flow cleavage	



In D. 9, 10, and 12 "o" is the pole to the bedding; in D. 11 "o" is the pole to the flow cleavage.

Diagram no.	13	14
Specimen no. and locality	VB101; Loc. 107, W. of Caolasnacon	VB110; Loc. 132, N. slope, Snor na Ciche
Formation: specimen description	<u>Binnéin quartzite</u> : quartzose quartzite, taken from upper limb of recumbent fold trending 129° , plunging 26° N.W. (Pl. I, Fig. 2); 2 fine lineations, L_1 a "b" lineation due to intersection of axial plane flow cleavage on bedding, L_2 an "a" lineation due to slippage of beds over bedding foliation	<u>Glencoe quartzite</u> : medium-grained quartzose quartzite with very thin intercalated black pelitic bands; 2 fine lineations: L_1 , approaching an "a" lineation, due to trace of false cleavage on bedding foliation, and L_2 , a "b" lineation due to intersection of axial plane flow cleavage and bedding foliation
Position of thin-section	$\perp L_1$ and a_2 ; almost $\perp F(b)$	$\perp L_2$ and a_1 ; almost $\perp F(b)$
Thin-section no. and description	VB101: Bands of medium to small quartz grains alternate with bands of small to tiny quartz grains and small mica laths; quartz sub-angular to subrounded, attenuated ca. 30° to bedding (trace of axial plane flow cleavage), a few large grains show strain shadows; individual mica laths inclined 31° , 40° , 51° to bedding foliation	VB110-1: Thick bands of medium to small quartz grains and mica laths alternate with thin bands of small to fine quartz and calcite grain individual mica laths inclined 24° , 39° , 55° , and 80° to bedding foliation
No. optic axes	280	283
Contours	1, 2, 3, 3.5%	1, 2, 3, 3.25%
General contour pattern	Peripheral (a_1, c) girdle + slight tendency for central (ab) girdle; one pair of shear planes inclined to L_1 and $F(b)$	Peripheral (a_2, c, b_1, c) girdle; one possible pair of shear planes cut bedding obliquely and straddle $F(b)$
Type of tectonite	$R=F(b)$, roughly $a_1=b_1=a_2$ $B \perp B'$	$B=F(b)=L_2=b_2$; almost a_1
Type of lattice orientation	j (?) with Max. IV (?)	h, with Max. IV
Fabric symmetry	Triclinic	Triclinic
Remarks		

Diagram no.	15	16
Specimen no. and locality	VB114; Loc. 140, shore section, Camas Callthaina	VB121; Loc. 147, River Laroch
Formation: specimen description	<u>Striped Transition Series:</u> flaggy quartzite, folded asymmetrically, with axis trending 78° , plunging 34° S. W.; 2 fine lineations: L_1 due to trace of false cleavage on bedding, L_2 due to axial plane false cleavage intersecting bedding	<u>Striped Transition Series:</u> 1-6 mm. thick bands of white quartzite alternate with 0.2 mm. thick bands of black slate; jointing prominent in 2 directions; part of N. W. limb of synform trending 74° , plunging 52° S. W. (Pl. XXII, Fig. 1); 2 fine lineations: L_1 approaching a "b" lineation and L_2 an "a" lineation, both due to false cleavages intersecting bedding foliation
Position of thin-section	$\perp L_1$, inclined to $F(b)$	Almost $\perp L_2$, inclined to $F(b)$
Thin-section no. and description	VB114: medium to small, sub-angular to sub-rounded, quartz grains, with occasional large ones in narrow cross-cutting veinlets; attenuation both parallel to bedding and normal to it (trace of axial plane false cleavage); minor mica laths inclined 30° to bedding.	VB121: Medium to tiny, sub-rounded to sub-angular quartz grains; some attenuation inclined to bedding foliation in micaceous bands marks trace of axial plane false cleavage; micaceous bands consist of clusters of tiny mica laths and small quartz grains; subordinate small grains of calcite and plagioclase scattered throughout
No. optic axes	249	301
Contours	1, 2, 3, 3.5	1, 1.75, 2, 2.5, 3
General contour pattern	Peripheral (a_1c) girdle; one pair of shear planes parallel but inclined quite steeply to bedding foliation	Peripheral (a_1c , a_2c) girdle + with tendency for a central (ab) girdle; one pair of shear planes parallel but inclined to bedding foliation; two pairs normal to bedding
Type of tectonite	$R=F(b)$, almost $=L_2=b_2$	$R=F(b) = L_1=b_1$ BIB'
Type of lattice orientation	h, with Max. IV(?)	j(?) with Max. IV
Fabric symmetry	Monoclinic	Triclinic
Remarks		



Diagram no.	17	18
Specimen no. and locality	VB130; Loc. 194, Glen Coe	VB142; Loc. 239, Camas Calltuinn
Formation: specimen description	<u>Ballachulish limestone</u> : quartzitic band in contorted limestone; part of small synform trending 52° , plunging 26° S. W.; 2 lineations: 1 medium (L_1) due to irregular bedding foliation intersecting measured bedding foliation, 1 fine due to false cleavage intersecting bedding	<u>Striped Transition Series</u> : part of quartzite band intercalated in contorted phyllite, having fold axes trending ca. 61° , plunging 67° S. W.; 2 fine lineations (L_1 and L_2) both due to false cleavages intersecting bedding foliation
Position of thin-section	Almost $\perp L_1$, gently inclined to $F(b)$	$\perp L_1$, somewhat inclined to $F(b)$
Thin-section no. and description	VB130: continuous bands of small to fine calcite grains marking bedding foliation alternate with narrow, discontinuous bands of medium to small, subangular to subrounded quartz grains; Böhm lamellae in some of the larger quartz grains; individual muscovite laths inclined 6° - 10° , 27° - 32° , and 59° to bedding foliation	VB142: medium to fine, angular to subangular quartz grains with subordinate tiny muscovite laths and blobs; some quartz attenuation parallel bedding foliation and some inclined ca. 40° to bedding (trace of axial plane false cleavage); individual mica laths inclined 27° and 39° to bedding foliation
No. optic axes	331	293
Contours	1, 1.5, 2, 3	1, 2, 3, 4
General contour pattern	Roughly peripheral (a_1c , a_2c) girdle + two central (b_1c , b_2c) girdles; two pairs of shear planes cut bedding foliation near L_1 and L_2	Peripheral (a_1c) girdle; one pair of shear planes parallel but inclined to bedding foliation
Type of tectonite	$R=F(b)$, almost $\perp L_1$ and b_1 $B \perp B'$	$R=F(b)$, almost $\perp L_1 = b_1$
Type of lattice orientation	j, with Max. IV	h, with Max. IV
Fabric Symmetry	Triclinic	Triclinic
Remarks		

Diagram no.	19	20
Specimen no. and locality	VB143; Loc. 142, shore section, Camas Calltuinn	VB324; Loc. 625, N. slope, Am Meall
Formation: specimen description	Banded Passage Beds: portion of contorted quartzite bands just E. of Bailey's slide; taken from fold trending 137° , plunging 34° S. E.; 2 lineations: coarse (L_1) and fine (L_2), both due to false cleavages intersecting bedding	Ballachulish limestone: thin-bedded ^{"ribbon" limestone with} paper-thin micaceous laminae; part of fold trending 71° , plunging 52° S. W.; 2 lineations: very fine (L_1) due to trace of false cleavage on bedding and coarse (L_2) almost a "b" lineation, due to axial plane false cleavage intersecting bedding
Position of thin-section	Roughly $\perp L_1$; gently inclined to $F(b)$	$\perp L_2$ and $F(b)$
Thin-section no. and description	VB143; large to tiny, angular to subangular quartz grains throughout, with some narrow, discontinuous bands of tiny quartz marking bedding foliation; attenuation both parallel bedding and inclined ca. 80° (trace of axial plane false cleavage); individual mica laths inclined 18° and 73° to bedding	VB324: narrow, straight bands of small, angular to sub-rounded calcite grains alternate with narrow bands of small, angular to sub-rounded quartz grains, with occasional sporadic lenticular bands of medium-sized quartz; both calcite and quartz attenuated parallel with bedding; tiny mica laths scattered throughout, many parallel with bedding others inclined 9° - 13° , 18° , and 26° to bedding
No. optic axes	234	366
Contours	1, 2, 3, 4	1, 2, 3, 4
General contour pattern	Peripheral (a_1c , a_2c) girdle; two pairs of shear planes out bedding foliation near L_1 and L_2	Peripheral (a_2c) girdle; two pair of shear planes parallel but inclined to bedding foliation
Type of tectonite	$R = F(b) = a_1$; $B \perp L_1$ and b_1	$R = F(b) = L_2 = b_2$
Type of lattice orientation	h, with Max. IV	h, with Max. IV
Fabric Symmetry	Triclinic	Triclinic
Remarks		



D17-VB130



D18-VB142



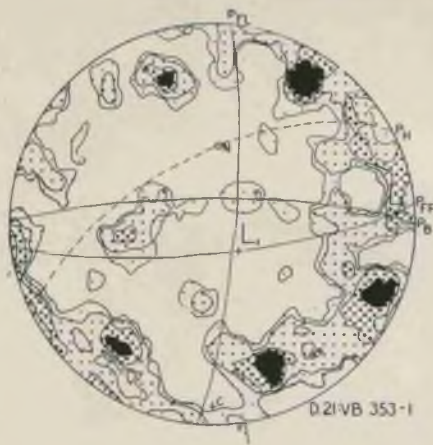
D19-VB143



D20-VB324

Diagram no.	21	22
Specimen no. and locality	VB353; Loc. 708, N. W. slope, Sgorr a' Choise	VB544; Loc. 1226, Tom Ban, Glen Coe
Formation: Specimen description	<u>Ballachulish slate</u> ; narrow, intercalated, folded quartz bands make bedding prominent on dominant false cleavage surfaces and result in a coarse to fine lineation (L_2); another fine lineation (L_1) due to trace of flow cleavage on false cleavage	<u>Ballachulish limestone</u> : alternate narrow, folded bands of bluish-gray calcite and silvery-gray tremolite and mica, with pockets of whitish quartz and with tremolite blades conspicuous on bedding foliation; 2 fine lineations: L_1 due to false cleavage crosscutting micaceous bands, and L_2 due to elongation of tremolite
Position of thin-section	$\perp L_1$; almost $\perp F(b)$	$\perp L_1$; inclined to $F(b')$
Thin-section no. and description	VB353-1: thick to thin bands of tiny mica laths alternate with thin bands of small to tiny, subangular to subrounded quartz grains; bands folded asymmetrically, thicken at crests and troughs, thin on limbs; flow cleavage trace inclined ca. 50° to bedding foliation (Pl. XVI, Fig. 2)	VB544: thick bands of tiny to medium-sized calcite grains with occasional mica laths and quartz grains alternate with narrow bands of mica and with discontinuous thin bands of coarse to medium-grained, angular to subrounded quartz; small-scale folding due to false cleavage crosscuts bedding foliation
No. optic axes	278	312
Contours	1, 1.5, 2, 3%	1, 2, 3, 4%
General contour pattern	Peripheral (a_1c) girdle + slight tendency for central (ab) girdle and for off-center (a_2c) girdle; three possible pairs of shear planes cut bedding foliation obliquely	Rough peripheral (a_1c, a_2c) girdle + tendency for central (b_1c) girdle and for off-center girdle passing from " a_2 " between " b_1 " and " c "; one possible pair of shear planes almost normal to bedding foliation
Type of tectonite	$B = F(b)$, almost $= L_1 = b_1$ $B \perp B'$	$B \neq F(b')$, $= L_2 (?) = b_2 (?)$ $B \perp B'$
Type of lattice orientation	j (?), with Max. IV	j (?), with Max. IVc
Fabric Symmetry	Monodinic	Monodinic
Remarks	Central (ab) girdle due to relict quartz orientation along bedding foliation	

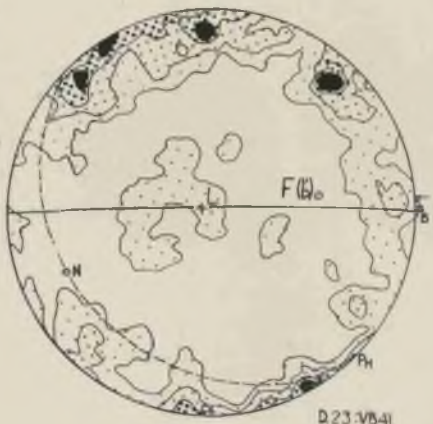
Diagram no.	23	24
Specimen no. and locality	VB41; Loc. 41, shore section, W. Ballachulish.	VB49; Loc. 43, shore section W. Ballachulish.
Formation: specimen description	<u>Striped Transition Series</u> : medium-grained flaggy quartzite, with one fine lineation (L) due to false cleavage in micaceous bands cutting bedding foliation; jointed	<u>Banded Passage Beds</u> : fine-grained, grayish, flaggy quartzite, with one fine lineation (L) approaching a "b" lineation and due to false cleavage in micaceous bands cutting bedding foliation; jointed
Position of thin-section	$\perp L$; inclined to $F(b')$	$\perp F(b)$; almost $\perp L$
Thin-section no. and description	VB41: bands of small to tiny, subangular quartz grains alternate with discontinuous narrow bands of small mica laths; individual laths may be parallel to bedding foliation or inclined 9° and 18° ; small grains of pyrite scattered throughout; vein of larger quartz grains crosscuts bedding	VB49: medium to tiny, subangular to subrounded quartz grains, some attenuated parallel to bedding, others inclined ca. 26° to bedding (trace of false cleavage); small to tiny mica laths inclined 29° and 51° to bedding foliation; medium-sized plagioclase grains scattered throughout
No. optic axes	388	373
Contours	1, 2, 3, 3.5	1, 2, 3, 4
General contour pattern	Peripheral (ac) girdle + slight tendency for central girdle passing from "b" between "a" and "c"; one possible pair of shear planes is parallel to bedding and steeply inclined to it	Peripheral (roughly ac) girdle; no possible pairs of shear planes
Type of tectonite	$B=L=b \neq F(b')$ $B \wedge B'$	$R=F(b)$; almost $=L=b$
Type of lattice orientation	J(?), with Max. II(?)	?h, with Max. IV(?)
Fabric Symmetry	Triclinic	Triclinic
Remarks		



D21VB 353-1



D22VB 544



D23VB 41



D24VB 49

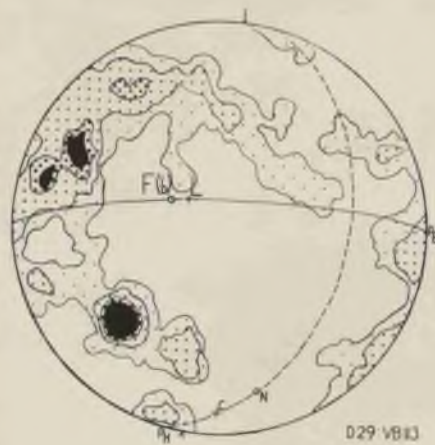
Diagram no.	25	26
Specimen no. and locality	VB60; Loc. 60, near junction of the Larock and Socaich rivers	VB98; Loc. 105, Caolas-nacon
Formation: specimen description	<u>Appin quartzite</u> : medium-grained, white, jointed quartzite with weathered feldspar grains; lineation(L) due to alignment of pyrite grains	<u>Binnein quartzite</u> : rather thin-bedded with intercalated micaceous laminae; part of a large fold trending 92° , plunging 42° N. W.; fine lineation (L) approaches a "b" lineation, due to axial plane false cleavage
Position of thin-section	Almost \perp L; gently inclined to axial direction	Almost \perp L; inclined to F(b)
Thin-section no. and description	VB60: large to medium, sub-rounded quartz grains; large ones show strain shadows; some large weathered microperthite and plagioclase grains with cleavages inclined 26° , 37° , and 43° to bedding foliation	VB98: thick bands of medium to small quartz grains alternate with thick bands of small to tiny quartz grains; quartz subangular to sub-rounded; narrow, more or less discontinuous bands of small mica laths inclined 15° , 31° , 40° , 49° , and especially 52° and 63° to bedding foliation
No. optic axes	353	257
Contours	1, 2, 3, 4%	1, 2, 3, 4%
General contour pattern	Distinct peripheral (ac) girdle; one possible structural plane, normal to bedding, along which pyrite has formed	Peripheral (ac) girdle; one pair of shear planes inclined to bedding foliation; second pair inclined to F(b)
Type of tectonite	$B ? = F(b'), \perp L, \parallel b$	$R = F(b) = L = b$
Type of lattice orientation	h, with Max. IV	h, with Max. IV
Fabric Symmetry	Triclinic	Triclinic
Remarks		

Diagram no.	27	28
Specimen no. and locality	VB100: Loc. 107, W. of Caolasnacon	VB123; Loc. 158, upper N. slope, Sgor na Ciche
Formation: specimen description	<u>Binnein quartzite</u> : quartzose quartzite taken from lower limb of recumbent fold (Pl. I, Fig. 2) and showing bedding well; one coarse lineation (L) parallel with fold axis (trending 129° , plunging 26° N. W.)	<u>Glencoe quartzite</u> : massive quartzose quartzite; one fine lineation (L) due to trace of false cleavage on bedding
Position of thin-section	Inclined to L and F(b)	Inclined to L and F(b')
Thin-section no. and description	VB100: large to tiny, subangular to subrounded quartz grains, attenuated 26° to bedding foliation (marks axial plane flow cleavage); small individual mica laths also parallel flow cleavage	VB123: bands of medium to tiny quartz grains alternate with bands of small to tiny quartz grains; grains subangular to subrounded; small muscovite laths in discontinuous bands mark bedding foliation; some laths inclined 13° , 33° - 38° (common), 64° to bedding; large cleavage sections of secondary biotite sometimes parallel bedding, sometimes are inclined 12° , 33° , and 76° to foliation
No. optic axes	351	343
Contours	1, 2, 2.5, 3%	1, 2, 3, 3.5%
General contour pattern	Rough peripheral (bc) girdle + slight tendency for central (ac) girdle + slight tendency for central girdle inclined to ab; one pair of shear planes cutting bedding near "a" and "b" (L)	Rough peripheral girdle passing from "c" between "a" and "b" + slight tendency for central girdle also passing from "c" between "a" and "b"; one pair of shear planes cutting bedding foliation near "a" and "b"
Type of tectonite	$R=F(b)=L=b$ $B \wedge B'$	$B=F(b')=L=b$ $B \perp B'$
Type of lattice orientation	j (?), with Max. VI(?)	j (?), with Max. VI(?)
Fabric Symmetry	Triclinic	Triclinic
Remarks		

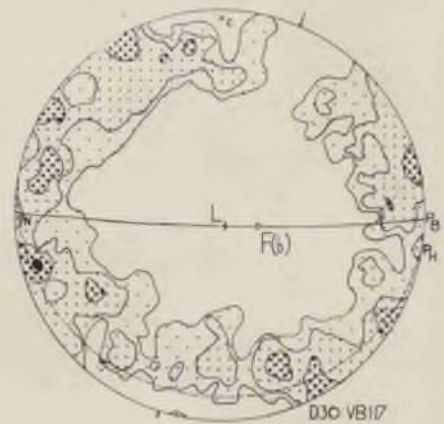


Diagram no.	29	30
Specimen no. and locality	VB113; Loc.140, shore section, Camas Calltuinn	VB117; Loc.141, shore section, Camas Calltuinn
Formation: specimen description	<u>Striped Transition Series:</u> part of massive quartzite band in broad open fold trending 102° , plunging 72° N. W.; 1 lineation: coarse to fine (L), approaching a "b" lineation and due to axial plane false cleavage intersecting bedding	<u>Striped Transition Series:</u> medium-grained flaggy quartzite; part of antiform trending 67° , plunging 59° S. W. (Pl. XXI, Fig.2); one fine lineation (L), approaching a "b" lineation and due to axial plane false cleavage intersecting bedding foliation
Position of thin-section	Almost \perp L and F(b)	\perp L; almost \perp F(b)
Thin-section no. and description	VB113: predominantly large, subrounded, interlocking quartz grains, with several showing strain shadows and with Böhm lamellae conspicuous in almost all grains, some attenuation inclined ca. 85° to bedding foliation; minor plagioclase grains throughout	VB117: broadly undulating bands of medium to small quartz grains alternate with bands of fine quartz grains with and without small mica laths; strain shadows in large quartz grains; individual mica laths inclined 15° - 20° , 30° - 32° , 37° - 44° , 49° , 56° , 76° to bedding foliation
No. optic axes	362	266
Contours	1, 2, 3, 4%	1, 2, 3, 4%
General contour pattern	Roughly peripheral (ac) girdle; one possible pair of shear planes cuts bedding obliquely	Distinct peripheral (ac) girdle; no possible pairs of shear planes
Type of tectonite	R=F(b); almost \approx L=b	R=F(b); almost \approx L=b
Type of lattice orientation	?h, with Max. VI ?	h, with Max. IV
Fabric Symmetry	Triclinic	Triclinic
Remarks		

Diagram no.	31	32
Specimen no. and locality	VB118; Loc. 141, shore section, Camas Callit/iunn	VB152; Loc. 72, N. W. slope, Am Meall
Formation: specimen description	Striped Transition Series: flaggy quartzite; part of antiform trending 67° , plunging 59° S. W. (Pl. XXI, Fig. 2); one medium-coarse lineation (L) due to false cleavage intersecting bedding foliation of micaceous bands	Ballachulish limestone: alternating bands of calcite and of calcite and mica; coarse-to fine-grained; part of fold trending 27° , plunging 23° N. E.; one fine lineation (L) due to false cleavage intersecting bedding foliation of micaceous laminae
Position of thin-section	\perp L; inclined to F(b), which lies in bedding foliation	\perp L; inclined to F(b), which lies in bedding foliation
Thin-section no. and description	VB118: about one-third medium-sized quartz grains, two thirds small quartz grains, subangular to subrounded, with embayment conspicuous in larger grains; the larger grains tend to occur in pockets and to show strain shadows; individual mica laths inclined 35 and 50° to bedding foliation	VB152; broad bands of tiny, angular to subrounded calcite grains alternate with narrow bands of medium-sized, angular to subrounded quartz grains; medium-sized blobs and small lath traces of muscovite usually admixed in both; individual laths inclined to 48° - 53° to bedding foliation
No. optic axes	301	320
Contours	1, 2, 3, 4%	1, 2, 2.5, 3%
General contour pattern	Peripheral (ac) girdle; no possible pairs of shear planes	Rough central (ac) girdle; one possible pair of shear planes parallel and inclined steeply to bedding foliation; second pair cuts bedding obliquely
Type of tectonite	$R=F(b)$	$R=F(b)$ with Max. III and Max. IV
Type of lattice orientation	h, with Max. II and Max. IV	Unlike a-m, when L is taken as "b", h, with Max. VI, when F(b) is taken as "b"
Fabric Symmetry	Triclinic	Triclinic
Remarks		



D29 VB13



D30 VB17



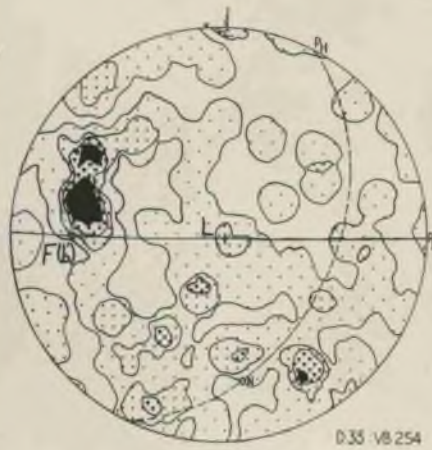
D31 VB18



D32 VB152

Diagram no.	33	34
Specimen no. and locality	VB187; Loc. 313, S. slope, Sgòr nam Fiannaidh	VB217; Loc. 360, spur S. of Caolasnacon
Formation: specimen description	Glencoe quartzite: coarse- to medium-grained quartzose quartzite; massive; "ac" jointing; one very coarse lineation (L) due to trace of false cleavage on bedding foliation of micaceous laminae	Binnein quartzite: medium-grained quartzose quartzite; massive; jointed; one fine lineation (L) due to intersection of false cleavage and bedding foliation in micaceous laminae
Position of thin-section	$\perp L$; inclined to $F(b')$	$\perp L$; almost $\perp F(b')$
Thin-section no. and description	VB187: predominantly large, sub-rounded quartz grains with no special attenuation; scatter of tiny grains throughout suggests incipient granulitisation; minor clusters of tiny mica laths with no preferred orientation; minor grains of weathered feldspar, Ca-garnet, and epidote	VB217: large to small, generally subrounded quartz grains attenuated both parallel to bedding and bedding (false cleavage); strain shadows in larger ones; occasional discontinuous bands of small muscovite laths mark bedding foliation, individual laths inclined 32° to bedding
No. optic axes	335	326
Contours	1, 2, 3, 4%	1, 2, 3, 4%
General contour pattern	Approximately peripheral (ac) girdle; no possible pairs of shear planes	Peripheral (ac) girdle; one possible pair of shear planes cuts bedding at large angle
Type of tectonite	$B=L=b$; $\neq F(b')$	$B=F(b')=L=b$
Type of lattice orientation	h, with Max. IV	h, with Max. IV
Fabric Symmetry	Triclinic	Triclinic
Remarks		

Diagram NO.	35	36
Specimen No. and locality	VB254; Loc. 406, summit, Sgòr nam Fiannaidh	VB295; Loc. 535, shore section N. W. slope, Sgòr na Ciche
Formation: specimen description	Glencoe quartzite: coarse-grained quartzose quartzite; massive; jointed; rough lineation (L) probably due to false cleavage intersecting bedding foliation	Glencoe quartzite: flaggy quartzite; one medium lineation (L) due to false cleavage intersecting bedding foliation of micaceous laminae
Position of thin-section	\perp L; inclined to $F(b')$, which lies in bedding foliation	Almost \perp L; inclined to $F(b')$
Thin-section No. and description	VB254: large, subrounded quartz grains, with no strain shadows but conspicuous Böhm lamellae; two fracture systems inclined 45° to bedding foliation; grains occasionally outlined by tiny muscovite laths inclined 15° , 35° , 42° , and 51° to bedding foliation	VB295: bands of medium to small, subrounded quartz grains alternate with narrow, discontinuous bands of small muscovite laths, frequently in a lacy pattern: individual laths inclined 22° and 52° to bedding foliation; a few large quartz grains show strain shadows
No. optic axes	129	310
Contours	1, 2, 4, 5.5%	1, 2, 3, 4
General contour pattern	Very rough off-center ($b'e$) girdle; one possible pair of shear planes cuts bedding at large angle	Peripheral (ac) girdle + slight tendency for off-center girdle (almost $b'e$); one possible pair of shear planes cuts bedding obliquely
Type of tectonite	$B = F(a')$	$B = L = b$, almost $= F(b')$ $B \perp B'$
Type of lattice orientation	?h, with Max. IV(?)	j(?), with Max. IV
Fabric Symmetry	Triclinic	Triclinic
Remarks		



Specimen No. and locality	VB525; Loc. 1090, upper S. W. slope, Sgòr nam Fiannaidh	VB647, Loc. 1223, Glen Coe
Formation: specimen description	Glencoe quartzite: massive, banded, white quartzite; micaceous films on bedding foliation have one fine lineation (L) approaching a "b" lineation and due to false cleavage intersecting bedding	Banded Passage Beds: alternating bands of whitish quartzite and dark gray phyllite folded into a small, slightly overturned synform trending 43° , plunging 79° S. W.; one medium lineation (L) parallels fold axis and is due to axial plane false cleavage (Pl. IV, Fig. 1)
Position of thin-section	\perp L and F(b')	\perp L and F(b)
Thin-section no. and description	VB525: predominantly medium-sized, subrounded to subangular quartz grains, the larger ones frequently showing strain shadows; occasional very narrow, discontinuous bands of mica laths largely inclined to bedding foliation and parallel to false cleavage	VB647: thicker bands of medium to small, angular to subangular quartz attenuated parallel with bedding alternate with thinner bands of long mica laths and small quartz grains; undulations of mica bands due to cross-cutting false cleavage
No. optic axes	292	320
Contours	1, 2, 3, 4%	1, 2, 3, 3.75%
General contour pattern	Almost peripheral (just off ac) girdle; no shear planes intersecting bedding foliation	Peripheral (ac) girdle; one pair of shear planes inclined to bedding foliation
Type of tectonite	$B = F(b') = b$	$R = F(b)$, roughly = b
Type of lattice orientation	?h, with Max. IV?	h, with Max. II and IV?
Fabric Symmetry	Triclinic	Triclinic
Remarks		

Diagram no.	39	40
Specimen no. and locality	VB707; Loc. 1607, Allt Socaich	VB3; Loc. 4, N. W. slope, Meall a' Chaolais
Formation: specimen description	<u>Ballachulish limestone</u> : 2 mm. thick whitish bands of quartzite alternate with 1-3 mm. thick greenish bands of mica and calcite; one very fine lineation (L) due to false cleavage intersecting the bedding foliation	<u>Banded Passage Beds</u> : very quartzose schist, cut by cubical jointing
Position of thin-section	\perp L; inclined to $F(b')$	\perp bedding foliation; possibly $\perp F(b')$
Thin-section no. and description	VB707: small to tiny, angular to subangular quartz, attenuated generally parallel to bedding, with small lath traces of mica both parallel with bedding foliation and inclined (marking false cleavage); several very large calcite porphyroblasts with tiny poikiloblasts of mica, quartz, and epidote	VB3: narrow bands of small, angular quartz grains alternate with narrow bands of tiny biotite lath traces; both quartz and mica are attenuated parallel bedding
No. optic axes	292	337
Contours	1, 2, 3, 4 $\frac{1}{2}$	1, 1.5, 2, 3 $\frac{1}{2}$
General contour pattern	Peripheral (ac) girdle; one pair of shear planes inclined to L	Peripheral (?a'c?) girdle; two pairs of shear planes cut bedding at large angles
Type of tectonite	$B = L(b) = b'$, inclined to $F(b')$	$B = F(b')$ (?)
Type of lattice orientation	h, with Max. IV	h, with Max. IV
Fabric symmetry	Triclinic	Monoclinic
Remarks		

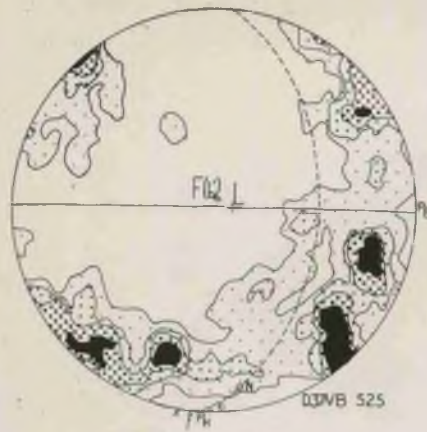


Diagram No.	41	42
Specimen No. and locality	VB35; Loc. 39, Neall a' Chaolais	VB36; Loc. 40, Neall a' Chaolais
Formation: specimen description	Striped Transition Series: whitish flaggy quartzite, with pyrite; jointed, no lineation	Striped Transition Series: same as VB35
Position of thin-section	⊥ bedding foliation; possibly F(b')	⊥ bedding foliation; possibly almost F(b')
Thin-section No. and description	VB35: large to tiny, sub-rounded quartz grains, with series of fine-grained quartz gross-cutting bedding foliation; some weathered, medium-sized, sub-rounded feldspar grains	VB36: regular bands of small to tiny, subrounded quartz grains alternate with discontinuous bands of mica blobs (tiny laths in a feathery pattern), with individual laths inclined 29° 36°, 52°-57°, and 76° to bedding foliation
No. optic axes	424	233
Contours	1, 2, 2.25, 2.75%	1, 2, 3, 4%
General contour pattern	Peripheral (? a'c?) girdle+ tendency towards central girdle (almost b'c); one possible pair of shear planes cuts bedding at large angle.	Peripheral (?a'c?) girdle+ tendency towards central (b'c) girdle; one possible pair of shear planes cuts bedding at large angle
Type of tectonite	B = F(b')? BLB'	B = F(b')? BLB'
Type of lattice orientation	j(?), with Max IV	j(?), with Max. IV
Fabric symmetry	Triclinic	Triclinic
Remarks		The lattice orientation corroborates that of VB 33, obtained nearby.

Diagram No.	43	44
Specimen No. and locality	VB68; Loc. 75, Clachaig, Glen Coe	Same as D. 43
Formation: specimen description	<u>Glencoe quartzite</u> : thick, whitish quartzite bands alternate with narrow, black pelitic bands; massive, jointed	Same as D. 43
Position of thin-section	\perp bedding; steeply inclined to $F(b')$	\perp bedding; $F(b')$ lies roughly in bedding foliation
Thin-section No. and description	VB68-1: large, subrounded quartz grains, with mica and quartz poikiloblasts, some attenuation parallel bedding foliation, Bohm lamellae, but no strain shadows; small mica laths scattered between quartz grains and parallel to bedding	VB68-2: very large, subrounded quartz, generally attenuated parallel bedding; streaks of muscovite parallel bedding, individual laths sometimes inclined 29°
No. optic axes	342	286
Contours	1, 1.5, 2, 3%	1, 2, 3, 4%
General contour pattern	Peripheral ($a'c'$) girdle + slight tendency for central ($b'o$) girdle; one pair of shear planes parallel to and steeply inclined to bedding foliation	Central ($a'c'$) girdle + tendency for peripheral ($b'o$) girdle; one possible pair of shear planes parallel and inclined to bedding; second possible pair cuts bedding at large angle
Type of teutonite	$B = F(b')?$ BAB'	$B = F(b')?$ BAB'
Type of lattice orientation	j(?), with Max. IV AND VI.	j, with Max. IV?
Fabric symmetry	Triclinic	Triclinic
Remarks		VB68-2 is approximately normal to VB68-1 and illustrates the value of studying differently oriented sections from the same specimen.



Diagram no.	45	46
Specimen no. and locality	VB69: Loc. 76, Clachaig, Glen Coe	VB73; Loc. 85, Allt a' Coire Riabhaich
Formation: specimen description	Banded Passage Beds: 10-12 mm. thick bands of pinkish-brown quartzite alternate with 0.2 mm. thick dark pelitic bands	Striped Transition Series: medium-grained quartzose quartzite mottled with whitish feldspar; jointed
Position of thin-section	\perp bedding foliation; steeply inclined to $F(b')$	\perp bedding foliation; $F(b')$ lies roughly in bedding
Thin-section no. and description	VB69: medium to small, sub-rounded quartz grains, with occasional large ones; continuous and discontinuous undulatory bands of small mica laths, some inclined 23° - 26° to bedding foliation	VB73: medium to tiny, sub-angular to subrounded quartz grains with small mica laths scattered throughout in discontinuous bands; some laths inclined 45° and 52° to bedding foliation
No. optic axes	649	295
Contours	1, 1.5, 2, 3%	1, 2, 3, 3.5%
General contour pattern	Annular girdle (passing from "a'" between "b'" and "c") + tendency for central (roughly $b'c$) girdle; three possible pairs of shear planes parallel to and inclined to bedding foliation	Roughly peripheral ($?b'c?$) girdle + slight tendency for central (almost $a'c$) girdle; one possible pair of shear planes cuts bedding plane at an oblique angle
Type of tectonite	$B = F(b')$? $B \wedge B'$	$B = F(a')$? $B \perp B'$
Type of lattice orientation	Roughly j, with Max. IV and VI(?)	j, with Max. III and IV(?)
Fabric Symmetry	Triclinic	Triclinic
Remarks		

Diagram no.	47	48
Specimen no. and locality	VB82; Loc. 90, S. slope, Sgorr Dhearg	VB136; Loc. 233, S. W. slope, Sgorr a' Choise
Formation: specimen description	Appin quartzite: medium-grained, whitish quartzite mottled with pink feldspar grains; jointed	Appin quartzite: medium-grained, white quartzite; jointed
Position of thin-section	\perp bedding; gently inclined to $F(b')$	\perp bedding; $F(b')$ lies roughly in bedding
Thin-section no. and description	VB82: large to medium, subangular quartz grains, with Bohm lamellae conspicuous but strain shadows singularly absent; large, rounded, weathered feldspar grains scattered throughout; minor mica laths inclined 44° and 57° to bedding	VB136: a generally even distribution of large to small quartz grains, angular to subangular, with strain shadows; medium-sized, weathered feldspar grains scattered throughout; some individual mica laths inclined 53° and 68° to rough bedding foliation
No. optic axes	361	298
Contours	1, 2, 3, 3.25%	1, 1.5, 2, 3%
General contour pattern	Two rough girdles, one approximately $b'o$, the other $a'b'$; two possible pairs of shear planes cut bedding at steep angles	Two rough girdles, one approximately $a'o$, the other $a'b'$; one possible pair of shear planes is parallel to and inclined to bedding, two other possible pairs cut bedding at steep angles
Type of teutonite	$B \neq F(b')$ $B \perp B'$	$B' = F(a')?$ $B \perp B'$
Type of lattice orientation	j (?); with Max. IV	j (?); with Max. IV?
Fabric Symmetry	Triclinic	Triclinic
Remarks		



D45 VB 69



D46 VB 73



D47 VB 82



D48 VB 136

Diagram no.	49	50
Specimen no. and locality	VB175; Loc. 300, N. slope, An t-Sron, Glen Coe	VB238; Loc. 386, N. slope, Sgòr na Ciche
Formation: specimen description	Glencoe quartzite: medium-grained, white, massive quartzite; jointed	Glencoe quartzite: medium-grained, glassy quartzite mottled with pink feldspar; jointed
Position of thin-section	⊥ bedding; F(b') lies in bedding foliation	⊥ bedding; inclined to F(b')
Thin-section no. and description	VB175: very large, angular quartz grains with tiny poikiloblasts of quartz and mica, Bohm lamellae conspicuous but no strain shadows; tiny mica laths mark bedding foliation	VB238: bands of medium-sized quartz grains alternate with bands of small quartz grains, subrounded; large microcline porphyroblasts and small muscovite laths scattered throughout; individual mica laths inclined 18° and 34° to bedding foliation
No. optic axes	280	353
Contours	1, 2, 3, 4%	1, 2, 3, 3.5%
General contour pattern	Central (a'b') girdle; one pair of shear planes roughly parallel to bedding and inclined to it	Rough peripheral (?a'e?) girdle; one possible pair of shear planes cuts bedding obliquely
Type of tectonite	B=F(b')?	B=F(b')?
Type of lattice orientation	e, with Max. IV and VII (?)	h, with Max. IV
Fabric symmetry	Triclinic	Triclinic
Remarks		

Diagram no.	51	52
Specimen no. and locality	VB242; Loc. 392, N. spur, Sgòr nam Fiannaidh	VB251; Loc. 403, summit, Sgòr nam Fiannaidh
Formation: specimen description	Glencoe quartzite: thermally metamorphosed quartzose quartzite; jointed	Glencoe quartzite: medium-grained, quartzose quartzite; jointed
Position of thin-section	⊥ prominent joint plane; inclined to bedding; $F(b')$ lies almost in bedding foliation	⊥ bedding; $F(b')$ lies in bedding foliation
Thin-section no. and description	VB242: medium to tiny, subangular to subrounded quartz grains, attenuation both parallel to mica foliation and normal to joint plane; minor mica laths inclined ca. 40° to joint plane; occasional small plagioclase grains	VB251: medium to small, generally subrounded quartz grains, some outlined by irregular blobs of tiny mica laths; individual laths inclined 56° and $70-78^\circ$ to bedding foliation
No. optic axes	394	299
Contours	1, 2, 3, 3.5%	1, 2, 3, 4%
General contour pattern	Rough peripheral ($b'c?$) girdle+tendency for an $a'c?$ girdle; no pairs of shear planes	Annular girdle, almost $b'c?$; one possible pair of shear planes cuts bedding obliquely
Type of tectonite	$B \neq F(b')$ BLB'	$B = P(a')$
Type of lattice orientation	j (?), with Max. IV	Reverse of h, with Max. IV
Fabric symmetry	Triolitic	Triclinic
Remarks		

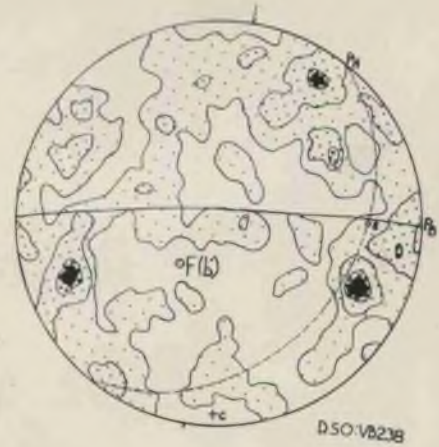
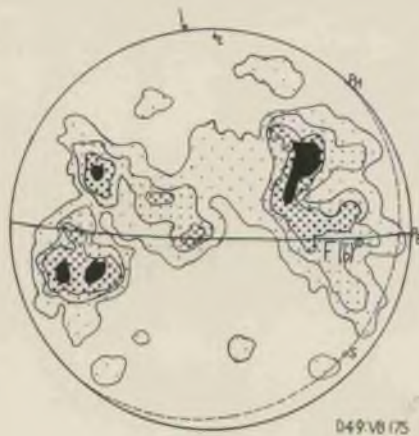


Diagram No.	53	54
Specimen No. and locality	VB263; Loc. 428, N. spur, Sgorr Dhearg	FB267; Loc. 431, summit, Beinn Rhiodha
Formation: specimen description	Appin quartzite: coarse, almost colorless quartzite mottled with pink feldspar; very massive; jointed; bedding crosscut by 10 mm. thick veinlet of white quartz	Striped Transition Series: medium-grained quartzose quartzite; massive; jointed
Position of thin-section	\perp bedding; steeply inclined to F(b')	\perp bedding; inclined to F(b')
Thin-section No. and description	VB263-2: bands of large quartz grains alternate with bands of medium to small quartz grains, generally subrounded; Böhm lamellae conspicuous, strain shadows absent; poikilitic arrangement of tiny mica laths on quartz parallels bedding foliation; individual mica laths inclined 17° and 30° to bedding foliation	VB267-1: predominantly medium-sized quartz grains with some narrow bands of tiny quartz grains; generally subrounded, larger ones frequently show strain shadows; occasional mica laths inclined 21° to bedding foliation
No. optic axes	330	389
Contours	1, 2, 3, 3.75%	1, 1.5, 2, 2.5%
General contour pattern	Rough peripheral (?a'c?) girdle + tendency towards central (b'c) girdle; no possible pairs of shear planes	Rough central (?a'b'?) girdle; three possible pairs of shear planes cut bedding obliquely
Type of tectonite	$B \neq F(b')$ $B \perp B'$	$B \neq F(b')$
Type of lattice orientation	j(?) with Max. IV?	j. with Max. II and IV(?)
Fabric symmetry	Triclinic	Triclinic
Remarks		

Diagram No.	55	56
Specimen No. and locality	VB269; Loc. 435, shore section, N. W. slope, Sgôr na Ciche	VB303; Loc. 563, Beinn Bhan
Formation: specimen description	Glencoe quartzite: medium-grained, massive quartzose quartzite, with micaceous film on bedding foliation	Appin quartzite: coarse-grained bands of glassy quartz and pink feldspar alternate with fine-grained, light-colored bands; massive; jointed (Pl. XXIV, Fig.2)
Position of thin-section	\perp bedding; $\perp F(b')$	\perp bedding; gently inclined to $F(b')$
Thin-section No. and description	VB269: medium-sized, sub-angular quartz grains, with Bôhm lamellae and strain shadows in the larger ones; individual small mica laths inclined 34° and 50° to bedding foliation	VB303-1: large to medium, partially embayed, partially recrystallized quartz grains with no preferred dimensional attenuation; strain shadows roughly parallel to or normal to bedding; abundant large microcline grains, partly weathered
No. optic axes	287	334
Contours	1, 2, 3, 4%	1, 2, 3, 3.5%
General contour pattern	Peripheral (?a'c?) girdle + slight tendency for a central (b'c) girdle; two possible pairs of shear planes cut bedding obliquely	Rough peripheral (?b'c?) girdle + tendency for central (almost an a'c) girdle; one possible pair of shear planes almost normal to bedding
Type of tectonite	$B = F(b')?$ $B \perp B'$	$B \neq F(b')$ $B \perp B'$
Type of lattice orientation	j, with Max. IV	j(?), max. not determined
Fabric symmetry	Triclinic	Triclinic
Remarks		

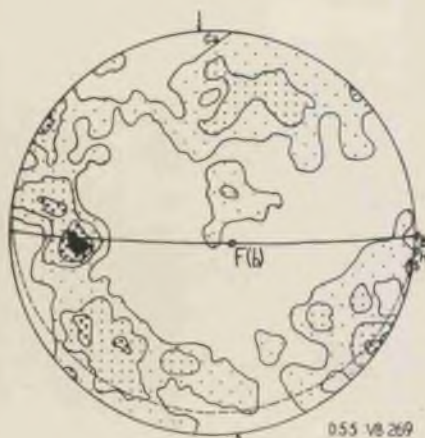
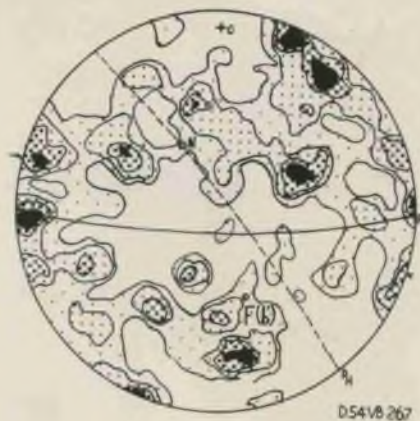
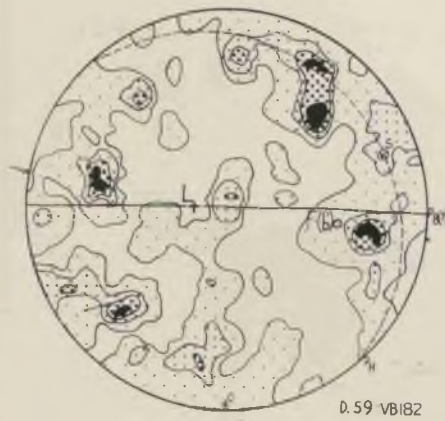
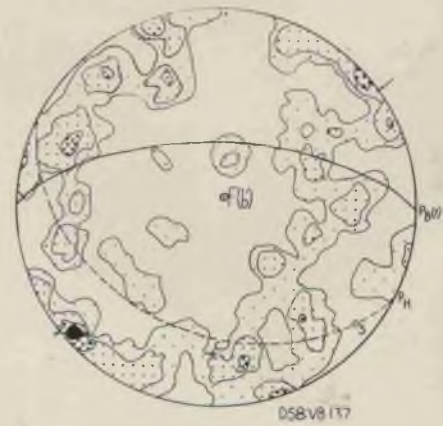


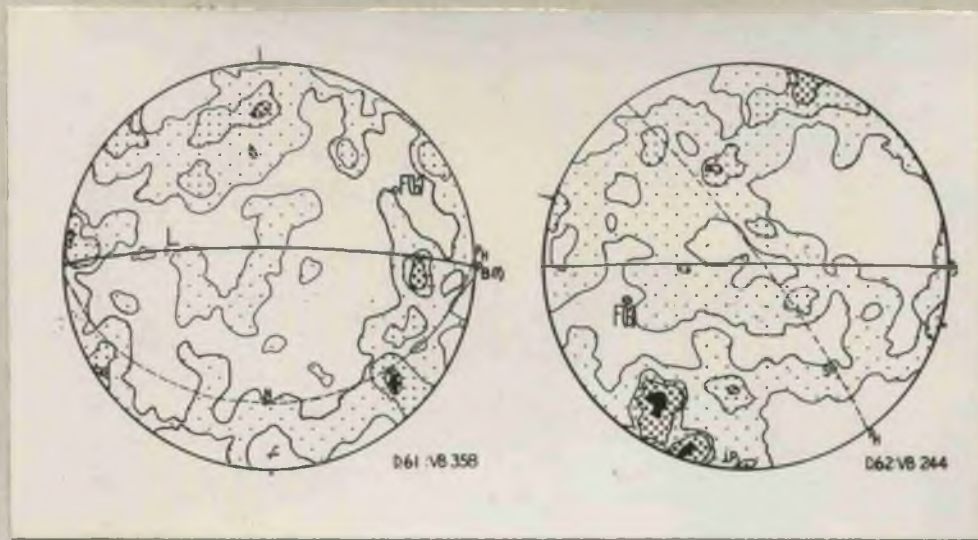
Diagram No.	57	58
Specimen No. and locality	VB16; Loc. 23, upper Gleann an Fhiodh	VB137; Loc. 234, S.W. slope, Sgorr a' Choise
Formation: specimen description	<u>Appin quartzite</u> : coarse-grained, light-colored, quartzose quartzite mottled with pink feldspar grains; massive; jointed	<u>Appin quartzite</u> : medium-grained, whitish, quartzose quartzite; massive; jointed
Position of thin-section	\perp ?bedding?; $F(b')$ lies almost in bedding? foliation	$\perp F(b')$; inclined to ?bedding?
Thin-section No. and description	VB16: very large to medium-sized, generally angular quartz grains, with Böhm lamellae but no strain shadows; medium to small, weathered microcline grains throughout	VB137: predominantly medium-sized, subangular to subrounded quartz grains, with Böhm lamellae and strain shadows conspicuous in the larger grains; occasional medium-sized feldspar grains
No. optic axes	319	257
Contours	1, 2, 2.5, 3%	1, 2, 3, 4%
General contour pattern	Rough girdle (b' and between a' and c); two possible pairs of shear planes cut ?bedding? obliquely	Peripheral (? $a'c$?) girdle; one possible pair of shear planes cuts bedding? at large angle
Type of tectonite	$B = F(b')$?	$B = F(b')$?
Type of lattice orientation	?e, with Max. IV? or VI?	h, with Max. IV
Fabric symmetry	Triclinic	Monoclinic
Remarks		

Diagram No.	59	60
Specimen No. and locality	VB182; Loc. 308, S. slope, Sgúor nam Fiannaídh	VB204; Loc. 73, upper Glen Coe
Formation: specimen description	<u>Glencoe quartzite</u> : fine-grained quartzose quartzite; massive; jointed; one very rough and coarse lineation (L), probably due to slippage along bedding (?) foliation	<u>Ballachulish limestone</u> : thermally metamorphosed to calc-silicate-hornfels; jointed; one very fine lineation (L), possibly due to slippage along ?bedding? foliation
Position of thin-section	\perp bedding(?); almost \perp L	Almost \perp bedding (?); L parallel with bedding foliation
Thin-section No. and description	VB182: large, subrounded quartz grains, sometimes surrounded by tiny quartz grains or narrow bands of tiny grains; Böhm lamellae conspicuous, some grains show strain shadows	VB204: tiny, almost indistinguishable mica laths in undulatory bands with tiny quartz grains; medium to small quartz grains in lenticles and pockets; quartz generally sub-angular; short bands of mica laths intersect bedding foliation at 22°
No. optic axes	319	427
Contours	1, 2, 2.5, 3%	1, 1.5, 2, 2.5%
General contour pattern	Peripheral (ac) girdle + tendency for central (bc) girdle; one possible pair of shear planes parallel but inclined to bedding; second pair cuts bedding at large angle	Peripheral (bc?) girdle; two possible pairs of shear planes cut bedding (?) foliation obliquely
Type of tectonite	$B \neq F(b')$? $B \perp B'$	$B = F(a')$?
Type of lattice orientation	j, with Max. IV(?) and VI(?)	Reverse of h, with Max. VI
Fabric symmetry	Triclinic	Triclinic
Remarks		

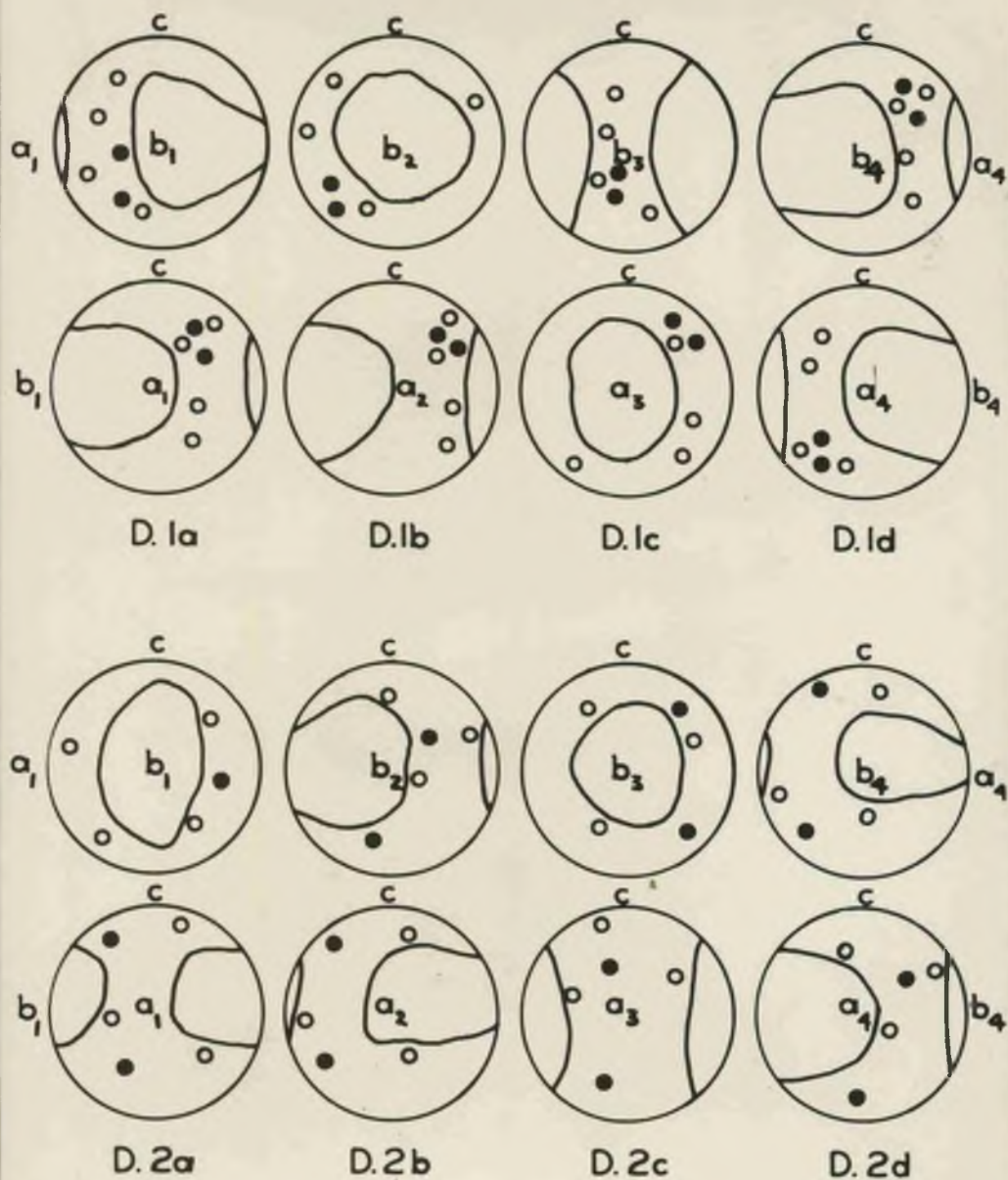


P_B represents the trace of foliation which may be bedding.

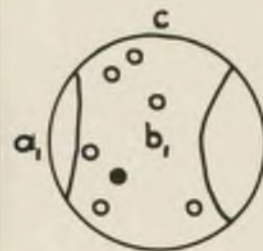
Diagram No.	61	62
Specimen No. and locality	VB358; Loc. 732, E. slope Gleann Leac-na-muidhe	VB244; Loc. 395, N. spur, Sgòr nam Fiannaidh
Formation: specimen description	<u>Leven schist</u> : thermally metamorphosed quartzose schist; one rough lineation (L)	<u>Glencoe granite</u> : fine-grained, with much pink feldspar; 3 main joint systems
Position of thin-section	\perp bedding?; inclined to L and to F(b')	\perp prominent joint plane; inclined to F(b')
Thin-section No. and description	VB358: fine mesh mica matrix with some feathery clusters in discontinuous, confused bands; individual small laths inclined 22° , 33° - 38° , and 59° to ?bedding?; conspicuous to subordinate, medium-sized, subangular quartz grains throughout	VB244: medium to small, subrounded to angular quartz grains, with large to small, weathered microcline and plagioclase grains scattered throughout
No. optic axes	292	342
Contours	1, 2, 3, 3.5%	1, 2, 3, 4%
General contour pattern	Rough peripheral (ac?) girdle + slight tendency for central (almost bc) girdle; one possible pair of shear planes cuts ?bedding? obliquely	Rough girdle (b' P _j ?); no possible pairs of shear planes
Type of tectonite	$B \neq b \neq F(b')$ $B \perp B'$	B roughly $\approx F(a')$
Type of lattice orientation	j (?), with Max. IV(?)	Reverse of h, with Max. VI
Fabric symmetry	Triclinic	Triclinic
Remarks		



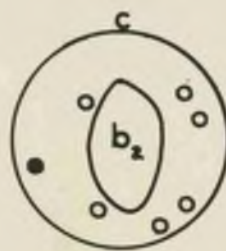
P_J represents the trace of a prominent joint plane.



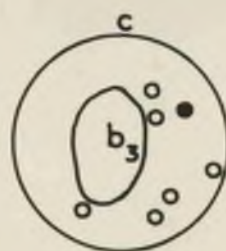
Quartz maxima and girdles of petrofabric diagrams 1 and 2, which have been rotated in terms of each lineation (b₁, b₂, b₃, b₄) and its concomitant "a"-axis (a₁, a₂, a₃, a₄).



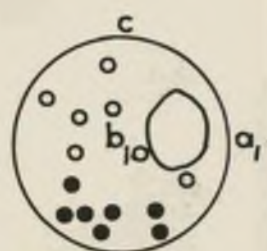
D. 3a



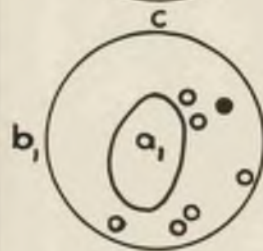
D. 3b



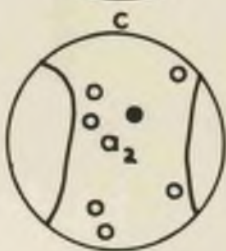
D. 3c



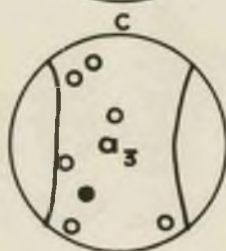
D. 4a



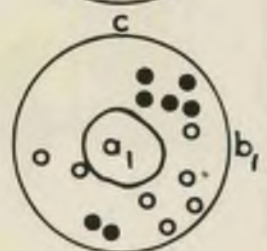
D. 4b



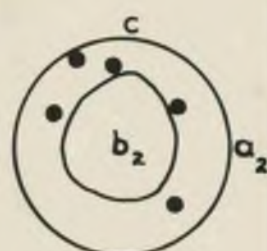
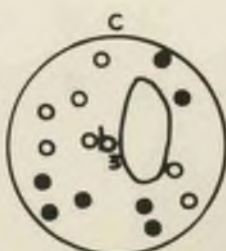
D. 4c

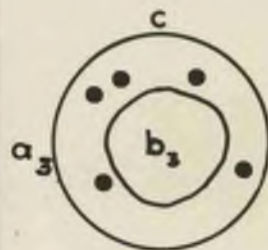


D. 5a



D. 5b

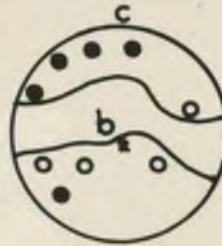




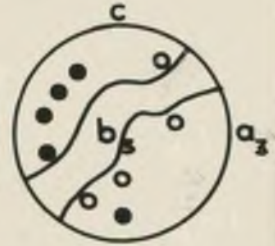
D.5c



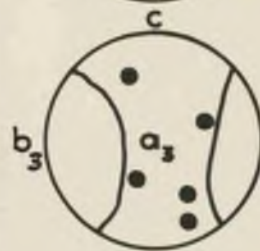
D.6a



D.6b



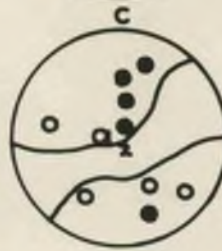
D.6c



D.7a



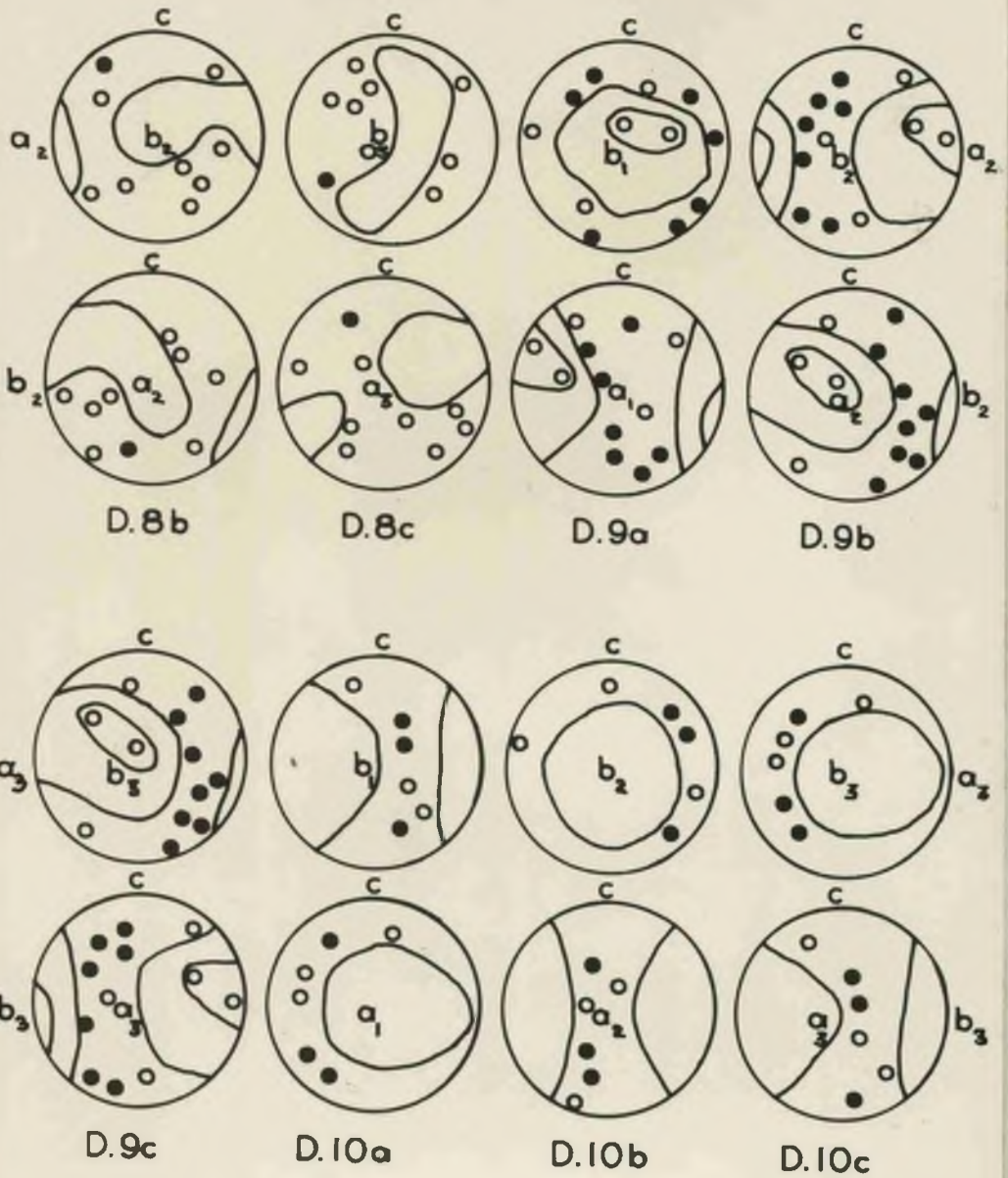
D.7b

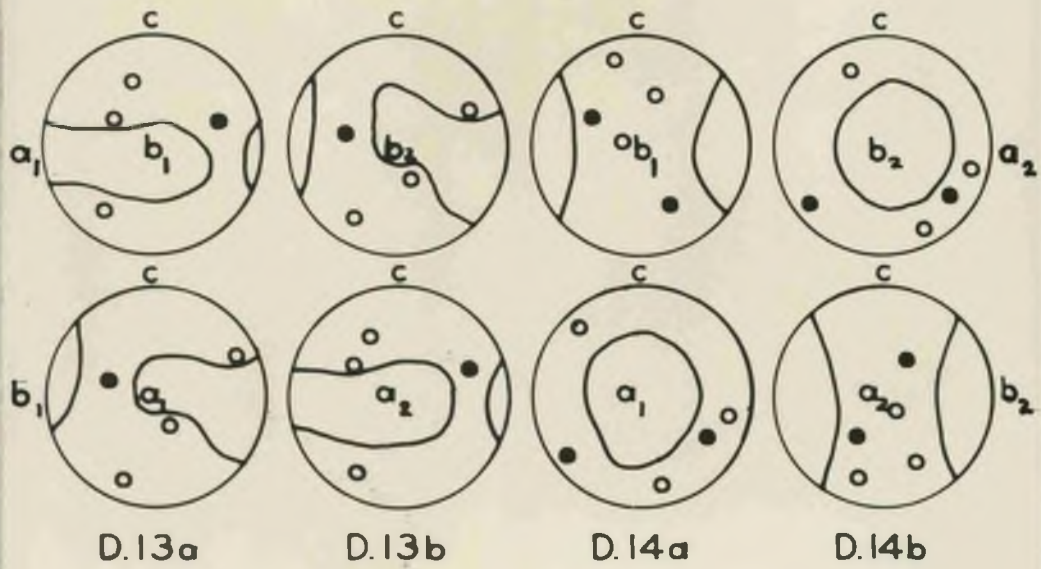
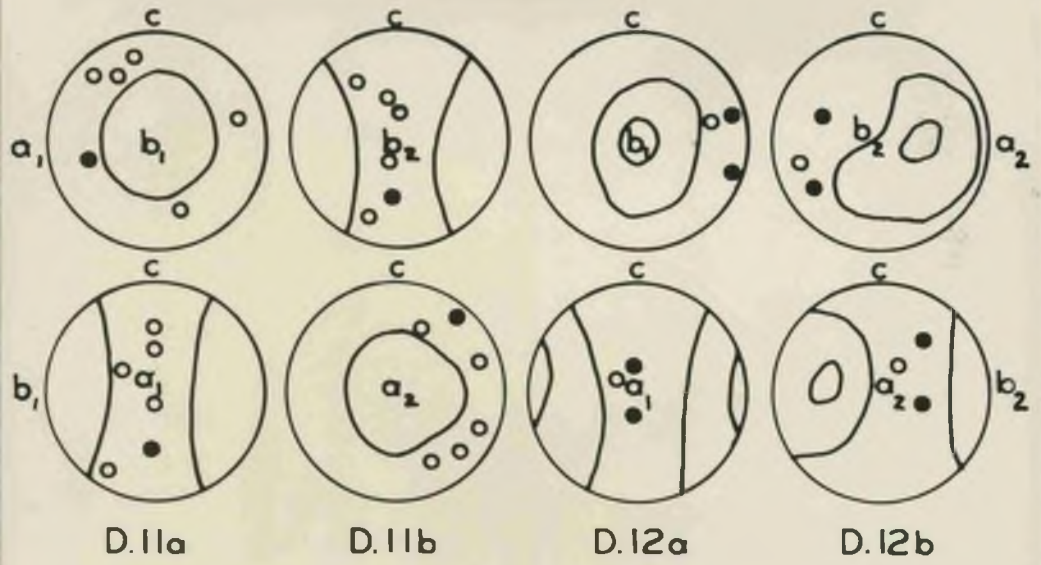


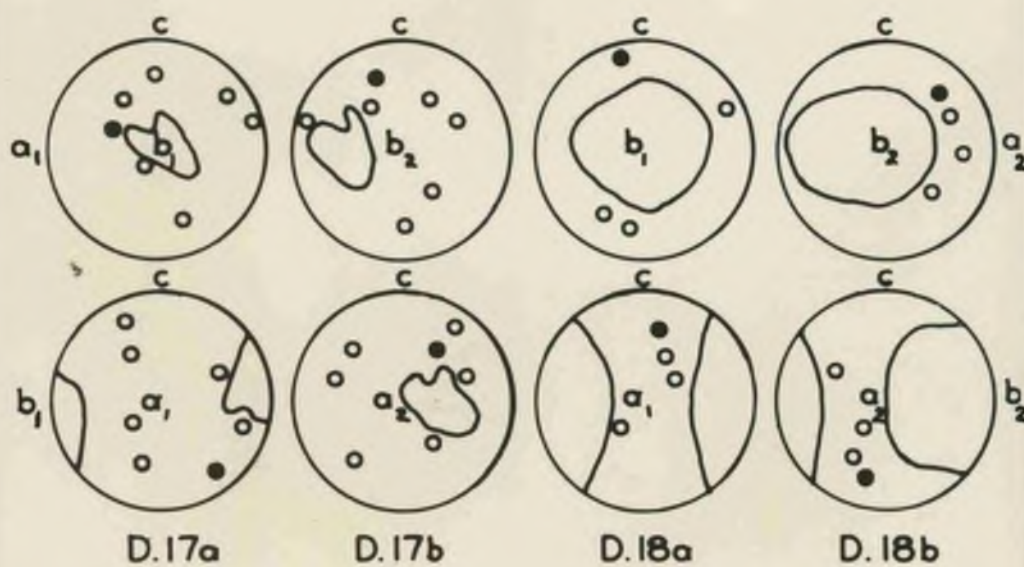
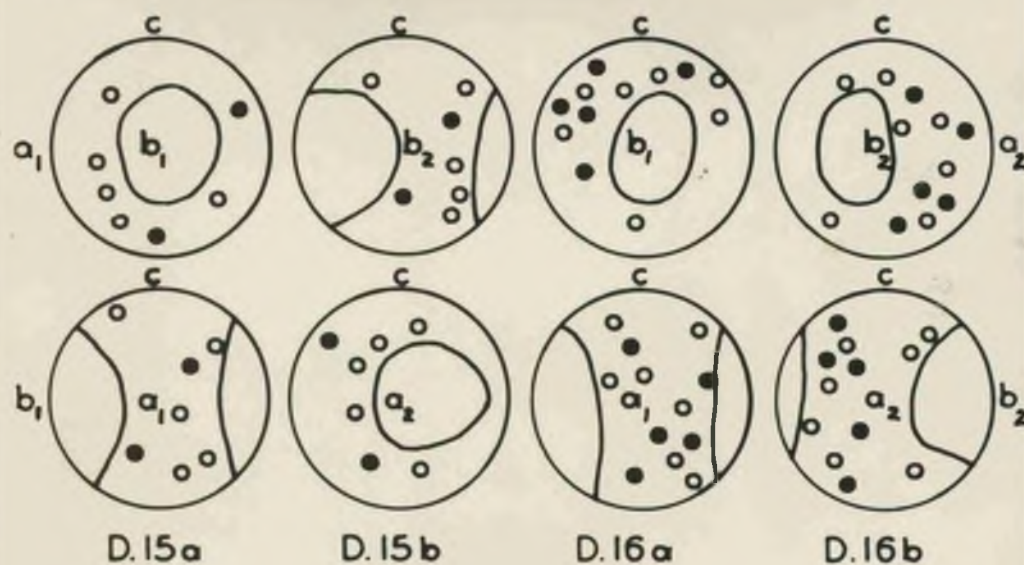
D.7c

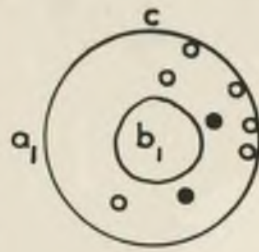


D.8a

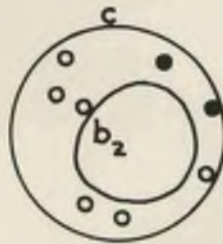




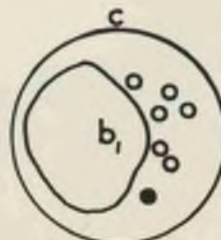




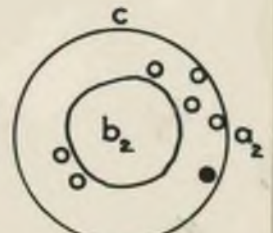
D.19a



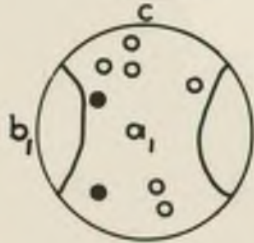
D.19b



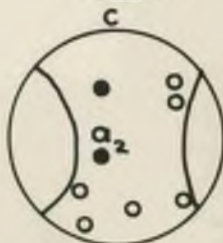
D.20a



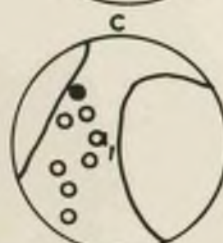
D.20b



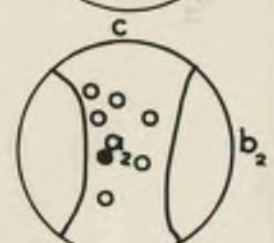
D.21a



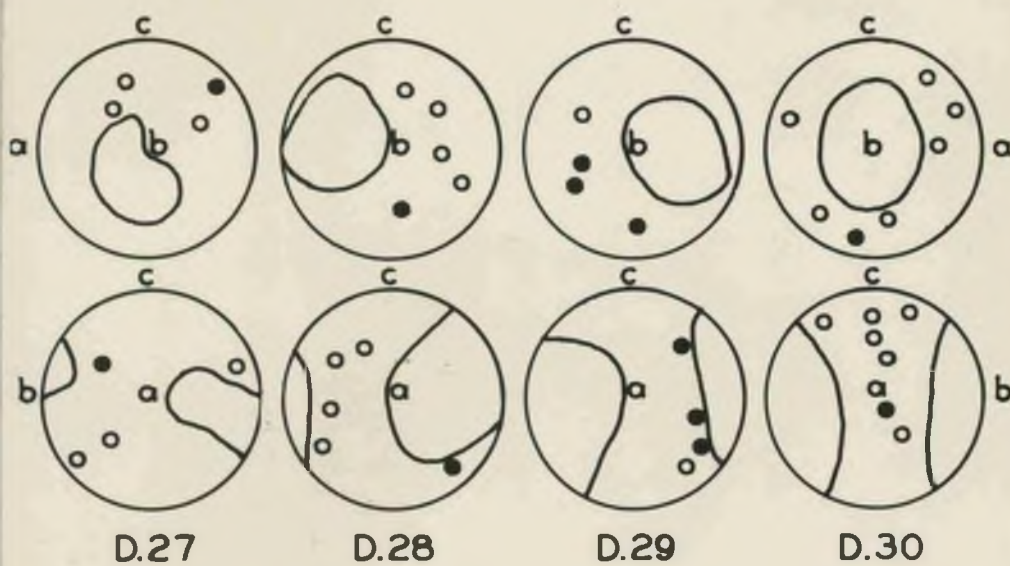
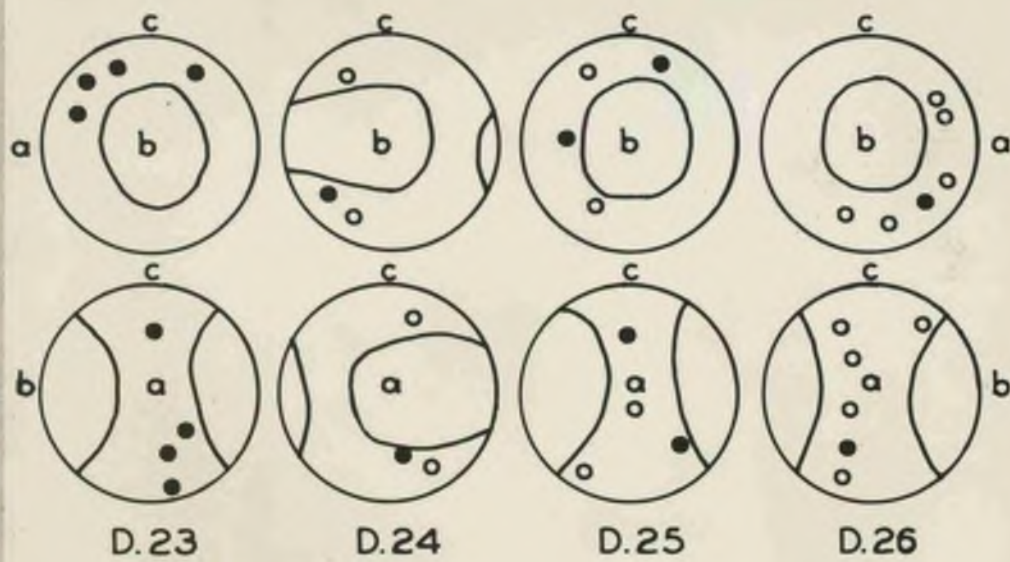
D.21b

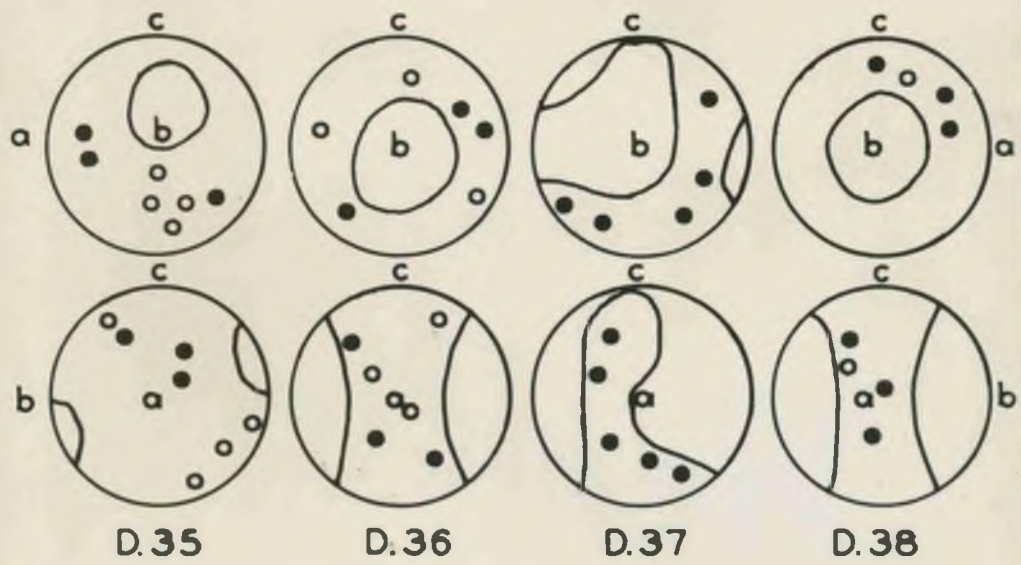
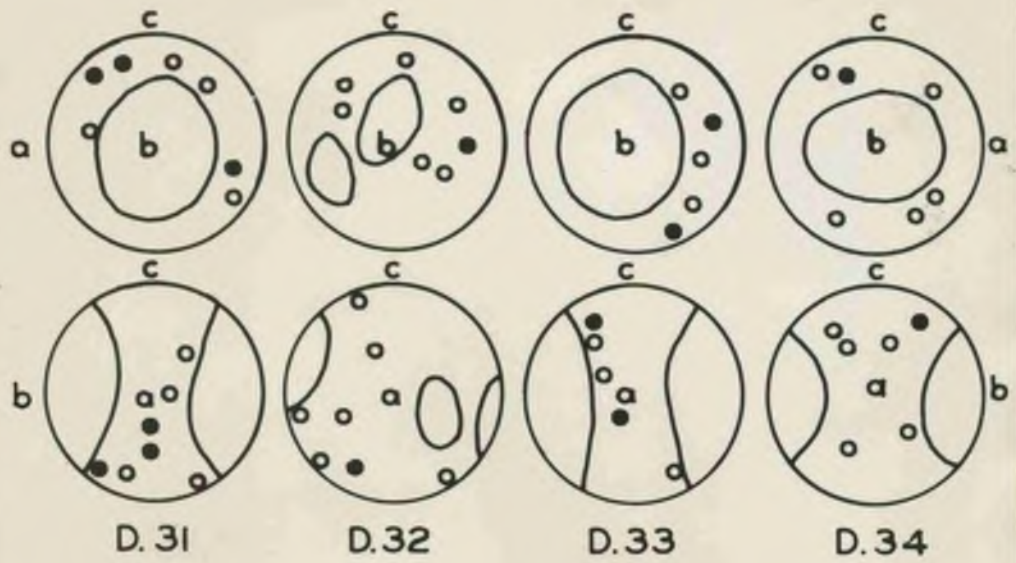


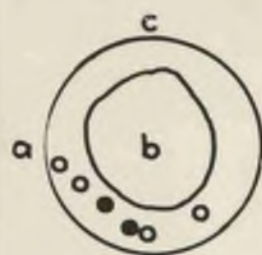
D.22a



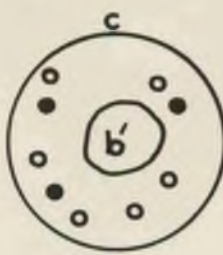
D.22b



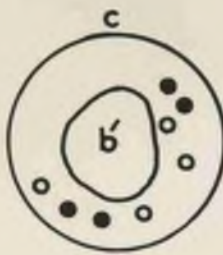




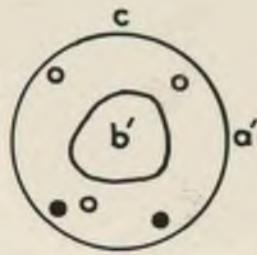
D.39



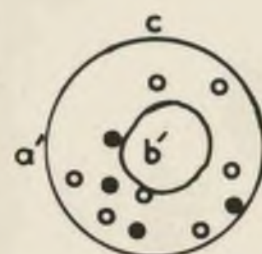
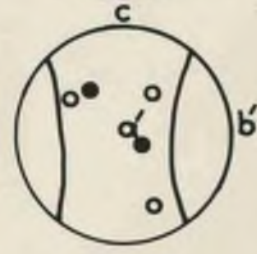
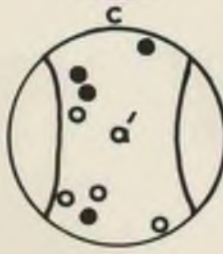
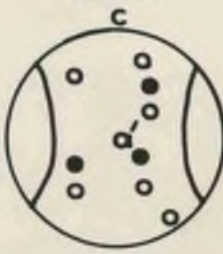
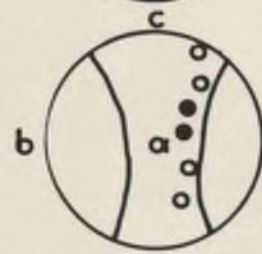
D.40



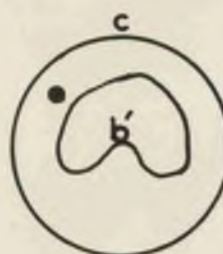
D.41



D.42



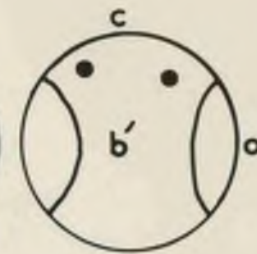
D.43



D.44



D.45



D.46



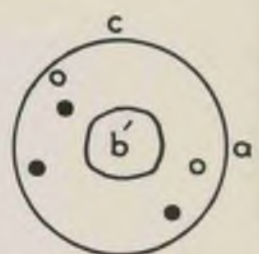
D.47



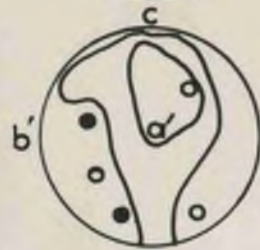
D.48



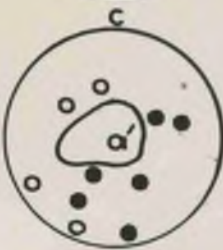
D.49



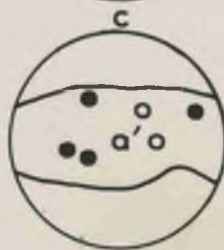
D.50



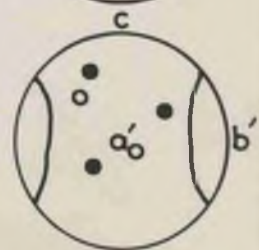
D.51



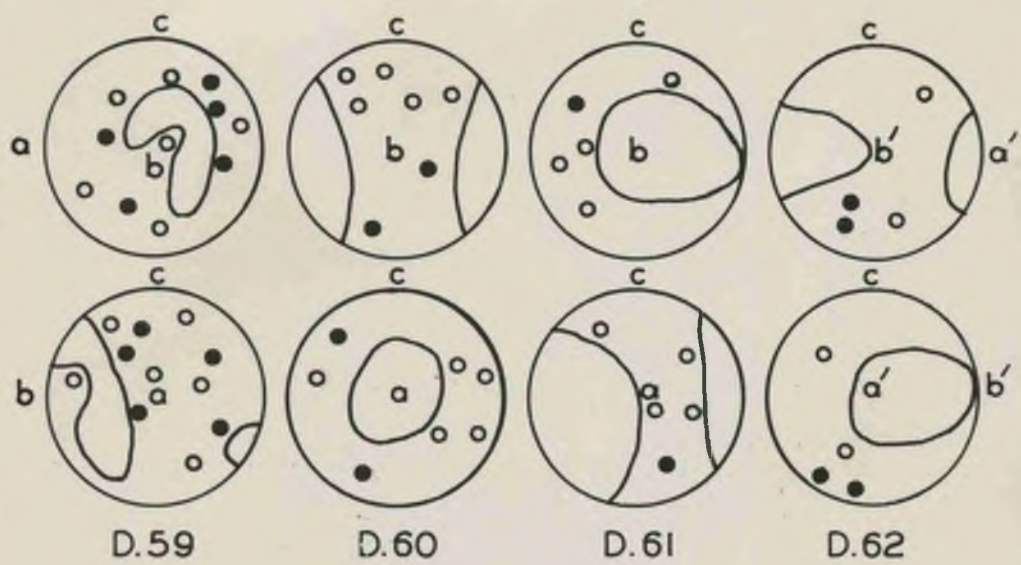
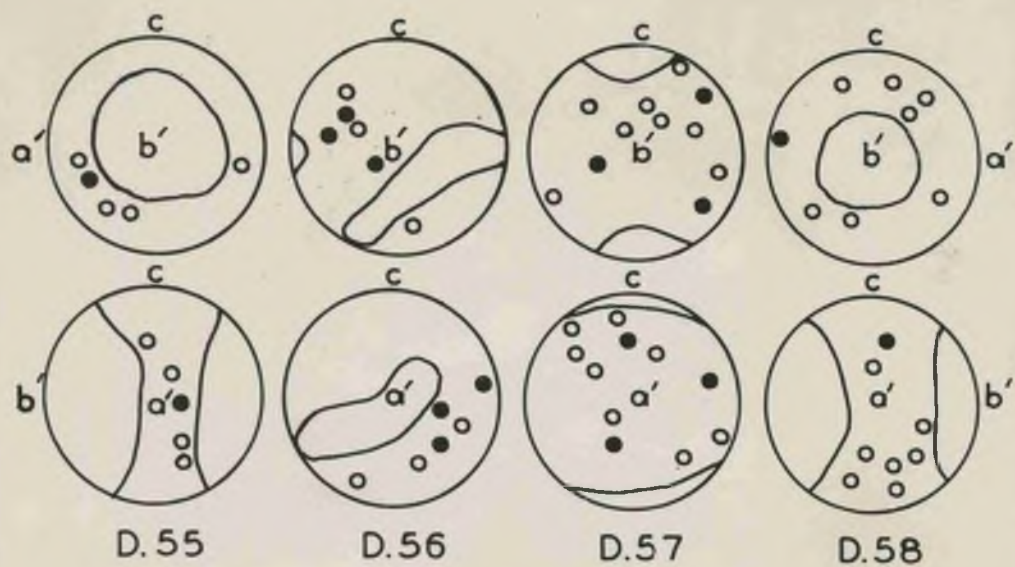
D.52



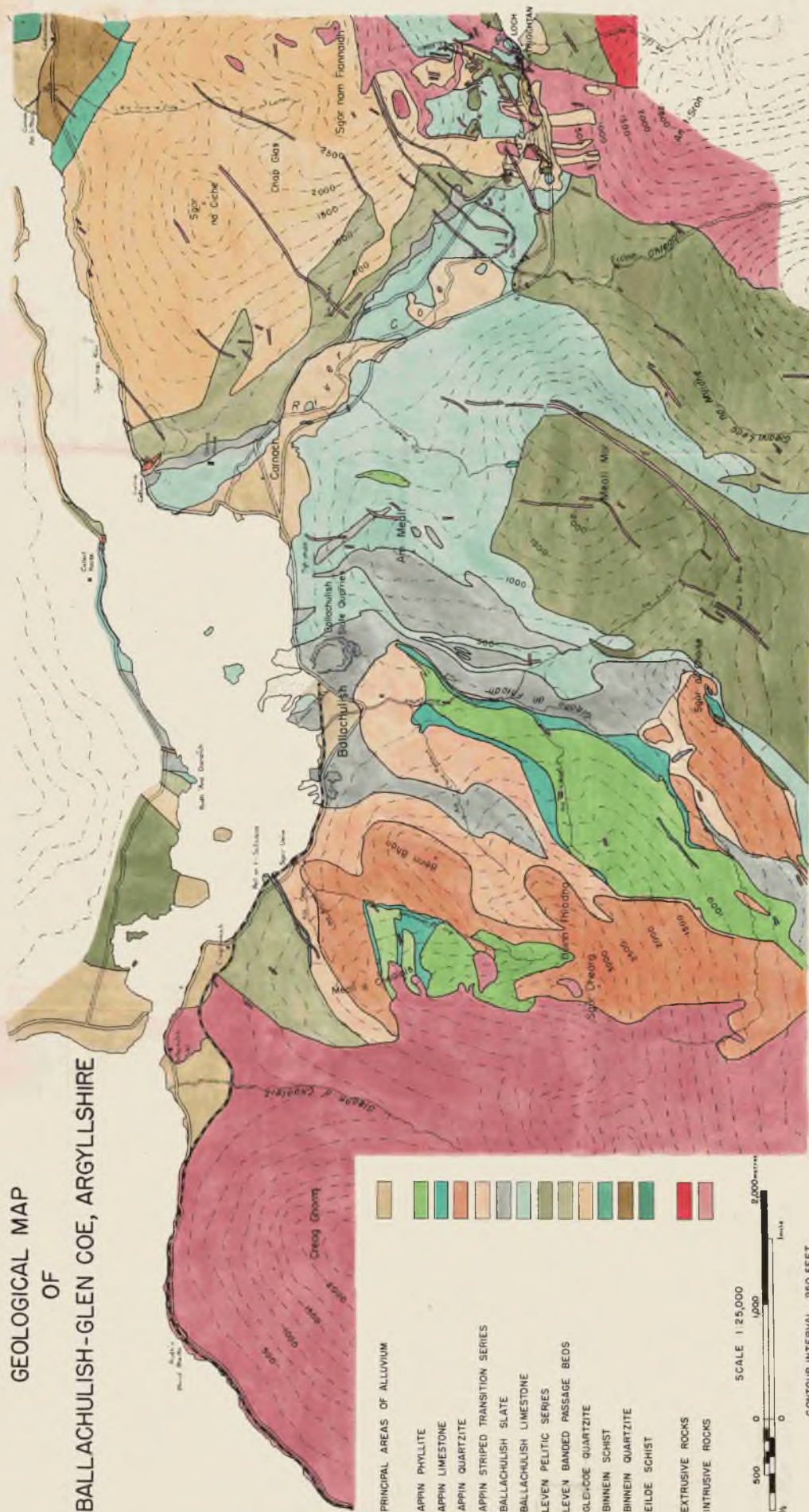
D.53



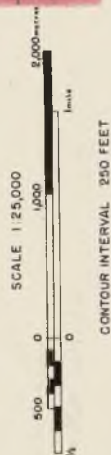
D.54



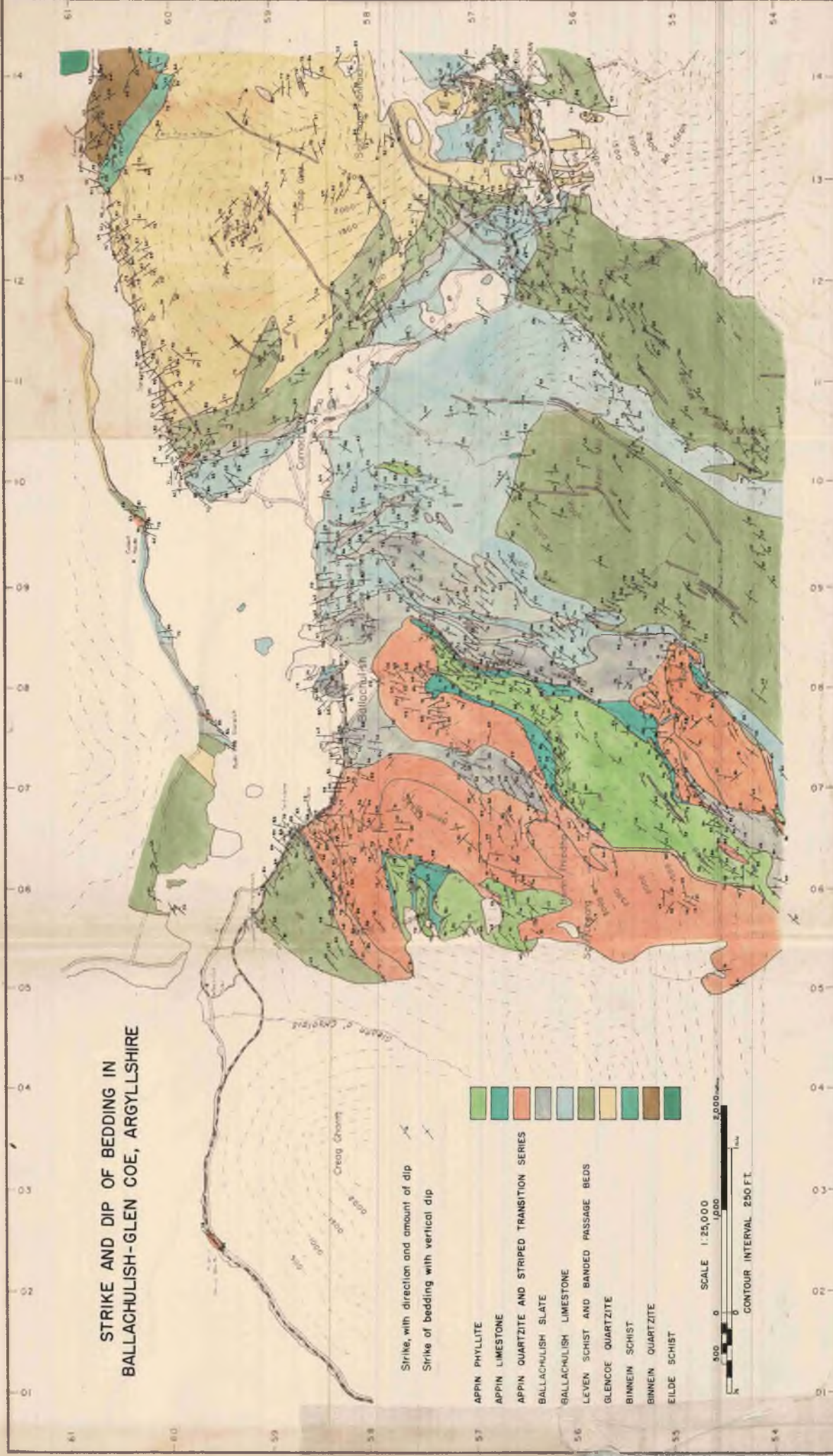
GEOLOGICAL MAP OF BALLACHULISH-GLEN COE, ARGYLLSHIRE



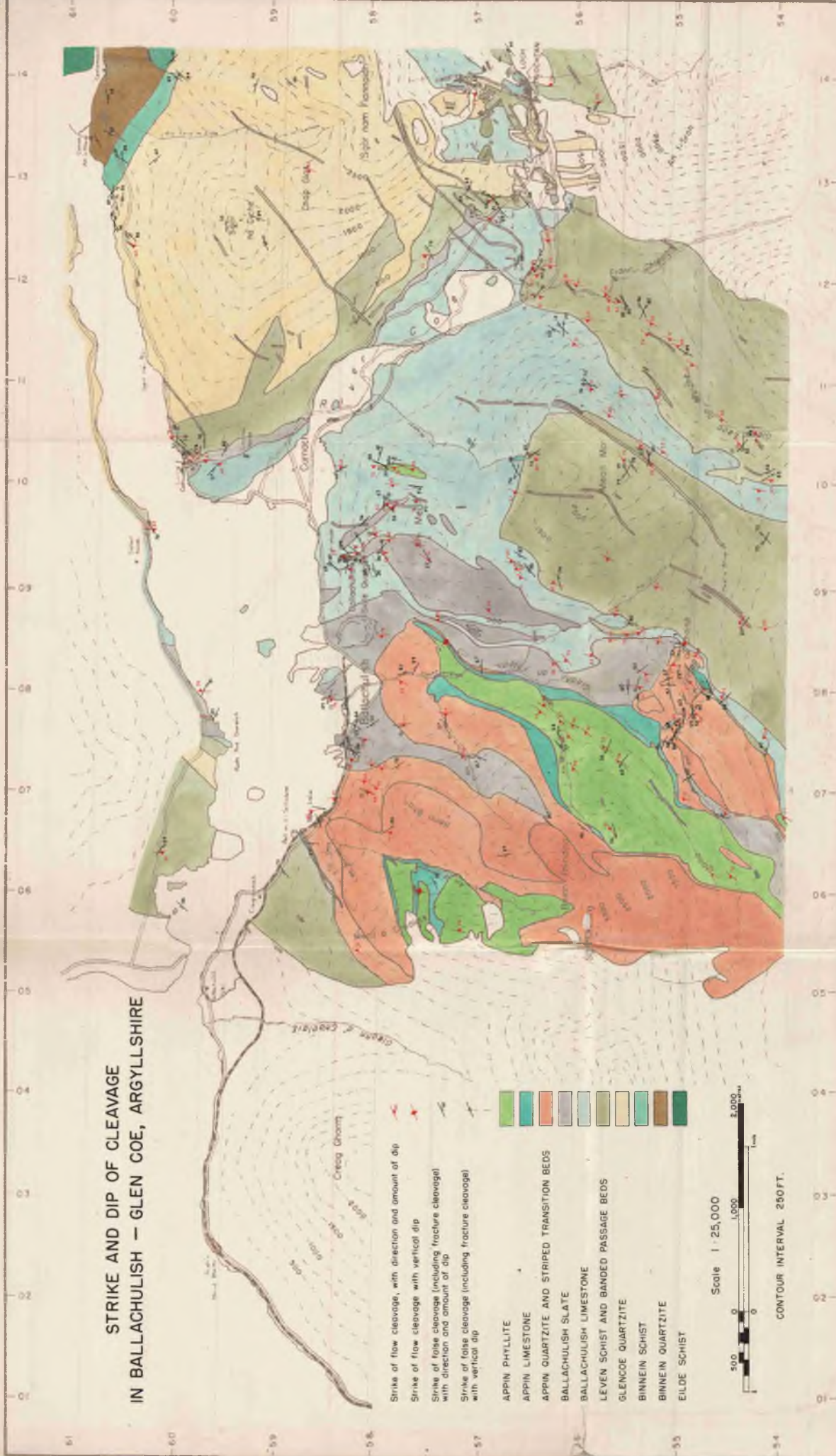
- PRINCIPAL AREAS OF ALLUVIUM
- APPIN PHYLLITE
 - APPIN LIMESTONE
 - APPIN QUARTZITE
 - APPIN STRIPED TRANSITION SERIES
 - BALLACHULISH SLATE
 - BALLACHULISH LIMESTONE
 - LEVEN PELTIC SERIES
 - LEVEN BANDED PASSAGE BEDS
 - GLENCOE QUARTZITE
 - BINNEN SCHIST
 - BINNEN QUARTZITE
 - EILDE SCHIST
 - EXTRUSIVE ROCKS
 - INTRUSIVE ROCKS



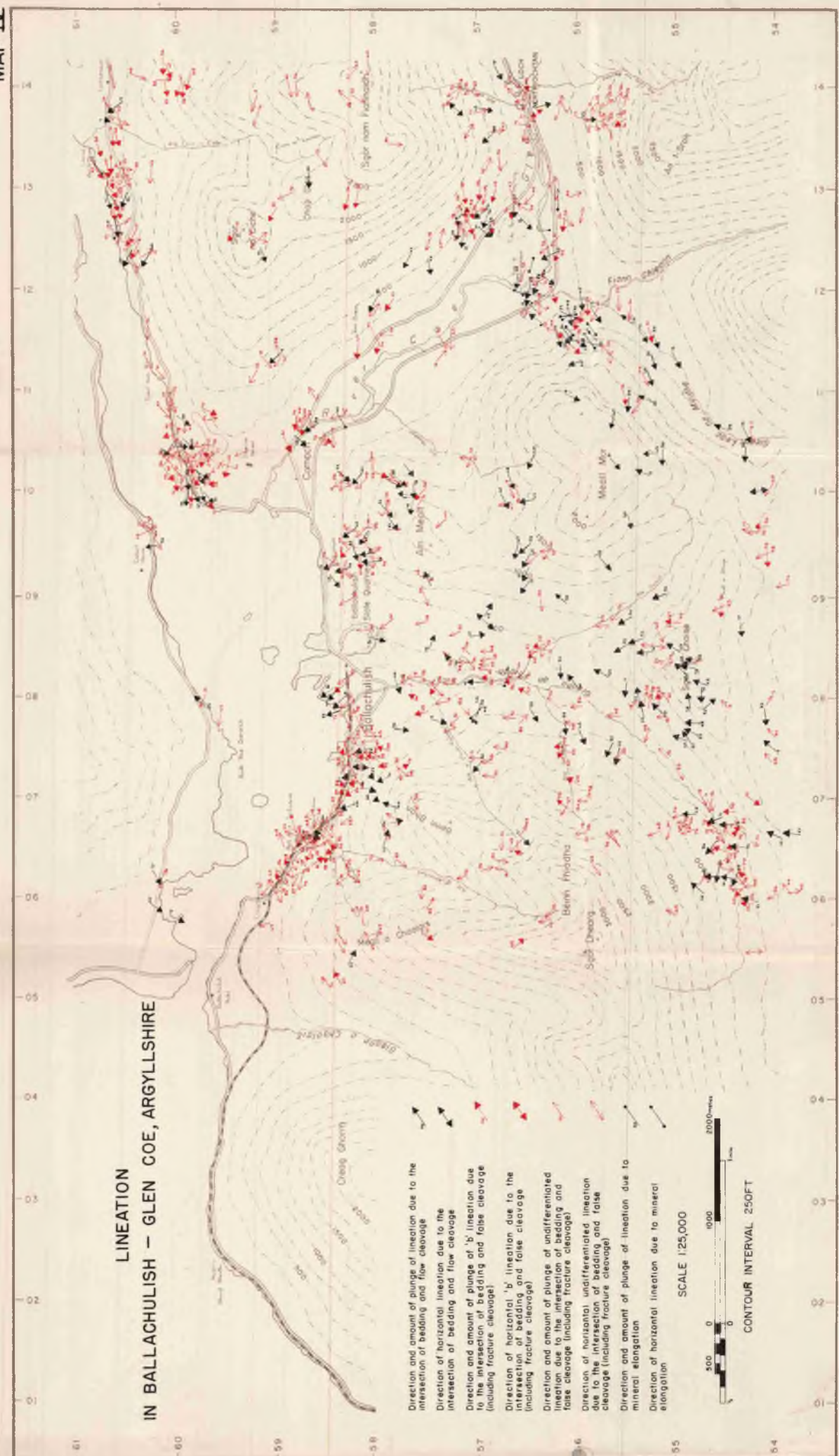
STRIKE AND DIP OF BEDDING IN BALLACHULISH-GLEN COE, ARGYLLSHIRE



STRIKE AND DIP OF CLEAVAGE
IN BALLACHULISH - GLEN COE, ARGYLLSHIRE



LINEATION
IN BALLACHULISH - GLEN COE, ARGYLLSHIRE



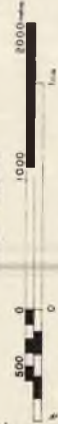
FOLD AXES IN BALLACHULISH-GLEN COE, ARGYLLSHIRE

Trend, with plunge in degrees,
of fold less than twelve inches in width
Trend, with plunge in degrees,
of fold more than twelve inches in width

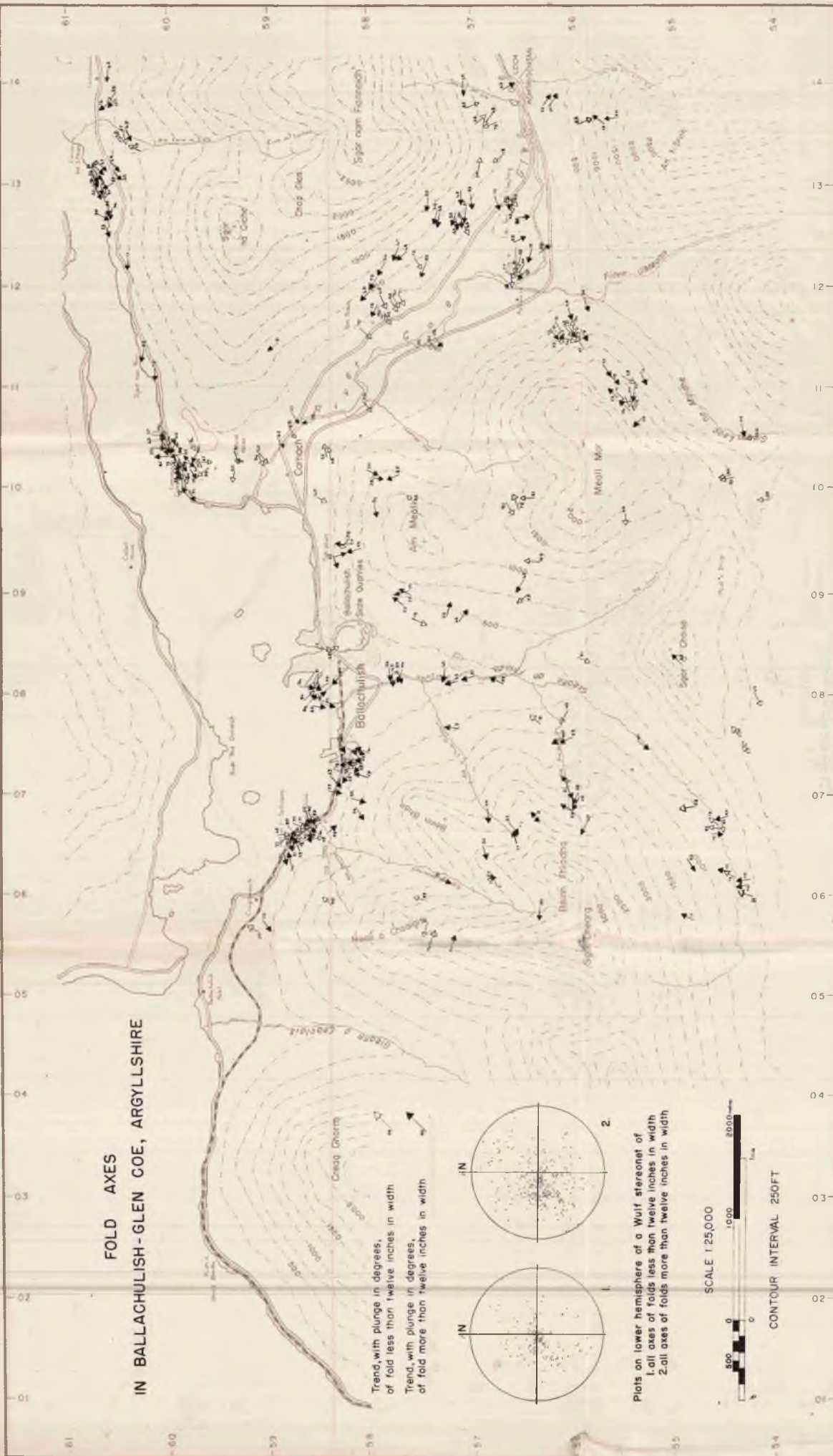


Plots on lower hemisphere of a Wulff stereonet of
1. all axes of folds less than twelve inches in width
2. all axes of folds more than twelve inches in width

SCALE 1:25,000



CONTOUR INTERVAL 250FT



AXIAL DIRECTIONS IN BALLACHULISH-GLEN COE, ARGYLLSHIRE

IV

III

II

I

Creag Chenn

Creag Chenn

BOUNDARY OF MAJOR DIVISION

AXIAL DIRECTION OF MAJOR DIVISION WITH
PLUNGE IN DEGREES

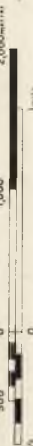
BOUNDARY OF SUBDIVISION

AXIAL DIRECTION OF SUBDIVISION WITH
PLUNGE IN DEGREES



ALL AXIAL DIRECTIONS WITH PLUNGES, OF SUBDIVISIONS ARE
PLOTTED ON A WULF STEREOGRAPH

SCALE 1:25,000



CONTOUR INTERVAL 250 FEET

IN BALLACHULISH - GLEN COE, ARGYLLSHIRE

